1980

Structural, biochemical, and inhibition studies of cell wall formation in the unicellular marine coccolithophorid alga Hymenomonas carterae

Ahmad Reza Safa-Esfahani
Iowa State University

SAFA-ESFAHANI, AHMAD REZA

STRUCTURAL, BIOCHEMICAL, AND INHIBITION STUDIES OF CELL WALL FORMATION IN THE UNICELLULAR MARINE COCCOLITHOPHORID ALGA HYMENOMONAS CARTERAE

Iowa State University PH.D. 1980

Structural, biochemical, and inhibition studies of cell wall formation in the unicellular marine coccolithophorid alga Hymenomonas carterae

by

Ahmad Reza Safa-Esfahani

A Dissertation Submitted to the
Graduate Faculty in Partial Fulfillment of the
Requirements for the Degree of
DOCTOR OF PHILOSOPHY

Major: Molecular, Cellular, and
Developmental Biology

Approved:

Signature was redacted for privacy.

In Charge of Major Work

Signature was redacted for privacy.

For the Major Department

Signature was redacted for privacy.

For the Graduate College

Iowa State University
Ames, Iowa

1980

TABLE OF CONTENTS

INTRODUCTION

At the present time, our knowledge of molecular details, spatial arrangement, morphogenesis, and particularly the self-assembly of wall components in different systems is not sufficient to present a complete detailed structural and biochemical model for individual plant systems. This in turn is due to the complexity of the structure and diversity of molecular species involved in construction of the cell wall. A common feature of most plant cell walls is the presence of cellulose and pectin which in turn are covalently linked to hydroxyproline-rich glycoprotein.

The interesting feature of the Hymenomonas cell wall is that it is composed of several discrete units which are assembled sequentially and intracellularly in Golgi cisternae. The coccoliths and scales which are the most morphologically distinct units of the wall have essentially similar but not identical structures. These wall components biochemically resemble the whole wall structure of higher plant cells simply by having cellulosic concentric microfibrils and pectic, radial microfibrils embedded in an amorphous polysaccharide and in turn connected to a hydroxyproline rich protein. Although morphologically different, the existance of similar components among the different systems provides a significant evolutionary relationship. Rapid production of Hymenomonas protoplasts by use of enzymatic methods devised for Petunia, tobacco, etc. provides another suggestion of similarities between this organism and higher plants.

The coccolith of H. carterae particularly offers an excellent model system for investigating biological calcification and the self assembly process, and also indicates the involvement of the Golgi membrane in such assembly. Although the exact mechanism of calcification is not completely known, the participation of polyanionic molecules which act as nucleators of crystallization have been reported.

The subject of this investigation is somewhat broad and includes the following purposes: 1) the determination of the detailed structural features of the cell wall of H. carterae by light, transmission, and scanning microscopy, 2) the isolation of the cell wall and its partial characterization, and also the self-assembly of some of the components which were partially solubilized from the cell wall, 3) the isolation of acidic polysaccharides from coccoliths which may be involved with calcification of the precisely formed calcite crystals, 4) speculation as to the nature of the interactions among the wall components, 5) the enzymatic digestion of the wall and formation of protoplasts, and finally 6) cell wall regeneration and the kinetics of wall formation under standard conditions and in the presence of cell wall inhibitors.

LITERATURE REVIEW

Life Cycle and General Features of *Hymenomonas carterae*

Hymenomonas carterae is a unicellular alga and a member of an old group of organisms, the so-called Coccolithophorida (coccolith-bearing) because of their production of calcified scales called coccoliths. The organism possesses two flagella and a haptonema; the latter is an organelle with a bulbous structure lying between the two flagella (Leadbeater, 1970, 1971; Paasche, 1968). Manton (1968) suggested that it may function as an attachment organelle and/or act like a rudder as an aid in controlling movement.

The life cycle of *H. carterae* (and other related organisms) has been investigated (Leadbeater, 1970, 1971; Paddok, 1968). Reviews by Leadbeater (1970, 1971) indicate that two major morphologically distinct stages have been established: (a) the coccolith-bearing "*Hymenomonas*" or "*Chrycosphaera*" stage and (b) a noncoccolith-bearing, vegetative or benthic, "*Apistonema*" or "*Pleurochrysis*" stage. Rayns (1962) and von Stosch (1967) found that the *Apistonema* stage of *Hymenomonas* was haploid and that the coccolith-bearing stage of *Hymenomonas* was diploid. According to von Stosch (1967), sexual fusion must occur before the *Hymenomonas* stage can arise (this claim has never been directly confirmed by any other investigator). Von Stosch (1967) believed that the two stages are linked through syngamy and meiosis (meiospores). Both stages, however, appear to have an unlimited capacity for vegetative or asexual reproduction. An alternative explanation would be the achievement of the diploid stage by apogamy (self-fusion) of motile

cells (Brown, 1969, 1975; Brown and co-workers, 1969, 1970, 1973; Romanovicz and Brown, 1976).

An additional stage (i.e., "Ochrosphaera" stage) in the life cycle of Hymenomonas has been reported by Lefort (1971). He has proposed on the basis of his observations of cultured material, that the coccolithophorid Ochrosphaera verrucosa, which bears heterococcoliths that are distinct from the coccoliths of Hymenomonas, is actually an additional stage in the life cycle of H. carterae. Thus, the life cycle of H. carterae may consist of three major stages as well as a number of transitional phases.

Parke and Adams (1960), working with Coccolithus pelagicus, have found that motile stages are haploid and the nonmotile stages are diploid; this information contradicts the Rayns (1962) and von Stosch (1967) work. However, the results of chromosome studies and a quantitative measurement of DNA content per nucleus by microspectrophotometry (Safa, 1977) showed that the motile, coccolith-bearing stages are haploid and the nonmotile, noncoccolith-bearing stages are diploid. Therefore, the life cycle data begins to suggest a unity of life cycle history relationships not only between Hymenomonas and other coccolithophorids (Parke and Adams, 1960) but also with green algae such as Chlamydomonas (Ebersold, 1963, 1967; Levine and Ebersold, 1960).

Cell Wall Characterization of H. carterae

Cell wall formation

Structural investigations The cell wall of H. carterae consists of several layers (Flesch, 1977; Williams, 1972). The outer part of the

wall contains calcified (calcite) plates, called coccoliths, which are formed in vesicles of the Golgi apparatus (Dorigan and Wilbur, 1973; Klaveness, 1976; Manton and Leedale, 1969; Manton and Peterfi, 1969; Outka and Williams, 1971; Pienaar, 1971; Williams, 1972). The inner portion of the wall is called columnar material (Manton and Leedale, 1969). This portion of wall consists of fibrils projecting from the plasma membrane which may be involved with holding the wall together. Also two or three cellulosic scales are connected together and in turn to outer and inner portions of wall by a component, the so-called "glue" (Flesch, 1977). In the Pleurochrysis stage of the life cycle, there are several layers of scales which are embedded in an amorphous electron transparent material (Brown and Romanovicz, 1976; Romanovicz and Brown, 1976). It is now also accepted that scales of the wall are made intracellularly in the Golgi apparatus (Brown, 1969; Brown and Romanovicz, 1976; Brown et al., 1970, 1973; Manton, 1967a,b, 1968).

The earliest fossil coccoliths first appear in the geological record some 180 million years ago and have many ultrastructural features in common with modern forms (Gartner, 1978). The structural investigations of coccoliths are restricted to electron microscopy. This is due to the small size of coccoliths (approx. 0.25-

observations have revealed that a coccolith can morphologically be divided into three distinct structural components. First, crystals of $CaCO_3$ are present in all coccoliths (Paasch, 1968). Second, there is a coccolith base (Brown and Romanovicz, 1976; Crenshaw, 1964; Outka and Williams, 1971; Paddock, 1968; Pienaar, 1969a, 1969b; Wilbur and Watabe,

1963). Third, a number of investigators have reported that an organic sheath or matrix (extracrystalline matrix) encases the $CaCO_3$ (Crenshaw, 1964; Klaveness, 1972; Manton and Peterfi, 1969). Recently, an intracrystalline polysaccharide has also been reported (Fichtinger-Schipman et al., 1979; DeJong et al., 1976; Westbroek et al., 1973).

The developmental sequence of coccolith formation has been studied by several authors (Wilbur and Watabe, 1963; Manton, 1966, 1967a; Manton and Leedale, 1969, Outka and Williams, 1971). In several of these reports, the authors found that scales and coccoliths were structurally determined before liberation from the parent Golgi cisternae. Isenberg and his co-workers (1966) hypothesized that the Golgi apparatus gives rise to a reticular body and a mineral reservoir which, in turn, gives rise to an intracellular coccolith precursor body (ICP). The ICP then forms a coccolith and a remaining portion which is either reincorporated into a new ICP or degenerates into a fat body. Pienaar (1969b) apparently accepted Isenberg's proposal. Investigations by Outka and Williams (1971) proved that coccoliths of H. carterae were formed sequentially in the Golgi apparatus. They showed that the first stages in formation of a coccolith involve synthesis and accumulation of electron dense bodies (coccolithosomes) in lateral ear-pockets of Golgi cisternae and the development of a scale-like base in the immature medial portion of the Golgi vacuole. The coccolithosomes are later transferred to the medial vacuole of the Golgi apparatus which contains the base, where they accumulate and condense at the periphery of the base and form a sheet-like matrix. Calcification

appears to occur from nucleation sites within the matrix. Coccoliths will be eventually transferred to the anterior region of the cell and finally extruded to the surface of the cell. The original mechanism suggested by Pienaar (1969b) to explain the formation of the coccolith has been modified (Pienaar, 1971) to say that the Golgi body is responsible for the formation of the coccoliths as well as the unmineralized scales. In addition to the proposal of Outka and Williams (1971) regarding the matrix function as a nucleation site for crystallization, Klaveness (1976), working with Emiliania huxleyi, proposed that the matrix acts to suppress uncontrolled nucleation by acting as a filtering medium to allow homogenous nucleation. Current investigation of other members of the Coccolithophorida (Cyclococcolithina leptopora and Gephyrocapsa oceanica) showed that coccoliths were formed within the Golgi apparatus but neither coccolithosomes nor scales were associated with coccoliths (Blackwelder et al., 1979). Therefore, formation and development of coccoliths in these species resemble processes in Emiliana huxleyi (Klaveness, 1976) but differ from those of H. carterae (Outka and Williams, 1971; Pienaar, 1971) insofar as they do not have coccolithosomes or scales and do not show the intracellular production of coccoliths one at a time.

The coccolith bases are presumed to be chemically and morphologically homologous to unmineralized scales except that the base of the coccolith is thicker, has sites for matrix deposition, and has calcified rim elements attached (Brown, 1969, 1975; Brown and co-workers, 1969, 1970, 1973; Romanovicz and Brown, 1976; Herth et al., 1972, 1975; Manton and

Leedale, 1969; Paddock, 1968; Pienaar, 1969a,b). The haptophyceae also have smaller scales that are found associated with the haptonema (Manton, 1968; Outka and Williams, 1971). Brown and his co-workers (Brown and Romanovicz, 1976; Brown et al., 1970, 1973) have described an elaborate developmental stage for scale formation in Pleurochrysis sherffelii. From morphological and cytochemical observations, they showed that the formation and secretion of scales can be followed along the maturing Golgi cisternae starting from a pronounced "polymerization center" as a completely intracisternal process, which ends in the exocytotic extrusion of the scales. So the complex role of membranes in the production of cell wall components and the assembly of such products occurs in a precise developmental sequence under genetic control, and infers that there has to be some kind of intracellular mechanism for determining coccolith or scale formation at different stages of the life cycle of the organism.

Physiological and nutritional studies

The correlation between light, photosynthesis, and coccolith formation has been investigated by several workers. Pintner and Provasoli (1968) have shown that coccolithophorids were capable of auxotrophic growth in the light. Crenshaw (1964) showed that light is required for coccolith formation in H. carterae and Coccolithus huxleyi. Although periodic exposure to light seems necessary for coccolith formation, Paasche (1968), Isenberg et al. (1965, 1967), and Blankley (1971) suggested that, under conditions of organic supplementation to the growth medium, H. carterae can grow and form coccoliths in the dark.

Paasche (1963, 1964) illustrated that in short term carbon-14 incorporation experiments, the saturating light intensity was considerably lower than that of photosynthesis. Paasche (1969) also found a similar result with Coccolithus pelagicus. Coccolith formation is independent of photosynthetic carbon assimilation and cell multiplication (Paasche, 1965). Coccolith formation does involve an expenditure of energy. ATP from cyclic photophosphorylation is used directly or indirectly in the accumulation of carbonate by coccolith forming cells (Paasche, 1964). A large supply of ATP in the light might be a prerequisite for a high level of coccolithogenesis. An immediate decline in the rate of coccolith formation in the dark was apparent. As Paasch (1964) found, the rate of coccolith formation in light was seven to ten times that measured when the culture was transferred to dark. It is not clear whether light-stimulated coccolith formation results exclusively from an altered energy supply, or whether some specific light reaction is involved. Paasche (1966a) determined the action spectrum of coccolith formation in Coccolithus huxleyi by measuring the uptake of C^{14} in coccolithogenesis and photosynthesis as a function of light intensity at various wavelengths. The two processes had similar action spectra, with absorption peaks at 440 nm and 670 nm. Blue light appeared to be relatively more efficient in coccolith formation than in carbon assimilation. The results suggest that light-dependent coccolith formation may be catalyzed by two photochemical reactions, one mediated by chloroplast pigments and the other by some pigment absorbing specifically in the blue part of the spectrum.

Although most physiological results reveal a relationship between light and coccolithogenesis, Blankley (1971), using glycerol as a sole energy source, showed that net coccolith production reached higher levels during growth in darkness than in light, presumably because in darkness there was no competition with photosynthesis for carbon. While Blankley (1971) reported that glycerol supported growth and provided a source of energy for calcification and division in Cricosphaera carterae in darkness, Dorigan and Wilbur (1973) reported that glycerol promoted no calcification or division during 7 days in darkness. The difference in findings may be due to cell strain differences or to their use, in the latter case, of shorter periods of observation and decalcified cells. Safa (1977) also showed that a lag period of about one week is required for adaptation to darkness and glycerol. After this period, cells start to divide and coccolithogenesis increases to a normal level.

The temperature, as well as other requirements, affects growth and coccolithogenesis. The optimum temperature for cell division and coccolith formation is in the range of 18 to 22^{o} C (Isenberg et al., 1963a; Paasche, 1966b).

Different investigations have been carried out to determine the effect of chemicals on growth, differentiation, and coccolithogenesis (Blackwelder et al., 1976; Crenshaw, 1964; Isenberg et al., 1963b, 1965, 1966; Paasche, 1964; Williams, 1972, 1974). The role of calcium, strontium, magnesium, and carbonate in the media have been characterized. It seems that the concentration of calcium and carbonate are important

not only in the formation of coccoliths, but also in the maintenance of coccolith structure (Crenshaw, 1964; Paasche, 1964, 1968; Williams, 1972). Using C^{14}, Paasche (1964) found the calcium saturation level for coccolith formation in C. huxleyi to be about 0.24 g/liter (2 x 10^{-3} M). Isenberg et al. (1963a) indicated that calcium concentrations of 10^{-2} M are optimal for growth of Hymenomonas, and coccolithogenesis is initiated at 10^{-5} M. Williams (1972) demonstrated that 10^{-2} M calcium was optimal for growth and coccolithogenesis and that, if the calcium concentration was increased (10^{-1} M) or decreased (10^{-4} M), the coccolith formation rate would be reduced. Blankwelder et al. (1976) showed similar results except that no coccoliths were made at 10^{-4} M calcium. Another evidence of the importance of calcium to coccolith formation comes from the work of Blankenship and Wilbur (1975). They showed that coccolith production was reduced in the presence of cobalt, a calcium transport inhibitor. Mg^{++} and Ba^{++} apparently play no role in coccolithogenesis (Isenberg et al., 1965). Neither Mg^{++} nor Ba^{++} was able to substitute as a growth requirement.

Generally, coccolith formation depends on an adequate supply of inorganic carbon, proper pH, light intensity, and the presence of an organic carbon source (Crenshaw, 1964; Isenberg et al., 1963a, 1965; Paasche, 1964; Williams, 1972, 1974). The effect of pH on coccolithogenesis is probably related to a pH dependent CO_2-carbonate equilibrium system. The optimum pH for coccolith formation in C. huxleyi is between pH 7.5 and 8.5 (Paasche, 1964) and for Cricosphaera elongata is 7.8 (Swift and Taylor, 1966).

The relationship between nutrient nitrogen concentration and coccolith calcification in cultures of Hymenomonas sp. was reported by Baumann et al. (1978). In their view, the degree of coccolith calcification is inversely proportional to the concentration of available nitrogen sources in the medium. These authors believe that this relationship makes possible a useful degree of control over the organism's calcifying activities. Although there is a possibility of shifting the life cycle of Hymenomonas from coccolith-bearing stages to naked, noncoccolith-bearing stages or vice versa by adding or deleting certain amino acids into growth culture (Brown and Romanovicz, 1976; Safa, 1977), we know essentially nothing about the molecular mechanisms of this alteration.

The report of Elder et al. (1971) indicated that Coccolithus huxleyi responded to the chlorinated hydrocarbon, DDT, by reduced calcification of surface scales. Paasche (1964) used several inhibitors of coccolith formation, including the compound 2,4-dinitrophenol (DNP), which acts primarily in uncoupling oxidative phosphorylation, with light-dependent phosphorylation being somewhat less sensitive to DNP. Protein synthesis inhibitors, cyclohexamide and chloramphenicol, and the transport inhibitors, $LaCl_3$, oligomycin, and ethacrynic acid, reversibly inhibit calcium uptake, coccolith formation, and cell wall division in H. carterae, according to Dorigan and Wilbur (1973). Glycerol (0.5 M) partially reversed the inhibitory effect of chloramphenicol on calcification but not on division.

Recently Weiss and Wilbur (1978) investigated the effect of cytochalasin B (CB) on cell division and calcium carbonate extrusion in Cricosphaera carterae. They found that CB at concentration of 100 ug/ml reversibly blocks cell division and caused the formation of abnormal cytoplasmic bodies in the cytoplasm. Coccoliths were not extruded but accumulated within the cell. It seems that CB alters the membranes of Golgi vesicles containing coccoliths in such a way that coccoliths will form but are not extruded through the plasma membrane. They also concluded that dimethylsulfoxide (DMSO) which is the solvent of CB at a proper concentration also inhibits cell division irreversibly.

Cell wall chemistry

Almost all investigations on the chemistry of Hymenomonas cell walls have been carried out on coccoliths and scales. The coccoliths contain calcium carbonate crystals in the form of calcite. These crystals have particular size and shape and well-determined crystallographic orientation (Watabe, 1967). The presence of an extracrystalline organic film has been demonstrated, which encases the calcite crystals (Crenshaw, 1964; Klaveness, 1972). Westbroek et al. (1973) reported the presence of a soluble intracrystalline fraction (SIF) from the coccoliths of C. huxleyi prepared from pronase and a strong alkaline oxidizing agent. Colorimetric tests of SIF prepared via oxidation by 1 M NaOCl in 0.1 N NaOH indicated that this material is a polysaccharide containing about 26% uronic acid, some methylpentose, and no aminosugars. This fraction was further characterized by DeJong et al. (1976). They found that this polysaccharide contained two types of monobasic

acid groups which were identified as uronic acids. Studies with $^{45}Ca^{++}$ using three methods--namely, gel filtration, equilibrium dialysis, and flow rate dialysis--demonstrated that the isolated polysaccharide is capable of binding Ca^{++}. These authors also showed that preferential binding of Ca^{++} occurred in a 100-fold excess of Na^{+} and Mg^{++}. A 100-fold excess of Sr^{++} inhibits Ca^{++} binding to a great extent while no Ca^{++} was bound in the presence of an equilibrium amount of La^{+++}. The Ca^{++}-binding properties of this fraction of coccoliths are in keeping with the hypothesis that this substance should play a role in cellular regulation of calcium carbonate crystallization. The work of Fichtinger-Schipman et al. (1979) established that the isolated acidic polysaccharide of coccoliths of Emiliania huxleyi contains residues of different monosaccharides including the presence of D-galacturonic acid. In addition, they established the presence of sulphate groups in this polysaccharide. Their data shows that galacturonic acid and sulphate in the polysaccharide bind Ca^{++} ions in a ratio of one mole of Ca^{++} per mole of acidic residue. This property supports the proposal of matrix function of the polysaccharide in the formation of coccoliths (DeJong et al., 1976; Fichtinger-Schipman et al., 1979; Westbroek et al., 1973). In view of the putative role of the acid polysaccharide in coccolith synthesis, DeJong et al. (1976) worked out a series of in vivo studies to give a preliminary characterization of a number of metabolic steps leading to coccolith formation. In their experiments, they used calcifying and noncalcifying cells of E. huxleyi. They concluded that, when calcifying cells were grown under light and

in the presence of radioactive calcium, bicarbonate, galactose, and sulfate, most of the calcium label and a small part of the label of the bicarbonate and galactose were incorporated into coccoliths. Radioactive sulfate was also incorporated into coccolith polysaccharide. They also demonstrated that noncalcifying cells fail to take up Ca^{++} and galactose and that these cells produced an acidic polysaccharide, resembling the coccolith-associated polysaccharide which was shed into the growth medium. It was even possible to label this polysaccharide by offering the cells radioactive bicarbonate.

A glycoprotein containing 5% protein with a hydroxyproline-rich peptide and a carbohydrate portion containing glucose, hexuronic acid, methyl pentose, but no amino sugars was isolated from coccoliths of H. carterae (Isenberg and Lavine, 1973; Isenberg et al., 1966). They believed that this glycoprotein contained 25% hydroxyproline and its estimated molecular weight was 40,000-50,000 daltons. Kuratana (1974) detected no hydroxyproline in a corresponding fraction obtained from coccoliths. Also her estimation of the molecular weight of this fraction was 8,000 daltons, based on sedimentation data. The presence of hydroxyproline in Isenberg's report may have been due to contamination from other cell material since cell walls usually contain hydroxyproline rich glycoproteins (Hills et al., 1975; Lamport, 1970, 1974, 1977; Roberts, 1974). Kuratana (1974) concluded that the coccolith is made up of about 50% calcite and 50% organic material, mostly carbohydrate Decalcified coccoliths of Hymenomonas were 12% protein and 70% carbohydrate. Her sugar analysis of isolated coccoliths revealed carbohydrate

monomers including glucose, galactose, mannose, arabinose, and a trace amount of xylose, fucose, and rhamnose. She did not detect uronic acid in her coccolith fraction, probably owing to a hydrolysis procedure which converted uronic acid to sugars such as glucose and galactose.

The chemical nature of scales of coccolithophorids has been investigated by Brown and Romanovicz (1976), Brown et al. (1970, 1973), Herth et al. (1972, 1975), and Romanovicz and Brown (1976) working with Pleurochrysis sherffelii and by Green and Jennings (1967) using Chrysochromulina chiton. The scale of P. scherffelii has been studied more extensively than any of the haptophycean scales. Chemical analysis (Brown et al., 1970) showed that scales were composed of 3-4% protein and more than 90% carbohydrate. The carbohydrate content was galactose and ribose with small amounts of arabinose and glucose. They also isolated the concentric microfibrils of the scales. This fraction was identified as cellulose. There has been the criticism that this fraction of the scale was not cellulose and that cellulose synthesis does not occur in the Golgi apparatus (Preston, 1974). Later investigations (Brown and Romanovicz, 1976; Brown et al., 1973) provided enough information to suggest that the alkali resistant spiral microfibril of the scale is synthesized and assembled in association with the Golgi apparatus. A careful study of the chemical composition of spiral microfibrils was carried out by Herth et al. (1972, 1975). These workers presented the electron and x-ray diffraction data and confirmed the cellulosic nature of concentric microfibrils. However, the absence of unequivocal crystallographic

evidence provided some doubts about the chemical nature of concentrics (Preston, 1974). In the latest report (Romanovicz and Brown, 1976), comparison of infrared absorption spectra, x-ray diffraction patterns, and sizes between cotton cellulose and isolated concentrics of scales confirmed that the concentrics are cellulose. The concentrics of scales are covalently linked with a peptide moiety (Brown et al., 1973). Chemical analysis of the radial and amorphous subcomponents of the scale revealed the presence of glucose, galactose, arabinose, and fucose. The radial microfibrils are thought to be pectin (Romanovicz and Brown, 1976) but no uronic acid was identified probably due to their particular analytical procedure for carbohydrate analysis. Serial extraction of isolated scales by trifluoroacetic acid, correlated with negative staining to find out the degree of extraction, revealed four subcomponents of scales (Romanovicz and Brown, 1976): a spiral microfibril covalently linked with a hydroxyproline rich protein (9%); 91% carbohydrate containing galactose, glucose, and mannose; spiral microfibrils of 37% protein and 63% carbohydrate containing only glucose; radial microfibrils with 7% protein and 93% carbohydrate containing galactose, glucose, and fucose; and an amorphous polysaccharide with 6% protein and 94% carbohydrate (galactose, glucose, and fucose).

The chemical nature of other fractions of the Hymenomonas wall (i.e., columnar material and "glue") are not known. However, Flesch (1977) tentatively identified certain carbohydrate molecules obtained from Hymenomonas cell walls as equivalent to the amorphous "glue". His data was based on cell wall solubilization, SDS-gel electrophoresis,

electron microscopic observations, and aggregation studies. He concluded that the cell wall is held together primarily by ionic interactions of its different molecular fractions.

The Cell Wall System in Relation to Other Algal Systems and Higher Plants

Algae other than coccolithophorids

Most studies on algal cell walls have been carried out on green algae such as Chlamydomonas (Catt, 1979; Catt et al., 1976; Davies and Lyall, 1973; Domozych et al., 1978; Good and Chapman, 1978; Hills, 1973; Hills et al. 1975; Homor and Roberts, 1979; Miller, 1978; Miller et al., 1974; Roberts, 1974, 1979; Roberts and Hills, 1976; Roberts et al., 1972), Scenedesmus and Siderocelis (Crawford and 1978; Homor and Roberts, 1979), and Oocystis (Brown and Montezinos, 1976; Preston, 1974). The red and brown algal polysaccharides have been also studied extensibly (Evans and Callow, 1976; Haug, 1974; McCandless and Craigie, 1978). The carrageenans of red algae are a group of alternative copolymers of various galactopyranose sulfates with molecular weights of several hundred thousand (Elias, 1977), which are the source of agar. Interestingly, monovalent cations like potassium, cesium, rubidium, sodium, and lithium cause the gelation of these molecules, while divalent cations have no effect on gel strength. Methods for isolation of polysaccharides from the red alga have been summarized (Craigie and Leigh, 1978) and excellent reports of their physical and chemical structures are available (Haug, 1974; Turvey, 1978). The alginic acid of brown algae is somewhat similar

to pectin (a polymer rich in α-1,4 linked D-galacturonic acid residues). It contains poly D-mannuramic acid and poly-l-guluronic acid, and exists as a mixed salt with calcium, magnesium, and sodium. Experiments have shown that guluronic acid has a high affinity for calcium and that the calcium ions are selectively bound in long sequences between the poly-guluronate chain in the gel (Haug, 1974). More detailed reviews of algal cell walls can be found in Haug (1974), Preston (1974), Evans and Callow (1976), McCandless and Craigie (1978).

Spectrophotometric titrations and conductivity measurements of Nitella flexilis cell walls have demonstrated that nonexchangeable Ca^{++} cations are present which are probably chelated by COO^{-} anions and donor groups such as OH from polysaccharides or NH from proteins (Wuytack and Gillet, 1978). These authors found that by acidification of the external medium, one can remove a large part of these calcium ions. The number of exchangeable sites available for H^{+} and K^{+} ions rises due to subsequent increase of COO^{-} groups. They concluded that the variation in the concentration of the carboxylic groups is accounted for by the pK of polygalacturonic acids and also by the changes within the constitutive calcium of the cell wall.

A wide range of carbohydrate monomers (glucose, galactose, rhamnose, fucose, mannose, and arabinose) can be found in algal polysaccharides (Haug, 1974; Huizing et al., 1979). Uronic acids and sulfate groups are also present but amino sugars are absent (Haug, 1974; Fichtinger-Schipman et al., 1979; Westbroek et al., 1973). The polysaccharides of the matrix components of algal systems can generally

be extracted with hot water or alkali. These molecules are usually polyanionic; under these conditions, fibrous materials are insoluble and are composed of cellulose, β-1,3-linked xylan or β-1,4-linked mannan with some heteropolymers (Haug, 1974).

Although a number of investigations proved that cellulose biosynthesis in Pleurochrysis takes place in Golgi cisternae, such is not the case in other algal systems and higher plants. Brown and Montezinos (1976), working with Oocystis have shown that cellulose biosynthesis occurs on the outer surface of the plasma membrane. They illustrated the presence of a linear enzyme complex (by freeze fracture techniques) which in their view is responsible for cellulose biosynthesis. They also observed the granules and some associated ridges which function to orient cellulose microfibrils. Terminal complexes or microtubular synthesizing centers which are localized in a zone or zones on freeze-fractured plasma membranes have been described in Glaucocystis which resembles the picture in Oocystis (Willison and Brown, 1978). In Glaucocystis, the plasma membrane is subtended by flattened sacs and terminal shields which become crosslinked to the plasma membrane after completion of cell wall formation. During wall deposition, microtubules lie underneath the shields, and polarized filaments lie between shields and plasma membrane. One of the functions assigned to cortical microtubules of plant cells is control of orientation in which cell wall microfibrils are deposited (Palevitz and Hepler, 1976). This hypothesis has received strong support from studies of colchicine-inhibited wall biosynthesis in Oocystis (Grimm et al., 1976) and in another green

alga, Mangeotia sp. (Marchant and Hines, 1979). In these systems, cellulose microfibrils continue to be synthesized in the presence of drugs which interfere with microtubule polymerization such as cholchicine (Grimm et al., 1976; Marchant and Hines, 1979; Robinson and Quader, 1978) or isopropyl-N-phenyl carbonate (Marchant and Hines, 1979). The microfibrillar orientation after treating cells with these drugs is random and remains that way even when the inhibitor is removed.

The cell wall of Chlamydomonas consists of a multi-layer glycoprotein structure (Hills et al., 1975; Roberts et al., 1972). The wall comprises several species of highly ordered high molecular weight glycoprotein subunits, which form a two dimentional crystalline layer around the cell. The whole wall has been shown to contain a high proportion of the unusual amino acid hydroxyproline (Catt et al., 1976, 1978; Homor and Roberts, 1979; Roberts, 1974, 1979; Roberts et al., 1972). The Chlamydomonas cell wall is an excellent system for the study of self-assembly processes, having the advantage that the entire assembly process can be monitored with the light microscope (Hills, 1973; Hills et al., 1975). These authors have developed a method by which the cell wall of Chlamydomonas may be dissociated into its components, and then reassembled in vitro into a product that is chemically and structurally identical to the original cell wall. Their method involves the use of chaotropic compounds, such as lithium chloride and sodium perchlorate to dissociate the wall into its components, removal of the salt from dissociated walls by dialysis and then bringing together both the salt soluble and salt insoluble fractions of the

wall for reassociation. They also demonstrated that the salt soluble glycoproteins alone can self assemble under various conditions to form fragments that have the same crystalline structure characteristics of the normal outer layer of the cell wall. Further studies by Catt et al. (1976, 1978) indicated that the major glycoprotein isolated from the cell wall contains about 50% protein glycosylated with simple sugars (mainly arabinose, galactose, and mannose). This major glycoprotein on its own is capable of reversible self-assembly into a crystalline lattice, characteristic of the native cell wall (Catt et al., 1978). Roberts (1979) has been able to cleave this main structural glycoprotein into three glycopeptides. These correspond to three distinct domains within the glycoprotein and are characterized by the asymmetric distribution of both sugars and amino acids, especially hydroxyproline. Crystalline periodicities in the range of 0.4-1.2 μm have been found in cell walls of many green alga (Domozych et al., 1978). Chemical analysis of purified cell walls in each of these alga revealed various amounts of protein in each case (Domozych and Cantral, 1978). These authors concluded from SDS gel electrophoresis of the cell walls that each cell type possesses a high molecular weight glycoprotein which separates into five or six bands. They also detected hydroxyproline in ranges from 0.2 to 0.3% of the wall.

Although chitin (a polymer of N-acetyl-D-glucosamine) is a compound found in fungal cell walls and invertebrate exoskeletons, Pearlmutter and Lembi (1976) reported the presence of chitin in the cell wall of the filamentous green alga, Pithophora oedogonia. Their approach for

chitin detection was based on using x-ray diffraction analysis, paper and gas chromatography, and enzymatic treatment by chitinase. They also developed a procedure to detect and localize chitin for light and electron microscopy (Pearlmutter and Lembi, 1978). In their method, chitin was visualized in cell walls after hydrolysis with potassium hydroxide and subsequent postfixation of the deacetylated polysaccharide (chitosin) in OsO_4. They concluded that areas of chitin deposition appeared dark brown by light microscopy. They found most of the chitin in the crosswall disc of the cell wall and small amounts in the outer longitudinal walls.

Higher plants

The structural aspects of higher plant cell walls are not completely known. Albersheim and his co-workers (Albersheim, 1975, 1976; Bateman and Basham, 1976; Bauer et al., 1973; Keegstra et al., 1973, Talmadge et al., 1973) have presented a model to explain the cell wall in general. In their model, the major polysaccharide components of the primary cell walls of dicots, and some features of the interactions of the wall polysaccharides have been described. In this model, many xyloglucan molecules bind to cellulose by H-bonding. A single xyloglucan covalently binds to a single arabinoglucan chain, which in turn is covalently linked to a single ramnoglucan chain, and this single rhamnoglucan is linked covalently to several arabinoglucan molecules, oriented radially to different cellulose microfibrils. These are also linked covalently to a glycoprotein called extensin. Each cellulose fiber also can be connected to several rhamnogalacturonan chains. The structure

goes backward from the extensin to another cellulose fiber. As finally visualized, the model contains many covalent bonds. Recently, Darvill et al. (1978) proposed that arabinan and galactan, two of the wall components, are attached to the rhamnogalacturonan (pectin). They were able to cleave the pectin into four different pectic substances using endopolygalacturonase followed by a chemical analysis of each fraction. The development of a model for primary cell walls has been achieved, in part, by the use of highly purified enzymes capable of selective digestion of the wall polysaccharides. This procedure is more favorable and specific than the use of acidic or basic extraction procedures, which result in the cleavage of a number of different linkages present in cell wall (Albersheim, 1974; Kaji and Sahelsi, 1975; Labavitch et al., 1976; Weinstein and Albersheim, 1979). Another model has been developed by Monro et al. (1976), which proposes fewer covalent bonds. Binding of cellulose to pectins, hemicellulose, and glycoprotein occur via ionic interactions.

Glycoproteins with high levels of hydroxyproline, covalently linked to arabinose or galactose are unique in plant cell walls (Lamport, 1974). Much speculation has been made about their possible function (Brown and Kimmins, 1977; Esquierre-Tugayé and Lamport, 1979; Esquierre-Tugayé et al., 1979; Lamport, 1977). Lamport (1977) also speculated on the shape of these molecules and the distribution of hydroxyproline within them.

The mechanism of assembly of cellulose microfibrils by higher plants involves some controversy. Two hypotheses which have been

developed mostly from the study of lower plants (algal cell wall) and bacteria (Acetabacter xylinum) describe microfibrillar formation (Brown and Montezinos, 1976; Brown et al., 1976; Willison and Brown, 1977). As previously mentioned, the first hypothesis postulated the presence of particular complexes within the cell membrane. These particles may represent enzyme complexes which by their activity control the synthesis of cellulose microfibrils. This hypothesis seems reasonably suitable for some of the algal cell walls. In contrast, freeze-etching techniques applied to cell walls of higher plants provided unconvincing evidence of terminal complexes attached to microfibrils (Muller et al., 1976; Willison and Brown, 1977). The second hypothesis postulates that hydrated polyglucan chains which are released from the cell associate to form a nascent fibril which is external to the cell but associated with the cell membrane (Colvin and Leppard, 1976). The intermediate of this process (hydrated polyglucans) has been partially characterized (Colvin et al., 1977).

Cell wall regeneration by isolated protoplasts offers an excellent experimental approach to the study of wall formation. Recently, Burgess and Linstead (1976, 1977, 1979) and Burgess et al. (1978) have reported scanning electron microscope observations of the surface of tobacco protoplasts. They reported short "fibers" appearing from randomly spaced centers which were discontinuously distributed over the protoplast surface. These fibers were sometimes associated with projections from the isolated protoplast surface which they think might correspond to granular centers involved in microfibrillar

biosynthesis. These results appear to be different from observations of similar material using freeze-etching techniques (Grout, 1975; Willison and Cocking, 1975; Willison and Grout, 1978). In their observations, short microfibrils were rarely found, and microfibril deposition did not occur in discontinuous zones nor were there distinctive structures associated with the terminal portion of the microfibrils. They, therefore, concluded that microfibril deposition does not occur in discontinuous zones on the surface of tobacco and tomato protoplasts. Willison and Grout (1978) also demonstrated the presence of globules associated with microfibril termini, a finding which supports the first hypothesis of cellulose biosynthesis mentioned above.

The synthesis of cell wall polysaccharides probably involves nucleotide diphosphates or similar intermediates as glycosyl donors (Karr, 1976). Such intermediates could function as specific primers or acceptors for the formation of polysaccharide. Lipid carriers or intermediates like dolicol phosphates have similar potential (Waechter and Lennarz, 1976), although such carriers have not been isolated from higher plants. The presence of lipid carriers in bacterial systems (Baddiley, 1975) suggests that eukaryotic cells may utilize a similar mechanism.

Ultrastructural and biochemical studies have shown that the Golgi apparatus is often involved in the biosynthesis of cell wall polysaccharides (Pickett-Heaps, 1966, 1967, 1968a, 1968b; Robinson and Ray, 1973). Autoradiographic and cytochemical methods (Pickett-Heaps, 1966, 1967, 1968a, 1968b; Vina and Roland, 1972) lead to the conclusion that certain Golgi vesicles undergo a maturation and finally become integrated in the cell plate or they secrete their contents by exocytosis.

It seems that this maturation involves a beginning of polymerization of the polysaccharide precursors in the vesicles (Pickett-Heaps, 1968b). This is accompanied by changes of their membranes in a direction which makes them more like the plasmalemma (Vina and Roland, 1972). Robinson and Ray (1973) reported that polysaccharides formed in the Golgi fraction have a composition similar to the pectin and hemicellulose fraction of the wall but containing no cellulose.

Recently, there has been particular interest in inhibition of cell wall formation in higher plants. Hara et al. (1973) found that coumarin (1,2-benzopyrone) inhibits the biosynthesis of cell wall formation in higher plants and prevents the formation of microfibrils on the surface of regenerating tobacco leaf protoplasts (Burgess and Linstead, 1977). Another inhibitor of cell wall formation is 2,6-dichlorobenzonitrite. This drug also is an inhibitor of cellulose synthesis (Hogetsu et al., 1974). The precise mechanism of the inhibition is not clear.

MATERIALS AND METHODS

Culture Methods and Standard Conditions

Hymenomonas carterae, Plymouth Culture Collection No. 181 obtained originally from Dr. L. Provasoli (Haskins Laboratory, New York, N.Y.), was maintained on a standard medium (PMW II), modified from that of Isenberg et al. (1963a) by Outka and Williams (1971, see also Appendix A). The cells were grown in sterilized 500 ml stainless steel-capped Delong flasks containing 100 ml of PMW II at pH 7.7-7.9. Cultures were kept at 17-19 C in a Precision Scientific controlled-temperature incubator with a light intensity of about 4450 Lux from 14-Watt cool-white fluorescent tubes delivering repeating photocylces of 16 hours light and 8 hours dark. Inocula usually resulted in an initial concentration of 5×10^3 to 6×10^4 organisms/ml. Inocula were maintained on a 48-hour transfer schedule (culture in exponential growth) and harvested for experimental studies at concentrations of $1\text{-}3 \times 10^5$ cells/ml. The standard initial concentration, approximately 10^4 cells/ml, was experimentally determined to result in the best combination of minimal length of lag phase and maximal number of generations in the culture. Growth determination (i.e., increase in cell number per unit volume of the culture medium) for experiments were carried out in triplicate using direct cell counts with a haemocytometer. For phase-change determination of cultures and life cycle studies, agar plates were prepared using 1% Ion agar #2 (IA-2), made up in PMW II. Plates were wrapped with parafilm to prevent evaporation of water from the agar surface. (For isolation and maintaining of different stages of

the life cycle, i.e., coccolith-bearing and noncoccolith-bearing cells, see Safa, 1977.)

Sufficient yields were required for cell fractionation and wall isolation. For this purpose, cells were grown in five-gallon carboys containing 15 liters of PMW II. Carboys were sterilized in an autoclave at a pressure of 15 PSI and at a temperature of 121 C for an hour. These large batch cultures were kept at 18-20 C with an incident light intensity of 2800-5500 Lux from the bottom to the top of the carboy. This light intensity was obtained from 8 ITTF-40 CW (cool-white) fluorescent tubes delivering repeating photo-cycles of 16 hours light and 8 hours dark. The method of forced-air carboy assembly was as described by Flesch (1977).

Microscopic Procedures

Light microscopic observations of experimental and control cells were carried out with a Zeiss photomicroscope. Cells were mostly examined in the Nomarski differential-interference-contrast mode. Original photographs were taken using Kodak Plus X film or Kodak High Contrast Copy film (HC 135-36) with or without using electronic flash. Numbers of coccoliths per cell and percentage of cells with flagella were counted using Nomarski differential interference contrast optics. Coccoliths were counted at a magnification of about 1250 diameters with a "plan" oil immersion objective stopped down to a numerical aperture of about 0.8. Accurate counts of surface coccoliths per cell could be made by counting them in different focal planes, focusing through cells carrying about 40-50 coccoliths. Reasonable approximations

(± 10 coccoliths/"average cell") could be made on cells carrying between 50 to 80 coccoliths. The number of cells counted to obtain coccolith number per cell in each population was 50.

For electron microscopic observations, samples were harvested at a concentration of 5×10^5 cells/ml. Cells were fixed in 4% glutaraldehyde, 0.1 M caccodylate buffer, 0.01 M CaCl, and 0.25 M sucrose, pH 7.4-7.6 for 5-7 hours at 4 C. They were then washed three times (10 minutes each) in cold cacodylate buffered wash solution containing 0.01 M $CaCl_2$ and 0.25 M sucrose. These cells were postfixed with 1% OsO_4 in 0.1 M cacodylate + 0.01 M $CaCl_2$ + 0.25 M sucrose, pH 7.4-7.8 for 10-12 hours at 4 C. After washing the cell three times (10 minutes each) in cacodylate-buffered wash solution containing 0.01 M $CaCl_2$ and 0.25 M sucrose, samples were decalcified for 30 minutes using 0.02 M uranyl acetate in 30% (v/v) ethanol (Williams, 1972). After dehydration through an acetone series (35%-100%), 10 minutes each, cells were treated with 3:1 acetone/ERL plastic (1 hour), 3:1 ERL/acetone (4 hours), and 100% ERL (Spurr low-viscosity embedding media; Spurr, 1969) for 16 hours using a roller apparatus inside a hood. Cells contained within as little plastic as possible were placed under vacuum for 30 minutes. Capsules were filled with fresh plastic and placed in a 60 C oven for 48 hours to polymerize.

Sections were cut with a DuPont diamond knife on a Reichert Om-U_2 ultramicrotome and floated on distilled water. The sections were picked up on parlodian-carbon coated grids and stained with 1% (w/v) uranyl acetate in 50% ethanol for 12 minutes and then aqueous lead citrate

according to Reynolds (1963) for 20 minutes. Sections were observed with a Hitachi HU-11E-1 electron microscope.

Negatively stained preparations were made on 200-mesh copper grids coated with 1% nitrocellulose in amyl acetate (Ernest F. Fullam, Inc., P.O. Box 444, Schenectady, N.Y. 12301) and then coated with evaporated carbon film. The stains used were 1% aqueous ammonium molybdate, 1% uranyl acetate in 50% alcohol or 5% sodium tangstate adjusted to pH 6.8 with formic acid.

For scanning electron microscopic preparations, cells were fixed according to the above procedure but for a shorter length of time (2 hours glutaraldehyde and 2 hours OsO_4). Then specimens were dehydrated through an alcohol series (35%-100%), 10 minutes each, followed by two changes of absolute alcohol; after dehydration, samples were critical-point-dried by gradual replacement of the alcohol with freon TF, exchanging freon TF with CO_2, and drying at the critical point of 72 atmospheres and 36.5 C. Dry samples were dispersed on the sticky surface of pieces of silver tape which were placed on brass discs that contained a moist overcoat of silver conducting paint. Discs were placed in a Varian VE-30M vacuum evaporator for a coating of carbon and gold during rotation. The specimens were observed with a JSM-35 scanning electron microscope.

Cell Wall Preparation and Coccolith Isolation

The standard procedure for cell wall preparation was based on utilization of cells from five gallon carboys. The cells were harvested at a cell density of 1-2 x 10^6 cells per ml. At this time, cultures are

usually 2 weeks old. The cultures were passed through a continuous flow rotor on a Sharples Super centrifuge (The Sharples Corporation, Philadelphia, Pa.). Cells were collected at a centrifuge speed of 22,000 rpm (14,000 g) at 4 C. Cells were used immediately or frozen at liquid nitrogen temperatures and stored at -20 C.

To isolate cell walls from the whole cell, different methods of disruption of the cell and purification were tried. These methods included various homogenization procedures, osmotic shock using high salt concentrations followed by distilled water treatment, and utilization of a detergent (Triton X-100). The most impressive method was a treatment involving Triton X-100. This detergent has been used to solubilize membrane lipoprotein (Vernon and Shaw, 1969) and it is considered to be a nonionic detergent. Solubilization of membranes with detergents may lead to the recovery of protein complexes in which native interactions may be maintained (Makino et al., 1973).

For isolation of cell walls, 1.5-2 g (wet weight) of cells were resuspended in 3X PMW II for 1 hour and centrifuged at 1000 g; the pellet was resuspended in 1/8 X PMW II or 37.5 mM Tris-maleate buffer, pH 7.5-7.8, and this wash cycle was repeated three times. Cells with weakened cell walls were then suspended in a solution containing 5% Triton X-100, 1.0 M KCl, and PMW II salts (20 g/liter NaCl, 0.6 g/liter KCl, 2.465 g/liter $MgSO_4 \cdot 7H_2O$, 1.11 g/liter $CaCl_2$, 0.5 g/liter $NaNO_3$, and 1×10^{-4} g/liter Na_2CO_3) for 12-15 hours with continuous shaking on a mechanical shaker. The solution was frequently changed. Green pigment, cell organelles, and membranes were removed by centrifugation.

A Nomarski differential interference contrast microscope was used to monitor the purity of the cell walls in different steps of this procedure. To remove the detergent completely, cell walls were washed for 8-10 times with PMW II or Tris maleate, pH 7.5-7.8. Distilled water was not used as a wash solution due to its solubilization effect on the calcareous rim of coccolith (DeJong et al., 1976; Isenberg et al., 1966; Kuratana, 1974). Cell walls prepared according to this procedure were used for ultrastructural observations, biochemical investigations, and cytochemical studies.

Free floating coccoliths were obtained from cultures (usually at exponential phase of growth) by differential centrifugation. Cells were removed from 500 ml of culture medium by centrifugation at about 1000 g for 5 minutes. Coccoliths were then centrifuged from the supernatant at 15,000 g for 20-30 minutes, resuspended and washed three times with PMW II.

Cell Wall Chemistry

Cell wall dissociation

Chaotropic solubilization Chaotropic agents such as LiCl and sodium perchlorate ($NaClO_4$-H_2O) have been used for the dissolution of membranes and enzyme complexes and the isolation of membrane-bound proteins (Hatefi and Hanstein, 1974). These agents also have been used for cell wall dissociation in Chlamydomonas (Hills, 1973; Hills et al., 1975) and were tested on H. carterae. The ultrastructural effect of 10 M LiCl on live cells was investigated. Mid-log phase cells

were centrifuged from their growth medium during the light period and were exposed to 10 M LiCl which was buffered in 37.5 mM Tris maleate at pH 7.5 for 2-4 hours. After washing the cells with PMW II three times, they were used for SEM or TEM preparations.

Isolated cell walls were treated with different concentrations of LiCl (2, 4, 6, 8, and 10 M) which were buffered in 37.5 mM Tris maleate at pH 7.5. A suspension from a 0.5-1.5 g wet pellet was made in 5-10 ml of 10 M LiCl for 48 hours at room temperature. After centrifugation at 15,000 g for 20-30 minutes, the supernatant or LiCl soluble fraction (LSF) was collected, dialyzed against 10 mM EDTA, pH 7.5, for 5-6 hours at room temperature. The dialysis bag was transferred to dH_2O, with several changes for 10-15 hours. This supernatant in 0.15 M NaCl was used for SDS gel electrophoresis, analytical ultracentrifugation, and TEM observations. To further characterize the solubilization effect of different concentrations of LiCl on the cell wall, isolated walls were oven dried at 40 C under vacuum. A suspension from 10 mg of dry cell walls was made in 5 ml of different concentrations of LiCl (i.e., 2, 4, 6, 8, and 10 M). The supernatant from each sample was collected by centrifugation (15,000 g for 15 minutes), then dialyzed against distilled water for 5-6 hours, and concentrated by the simple process of hanging the dialysis bag in front of a fan. Finally the carbohydrate and protein concentrations of each sample were determined (see the procedure for protein and carbohydrate assay). The pellet or LiCl insoluble fraction of the cell wall (LISF), after 10 M LiCl solubilization, was collected for TEM and SEM observations. LISF was dialyzed

against distilled water for 5-6 hours to remove the LiCl. Then for TEM preparations, samples of LISF were either processed for thin section observations or one drop of suspension was placed on 200 mesh, collodion coated, copper grids and negatively or positively stained with 1% uranyl acetate. SEM preparations were carried out according to procedures previously described.

EDTA solubilization

Selective solubilization of live cells and isolated cell walls were performed with EDTA. Mid-log phase cells were collected by centrifugation at 250 g and were treated with 10 mM EDTA adjusted to pH 7-7.5 for 2 hours. The cells were washed 3 times with PMW II and then were used for TEM and SEM preparations.

The effect of different concentrations of EDTA on isolated walls was determined by using 10 mg dry wall (walls were oven dried in a vacuum desiccator at 40 C) in each experiment, treating different samples with 1, 5, 10, 25, 50, and 100 mM EDTA at pH 7-7.5 for 48 hours, then dialyzing against distilled water for 5-6 hours, and concentrating the samples through evaporation while in the dialysis bag. Then, carbohydrate and protein concentrations released per ml due to the treatment were determined.

Preparation of the EDTA soluble fraction of the wall (ESF) for electron microscopic observations, and biochemical analysis was carried out as follows. A suspension from 1-1.5 g wet weight of isolated cell walls was made in 5-10 ml of 10 mM EDTA, pH 7.5 for 48 hours. Insoluble residues were removed by centrifugation at 15,000 g for 20 minutes

and the supernatant was dialyzed against distilled water overnight with frequent changes. The preparation was concentrated while in the sterile dialysis bag by forced air (from a fan) evaporation. Dialysis was done in "Spectropor" membrane tubing No. 3 with a cylindrical diameter of 11.5 mm and a molecular weight cut-off of approximately 3500 (Spectrum Medical Industries, Inc.).

The EDTA insoluble fraction of the cell wall (EISF) obtained after solubilization was washed with PMW II and used for TEM observations. These samples were either negatively stained or were processed for thin section observations.

Reassociation

The EDTA soluble fraction of the cell wall (ESF) in 1-5 ml amounts was dialyzed against double distilled water (d_2H_2O) at room temperature overnight. The supernatant was filtered through a 0.22 um millipore filter and the filtrate was collected. The effect of monovalent and divalent ions on reassociation was tested on the filtrate. The filtrate was then dialyzed against 100 ml of 0.01 M $CaCl_2$, 0.3 M $CaCl_2$, 0.3 M $CaSO_4$, 0.3 M $MgSO_4$, 0.3 M $MgCl_2$, 0.15 M NaCl or 0.15 M KCl, pH 7.5 at room temperature for 2-4 hours. The reassociation was monitored by Nomarski differential interference optics and TEM.

Biochemical Analysis of the Cell Wall Soluble Fractions (LiCl-soluble Components and EDTA-soluble Materials)

Protein and carbohydrate analysis

Protein determinations were carried out according to Lowry et al. (1951). Bovine serum albumin fraction (Miles Laboratories, Inc.,

Kankakee, Ill.) was used as a standard. Total carbohydrate was estimated with the phenol sulfuric method (Hodge and Hofreiter, 1962), with D-glucose (Mallinckrodt Chemical Works, St. Louis, Mo.) as a standard. Uronic acid was assayed with the carbazole test according to Dische (1947), with glucuronic acid as a standard.

Ultracentrifugation

For ultracentrifugation, a Spinco Model E analytical ultracentrifuge (Beckman Instruments, Inc.) with a Spinco An-D rotor and a single sector cell was used. Ultracentrifugation was carried out at a rotor speed of 60,000 rpm and a temperature of 20-21 C. Schlieren patterns were recorded on photographic plates. Pictures were taken at 16-minute intervals. Sedimentation coefficients were determined by using a Nikon Model 6C micro-comparator and measuring the schlieren patterns on each plate.

Gel Electrophoresis

Samples already in solution, isolated cell walls, and insoluble substances of the wall were treated with 2% SDS in 0.15 M NaCl and heated in boiling water for 2 minutes. For a comparison of the effect of heat, soluble fractions were heated for 2, 4, and 6 minutes. After boiling, the tubes containing isolated walls or insoluble substances of the wall were centrifuged at 15,000 g and room temperature for 10 minutes to sediment any small amount of insoluble material.

SDS-polyacrylamide gel electrophoresis was performed essentially according to the procedure of Weber and Osborn (1969). The 7.5%

polyacrylamide gels were made routinely and were 5 x 80 mm. The amount of component submitted to electrophoresis was 50-100 µl (about 40 µg) of sample, and 50-100 µl of tracking dye (2 ml β-mecaptoethanol, 0.45 ml of 0.05% Bromphenol blue, 1.25 ml of 8 M urea and glycerol and 2.46 ml of 1% SDS in 1 M Tris acetate buffer). The electrophoresis was done in 0.1 M sodium phosphate buffer containing 0.1% SDS, pH 7.0 and at 2.5 mA/gel with the positive electrode in the lower chamber. It took about 8-10 hours for the tracking dye to move to 1 cm from the bottom of the gel.

For comparison of proteins and carbohydrates, samples were run in duplicate. For proteins, gels were stained with Coomassie blue (0.3 g Coomassie Brilliant Blue R, Sigma Chemical Company, St. Louis, Mo.; 150 ml methanol, 129 ml H_2O, and 21 ml glacial acetic acid) for 6-8 hours. Gels were destained electrophoretically in two destaining solutions. First they were destained overnight in a 50% methanol, 9.2% glacial acetic acid solution and then transferred to 7% acetic acid, 5% methanol. Gels were also stored in the latter solution.

Carbohydrate staining was performed using the periodic acid-Schiff (PAS) method of Zacharius et al. (1969). Each gel was immersed in 12.5% trichloracetic acid (25-50 ml/gel) for 30 minutes, rinsed lightly with distilled water for 0.25 minute, immersed in 1% periodic acid (made up in 3% acetic acid) for 50 minutes, washed for 2 days in 200 ml distilled water/gel with frequent changes until it was completely clear, immersed in Schiff reagent in the dark for 50 minutes, washed three times with freshly prepared 0.5% (w/v) metabisulfite for 10 minutes

each (25-50 ml/gel), washed again in distilled water with frequent changes and agitation until excess stain was removed (2-3 days), and finally it was stored in 7.5% acetic acid at room temperature. The Schiff reagent was made up according to McGuckin and McKenzie (1958). For preparing the reagent, 2 liters distilled water, 16 g sodium metabisulfite, and 21 ml concentrated hydrochloric acid were used. When solution was attained, 8 g of basic fuchsin was added and the solution was stirred gently with a mechanical stirrer for 2 hours at room temperature, and then decolorized with charcoal, filtered through glass wool until clear and colorless and stored in a brown bottle at 4 C.

To obtain further information about the nature of the EDTA-soluble fraction of the cell wall (ESF), polyacrylamide gel electrophoresis in the absence of SDS was carried out. The procedure was basically the same as SDS gel electrophoresis. Sodium phosphate buffer was used (0.01 M, pH 7.0) along with a tracking dye (0.45 ml of 0.05% (w/v) Bromphenol blue, 1.25 ml glycerol, and 2.5 ml dH_2O). In this technique, molecules migrate along the gel according to their net charges. Gels were stained for proteins with Coomassie blue as described before and for carbohydrates with 0.5% alcian blue (Eastman Kodak Co., Rochester, N.Y. 14650) in 3% acetic acid. Destaining was done overnight in 7% acetic acid and the gels were stored in the same solution.

Isolation of Acidic Polysaccharides from Gels

On each of 24 gels and in different runs, about 80 µg ESF was applied. Electrophoresis was performed until the tracking dye

traversed about 70% of the length of the gels. Gels were stored in 0.1 M sodium phosphate buffer pH 7.0 at 4 C. One gel was stained with 0.5% alcian blue as described before. To localize the polysaccharide bands, the corresponding volumes of the other gels were cut out. The gel material corresponding to each carbohydrate band was frozen until sufficient amounts of material were obtained. The gel material obtained from the individual carbohydrate bands was suspended in a small amount of 0.01 M sodium phosphate buffer pH 7.0 and was homogenized with a Servall Omni Mixer (Ivan Sorvall, Inc., Norwalk, Conn.) attached to an Adjust-A-volt (Standard Elect. Product Co., Dayton, Oh.) for variable speed adjustments. Each gel homogenized was centrifuged at 15,000 g for 30 minutes. The supernatant was collected and a second elution was performed on the pellet. The combined eluent of each sample was filtered through a 0.22 um millipore filter to remove the gel residues. The filtrates were collected, dialyzed against distilled water overnight with frequent changes to remove the residual salts, and lyophylized in round flasks. These samples were dissolved in 0.15 M NaCl and were used to determine their purity and also their electrophoretic and ultracentrifugal behavior. The same samples were used for transmission electron microscopic observations.

Gel Filtration

The cell wall preparations were solubilized in 10 mM EDTA, pH 7.5 (ESF). The supernatant was collected after 20 minutes centrifugation at 15,000 g, then dialyzed against distilled water overnight, concentrated in the dialysis bag, and applied at concentrations of 1-2 mg/ml

on Biogel P10, Biogel P60, and Biogel P100. Columns were eluted with 0.15 M NaCl or distilled water and fractions of 1 ml were collected. From each fraction, 0.5 ml samples were assayed for carbohydrates with the phenol sulfuric test (Hodge and Hofreiter, 1962). The remaining 0.5 ml portions were concentrated and used for gel electrophoresis and analytical ultracentrifugation studies.

Uronic Acid Assay from Pectinase-treated Walls

Isolated cell walls were oven dried in a vacuum inside a desiccator at 40 C. Different concentrations (5 mg/ml-40 mg/ml) of pectinase (Sigma Chemical Company, P.O. Box 14508, St. Louis, Mo. 63178) were prepared. These enzyme samples were incubated for 30 minutes at 30 C, pH 4.5, and were filtered through 0.45 μm Millipore membrane filter. The filtrate was frozen in 2 ml vials. Dry cell walls (10 mg) were incubated in 2 ml of 5 mg/ml, 10 mg/ml, 15 mg/ml, 20 mg/ml, 25 mg/ml, 30 mg/ml, 35 mg/ml, and 40 mg/ml pectinase pH 4.5 for 48 hours. Samples were centrifuged at 15,000 g for 10 minutes, supernatants were collected, and the amount of uronic acid released from 10 mg cell walls at different concentrations of pectinase was assayed with the carbazol test (Dische, 1947). Since the uronic acid test on pectinase was also positive (i.e., pectinase contains some impurities including uronic acid), samples from different concentrations of pectinase were also assayed and the absorbance of each sample was subtracted from the absorbance of the corresponding extracts obtained from cell wall treatment. The effect of 40 mg/ml pectinase on 10 mg dry wall at different periods of treatment was also determined. Pectinase at

a concentration of 40 mg/ml pH 4.5 was used for 5, 10, 20, 30, 40, 50, 60, 70, 80, and 90 hours, and the concentrations of uronic acid released during these periods were determined according to the above procedure. After pectinase treatment, the insoluble fraction of the cell wall was collected, washed with PMW II (2 times), and used for TEM observations.

Cytochemical Localization of Acidic Polysaccharides and Ionic Interactions of the Wall Components

Ruthenium red

This has been used as a standard stain for pectins in plant tissues for light microscopy. For electron microscopy, it was introduced probably by Reimann (1961). To demonstrate the staining effect of ruthenium red on Hymenomonas, mid-log-phase cells on 16 hours of light and 8 hours of dark were harvested, fixed in 4% glutaraldehyde, 0.1 M cacodylate buffer, and 0.2 M sucrose pH 7.8-7.9. Chloride-free cacodylate buffer is considered the most ideal buffer for the maximum contrast in this method (Hayat, 1975). Cells were postfixed in a filtered, saturated solution of ruthenium red in 0.1 M cacodylate buffer containing 1% osmium tetroxide and 0.2 M sucrose. The rest of the procedure was the same as previously described. Sections were observed directly or poststained with 1% uranyl acetate in 50% ethanol and aqueous lead citrate (Reynolds, 1963).

Cationized ferritin

In the first experiments, cationized ferritin (Miles Laboratories, Inc., Elkhart, Ind.) was diluted to a final concentration of 0.5 mg/ml

with PMW II. This working dilution was added to a 10% cell suspension (i.e., 0.1 ml of pellet was resuspended in 1 ml of 0.5 mg/ml cationized ferritin in PMW II) for 30 minutes at room temperature, and after washing the cells three times in PMW II, they were processed for electron microscopic visualization. The second sample was first fixed with 4% glutaraldehyde in 0.1 M cacodylate buffer pH 7.5 for 2 hours (two changes). After washing the cells three times in washing buffer, they were treated with 0.5 mg/ml cationized ferritin (added to 10% cell suspension) for 30 minutes at 4 C. Cells were washed three times in washing buffer and then were processed for electron microscopic observations.

Protoplast Isolation and Cell Wall Regeneration

Enzyme incubation and protoplast isolation

Mid-log phase cells were collected by centrifugation (500-1000 x g) and were resuspended in enzymes. Macerozyme R-10 and "Onozuka" cellulase R-10 (Kinki Yakult Mfg., Co., Ltd., 8-21 Shingikan-Cho, Nishinomiya, Japan) were used individually, as a sequential two-step enzyme treatment, or as a mixed one-step treatment. Enzymes were dissolved in 0.6 M mannitol, the solutions were centrifuged (15,000 x g) to remove the insoluble fraction and then sterilized by filtering through a 0.45 μm Millipore membrane filter.

For individual enzyme procedures, sterile cells were either treated with a filtered-sterilized solution containing 0.6 M mannitol and 3% macerozyme pH 4.5 or with a solution of 0.6 M mannitol, 5% cellulase,

and 8 mM $CaCl_2$ pH 5.2 for 2-3 hours. In the mixed one-step enzyme procedure, cells were incubated for 4-5 hours at 25-26 C in a solution of 3% macerozyme and 5% cellulase in 0.6 M mannitol pH 5.2. This procedure was carried out either in the presence or in the absence of 8 mM $CaCl_2$. For the sequential, two-step enzyme procedure, sterile cells were preincubated in a solution of 0.6 M mannitol and 3% macerozyme pH 4.5 for 2 hours (cells were incubated on a reciprocal shaker at 60 cycles per minute and 25-26 C). The sample was centrifuged (500 x g), cells were collected, and washed 2 times with 0.75 M mannitol. These cells were then incubated in a solution containing 0.6 M mannitol, 8 mM $CaCl_2$, and 5% cellulase pH 5.2 for 4-5 hours. Protoplasts were washed once with 0.75 M mannitol and then two times with PMW II. Different stages in the protoplast isolation procedure were monitored by Nomarski differential interference contrast light microscopy, an optical method in which it is possible to identify the naked protoplasts. For further confidence, these protoplasts were also stained with 0.1% calcofluor white M_2R as a stain for cellulose (Nagata and Takebe, 1970). Protoplasts were also prepared for SEM and TEM preparations.

Growth study

Protoplasts at a concentration of 7×10^3 cells/ml were kept under standard conditions and growth determination in triplicate were completed using direct cell counts on an A. O. Spencer haemocytometer chamber.

Kinetics of cell wall formation

Coccolithogenesis after protoplast isolation Protoplasts (7×10^3 cells/ml) were transferred to PMW II and kept under standard conditions (17-19 C in the light at an intensity of 4450 Lux in 16 x 25 mm screw-cap tubes). Samples were removed at specific times, and the number of coccoliths per cell was counted for 50 cells, using Nomarski differential interference contrast (Williams, 1972, 1974).

Samples of protoplasts at various stages of recovery were processed for observation with the transmission and scanning electron microscopes.

Chemical inhibition of cell wall formation by coumarin and 2,6-dichlorobenzonitrile (DBN) and release from inhibition

For the inhibitor studies, protoplasts were isolated and transferred to different concentrations of filter sterilized coumarin (10-500 mg/liter) dissolved in PMW II or 2,6 dichlorobenzonitrile (DBN, 0.1-40 mg/liter) in PMW II. The effects of different concentrations of coumarin and DBN on protoplasts were monitored by Nomarski light microscopy and TEM. Samples for electron microscopic observations were prepared from 48-hour or one-week inhibited protoplasts.

For recovery studies, $7\text{-}8 \times 10^3$ protoplasts/ml from the most effective concentration of inhibitors were transferred to PMW II under standard conditions. The growth of protoplasts was determined using direct counts on a haemocytometer. Cell wall regeneration was also monitored by Nomarski light microscopy and TEM.

RESULTS

The Structure of the Cell Wall as Correlated with Different Stages of the Life Cycle

Hymenomonas carterae presents a complex life cycle with different morphological stages (Safa, 1977). Ultrastructural aspects of the two major stages are presented here. Under standard conditions, cells divide once a day (0.85-1 division/day), with the division peak occurring at the end of the dark period (16 hours light, 8 hours dark). At low population densities (2-5 x 10^5 cells/ml) and a 48-hour transfer (subculture) schedule, no phase change is observed. However, about the fifth day of cultures initiated at a population of 2-5 x 10^5 cells/ml, cells start to clump, the synchrony is lost and in addition to motile cells which are 10-14 μm in diameter and are covered with coccoliths, there are present some single cells and clumps of cells which are nonmotile, have no coccoliths and are 14-18 μm in diameter. Further analysis of samples were done by plating cells onto agar surfaces. After several days, two kinds of colonies were observed, smooth and rough. Light microscopic examinations showed that smooth colonies have coccoliths on the surface. The cells in smooth colonies are close together and seem to share a common transparent fluid or gel. Rough colonies appear surrounded by a sac of higher density. In smooth colonies, coccoliths are visible only at the outer edges of the colony. Rough colonies grow as clumps and have no coccoliths on the surface.

Scanning electron microscopic observation of noncoccolith-bearing cells (Figure 1) confirms that at this stage cells are in a sort of colony in a common matrix. They are essentially naked with a "lumpy"

Figure 1. Scanning electron micrograph of noncoccolith-bearing stage of the life cycle of H. carterae. Cells in this stage are nonmotile in a sort of colony in a common matrix. X 4,900

Figure 2. Transmission electron micrograph of the wall in noncoccolith-bearing (or naked) stage of the life cycle. Section was double stained with uranyl acetate and lead citrate. At this stage, the wall is composed of several layers of cellulosic scales and no coccoliths on the surface. Note the presence of electron dense material on cross-sections of scale networks (arrows). Also note the presence of amorphous electron dense material connecting scales together (arrowheads). X 56,400


1


2

appearance which we assume represents the layers of scales. Also the micrograph shows the presence of some material adhering to the cell surface. A section through the wall of a noncoccolith-bearing cell (Figure 2) revealed different layers of scales connected together by an amorphous electron dense material. This micrograph shows the scale network and especially the presence of very small electron dense dots arranged in a regular fashion along the radial microfibrils. A scanning electron micrograph of coccolith-bearing cells (Figure 3) shows that the cell surface is covered with 75-100 coccoliths. The coccolith is the largest component of the cell wall of H. carterae; it is an external oval disc about 1.5 μm by 1.0 μm by 0.3 μm (Figure 5), consisting of a base (Figure 6) which includes cellulosic microfibrils and a rim composed of about 32 rim elements. These last are calcite microcrystals which are formed inside of a special "matrix." Another most interesting structure associated with coccoliths is the stranded fibrous material which is contiguous over the top of the coccolith and has been given the general name of coccolithonet (Figure 5). Coccolithonets measure 0.045-0.05 μm in diameter and appear to originate from inside of the wall (Figure 5). Their function is probably to maintain coccoliths on the surface of the cell.

Figure 4 is a survey transmission electron micrograph showing the cell wall and internal morphology of H. carterae. Outside of the cell or plasma membrane, coccoliths and scales are visible. Inside of the plasma membrane, chloroplasts surround the nucleus and two vacuoles are visible. A cross section through a cell (Figure 6) illustrates several components of the wall, namely, fibrous strands (columnar material)

Figure 3. SEM micrograph of the coccolith-bearing stage of the life cycle. Many coccoliths are visible on the surface of these cells. X 3,520

Figure 4. A survey transmission electron micrograph of H. carterae. The following structures are visible: chloroplast (Ch), nucleus (N), coccolith (C), scale (S), and pyrenoid (P). X 15,000


C
Ch
S
P
4

Figure 5. High magnification SEM micrograph of the external surface of H. carterae. A major part of the cell wall is coccoliths; each is an external disc of about 1.5 μm by 1 μm. The coccolith consists of a base and a rim with 32 radially arranged elements. The latter are calcite microcrystals which often appear to be fused, giving the disc-like shape observed on the surface. Note the strands of fibrous material over the top of the coccolith (coccolithonets). It seems that these strands originate from inside of the wall (arrows). X 45,000

Figure 6. TEM micrograph of coccolith-bearing stage. The wall in this stage consists of coccoliths (C), scales (S), and columnar material (CM). Mitochondria (M) and chloroplast (Ch) are also present. X 139,000

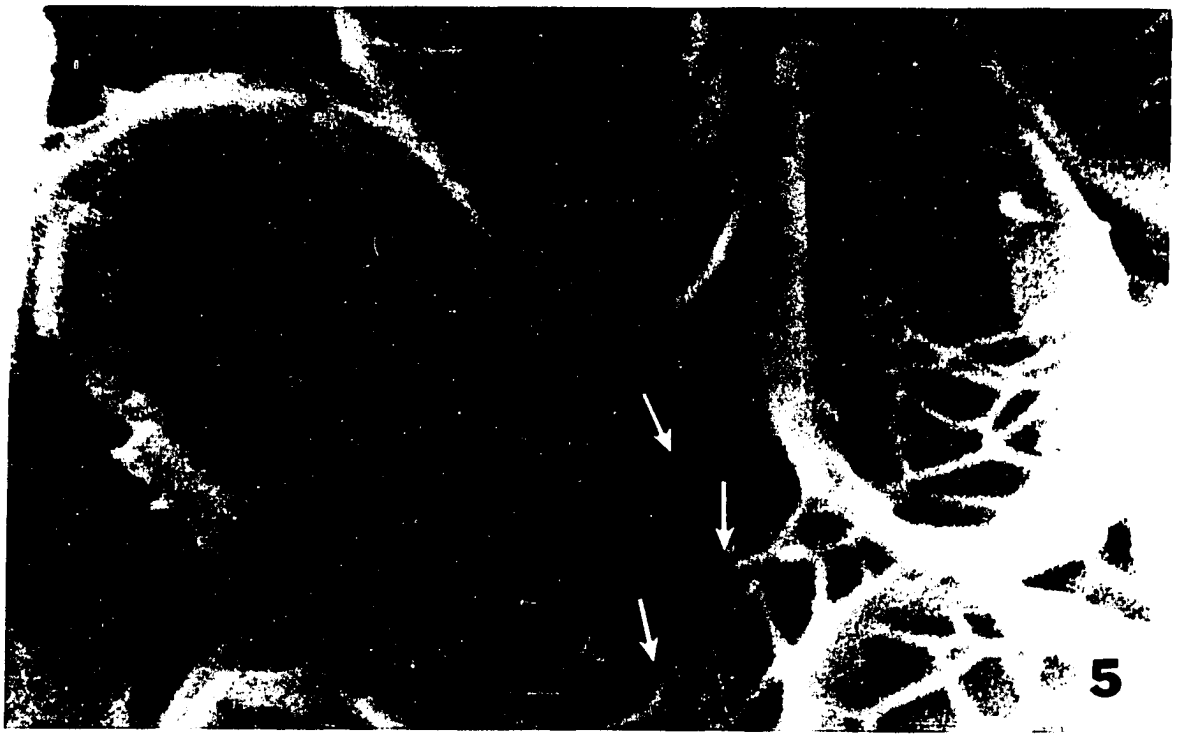

5

6

which appear attached to the cytoplasmic membrane, 1-2 layers of scales attached together by an amorphous component of the wall (so called "glue"), and coccoliths.

Ultrastructure of Cell Wall Fractions

To obtain the cell wall (ghost) of H. carterae, it is necessary to disrupt the cell structure and separate the wall from cell fragments. The use of osmotic shock and Triton X-100 provided an appropriate procedure for cell wall isolation. The nonionic detergent Triton X-100 solubilizes membrane lipoprotein (Vernon and Shaw, 1969). Makino et al. (1973) described the binding of Triton X-100 to high affinity hydrophobic sites which was not accompanied by a conformational change. The use of 5% Triton X-100 in salt solution provided a yield of about 1-1.2 g (dry weight) of cell wall from 90 liters of culture. Since distilled water solubilizes some coccolith fractions (Isenberg et al., 1965; Kuratana, 1974; DeJong et al., 1976), it was not used by itself for the cell wall isolation procedure. The relative purity of cell walls (ghosts) at different steps of the cell wall isolation procedure was monitored by light and electron microscopy. A scanning electron micrograph (Figure 7) of an early step of wall isolation shows that Triton X-100 caused degradation of the internal components of the cell beginning from the flagellum and proceeding distally after 2-3 hours treatment with 5% Triton X-100 in the presence of PMW II salts and 1.0 M KCl. After 10-15 hours treatment, pure walls can be obtained (Figure 8). These walls were used for further microscopic and biochemical investigations.

Figure 7. SEM micrograph of the cell wall at an early stage of the cell wall isolation. Cells were treated for 2-3 hours with Triton X-100. Note the appearance of a hole at the anterior portion of the cell. X 10,800

Figure 8. Ghosts of H. carterae. Cell walls are intact and pure. X 6,500


7


8

The negatively or positively stained walls as well as thin sections (Figures 9, 10) were also examined by transmission electron microscopy for further assessment of purity, based on the presence or absence of different components of the wall. Figure 9 shows most of these wall components. Coccoliths are connected to scales via "glue," scales tend to be stacked in layers, with "glue" adherent to different parts of scales (Figure 9). Figure 10 illustrates a section which also shows different fractions of the wall. The interesting observation in both figures (9, 10) is that the rims of coccoliths are intact including no evidence of degradation of calcite crystals due to Triton X-100 treatment. The "glue" is probably a loosely defined term as will be shown later (next section of Results). It is not present as a single component of the wall but rather shows a tendency to aggregate at different levels. Figure 11 shows the "glue" fraction of the wall in different morphological states.

For the purpose of correlating microscopic and biochemical data, it is necessary to bring together particular biochemical fractions which correspond to morphologically identifiable parts of the cell wall. For this purpose, it is important to have at least one component of the wall in something resembling a pure form which would serve as a standard reference for significant comparison. Probably the best candidate would be the coccolith, which we view as a model cell wall unit. Free floating coccoliths were collected by differential centrifugation from the growth medium in logarithmic growth phase or early stationary phase. Figure 12 shows the free floating coccolith collected by centrifugation and washed 3-5 times with artificial sea water (PMW II). Most coccoliths are intact

Figure 9. TEM micrograph of isolated cell wall. Note the presence of coccoliths (C), scales (S), and "glue" (arrows). X 24,900

Figure 10. TEM micragragh showing a section through a ghost of H. carterae. Coccoliths (C), scales (S), and "glue" can be seen in this cross-section. X 14,100

9

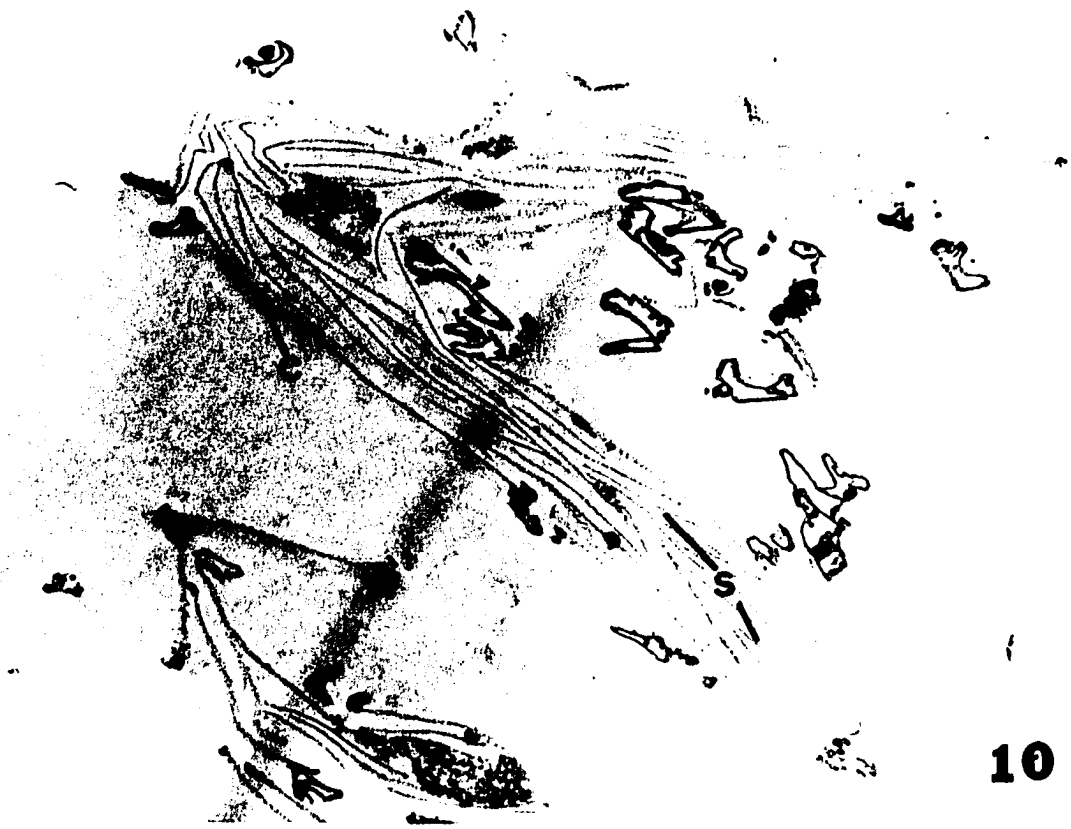

10

Figure 11. TEM micrograph of the aggregated component of wall called "glue." Glue can be seen at different levels of aggregation and serves as an adhesive compound to maintain the wall structure. X 31,800

Figure 12. TEM micrograph of free floating coccoliths collected from the Hymenomonas growth culture at late exponential phase. Note a few calcite crystals are degraded (arrow). X 32,400

Figure 13. SEM micrograph of free floating coccoliths. Note the absence of coccolithonets and presence of some damage to the calcite portion of coccoliths (arrows). X 20,900

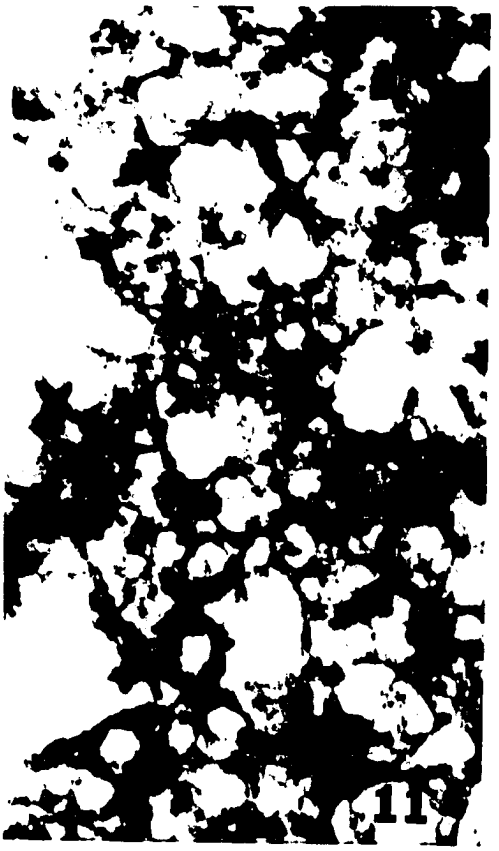
11

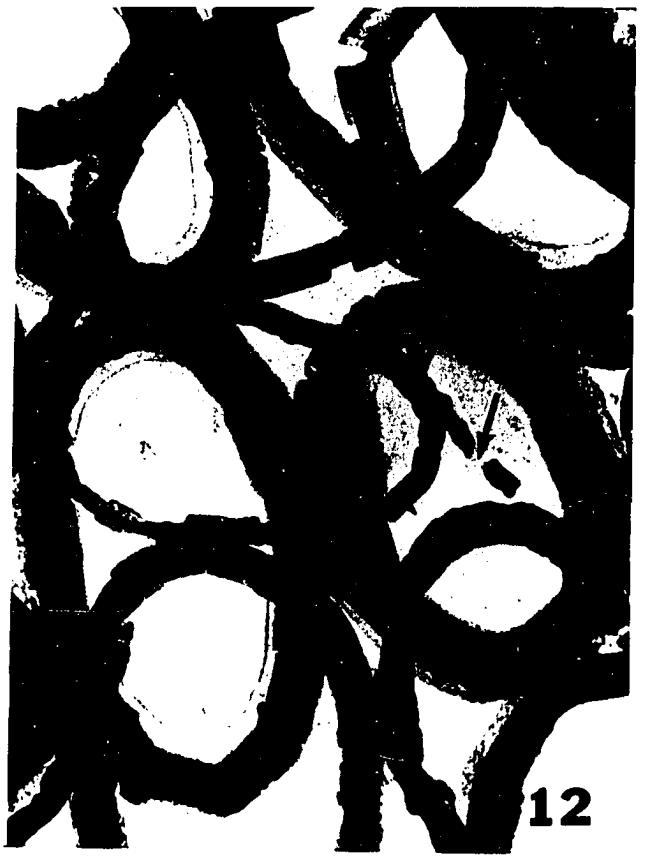
12

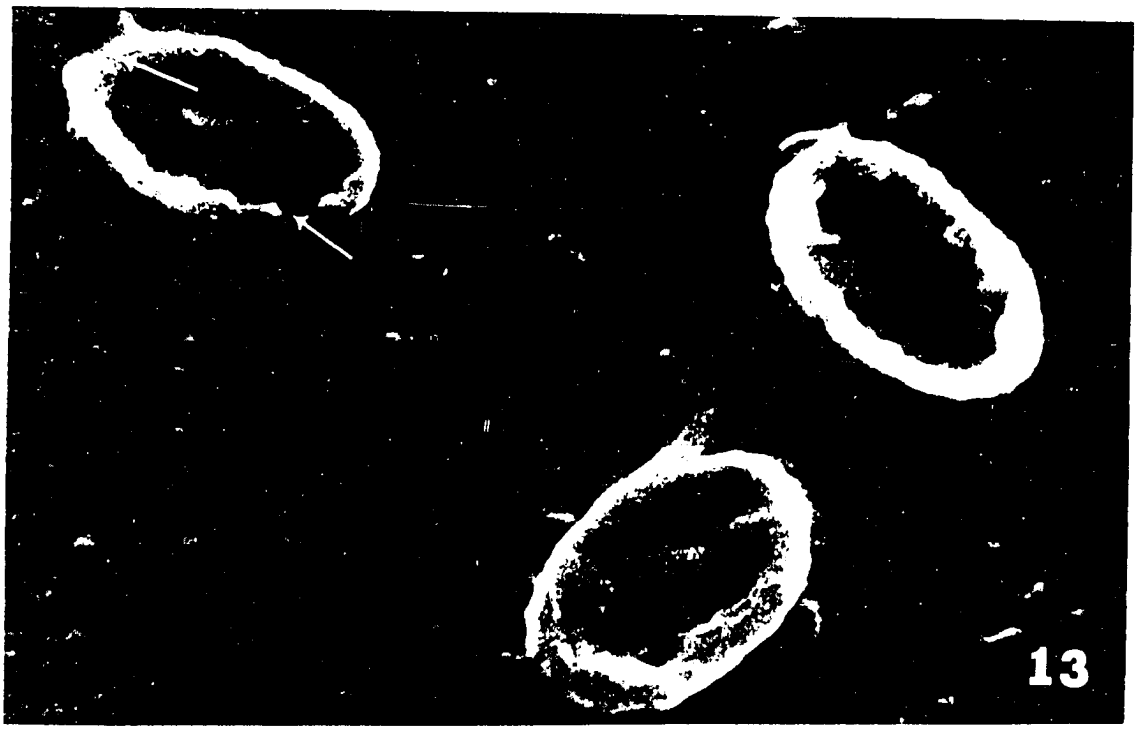
13

with complete calcite rims. Figure 13 is a scanning electron micrograph of free floating coccoliths showing some degradation in parts of coccolith rims. The minor destruction of coccolith rims may have occurred during preparation of the sample or could be caused by enzymatic or pH degradation which seems to become more pronounced as cultures age. However, the degree of disorganization is not as great as free floating coccoliths used in the work of Kuratana (1974). These later coccoliths were from older cultures under less controlled conditions. Also coccoliths shown in Figures 11 and 12 have not been subjected to Triton X-100 treatment as described by Kuratana (1974).

Cell wall chemistry

The approach to the study of cell wall chemistry has been to selectively remove the various cell wall components utilizing chaotropic agents (such as lithium chloride and sodium perchlorate), EDTA to chelate calcium, a pH shift to solubilize calcium, sodium dodecyl sulfate (SDS), and enzymes such as pectinase and cellulase. The following results present some information about chemical interaction and the nature of some of the wall components.

Chaotropic solubilization

Lithium chloride (LiCl) and sodium perchlorate ($NaClO_4$) are well-known as chaotropic agents and have been used in various systems especially in Chlamydomonas for the solubilization of protein and glycoprotein aggregates (Hatefi and Hanstein, 1974; Hills et al., 1975). Suitable conditions for dissociating the cell wall were developed by subjecting cells and suspensions of wall to different concentrations of

LiCl (2-10 M). Dissociation was monitored by measuring the release of protein and carbohydrate from the wall, electron microscopic observations, SDS gel electrophoresis, and analytical ultracentrifugation studies. In order to find some information about the nature of interactions among various components of the wall and in turn with internal portions of the cell, LiCl solubilization was carried out on whole cells. Figure 14 is a TEM micrograph of cells treated with 10 M LiCl for 2 hours. As seen in Figure 14, the most interesting effect of this chaotropic ion is its ability to destabilize membranes. No membrane is visible in this section. LiCl also causes the destruction of calcite crystals and dissolves columnar material and "glue" components of the wall. Scanning electron micrographs of cells treated with 10 M LiCl for 4 hours (Figure 15) show the release of almost all coccoliths from the wall, leaving behind cells with many blebs on the surface. The important feature of this micrograph is that coccoliths remain on the outer cell surface, apparently maintained there by strands of fibrous material which are contiguous over the top and under the coccoliths (see arrows in Figure 15). This kind of morphology supports the hypothesis that coccolithonets originate from the interior of the wall. Such an arrangement could make the cell wall a more stable structure.

Chaotropic solubilization of isolated walls revealed that lower molarities of LiCl did not achieve complete dissociation (Figure 16). This figure illustrates the effect of different concentrations of LiCl on dry walls. Note the release of protein and carbohydrate after 48 hours treatment. The most effective concentration is 10 M. At

Figure 14. TEM observation of the cross-section of a cell treated with 10 M LiCl for 2 hours. Note the effect of LiCl on membranes of the cell. After LiCl solubilization, the cell wall seems to be "loose" and no columnar material or glue can be seen. Also note the destructive effect on the rims of coccoliths (arrows). X 30,000

Figure 15. SEM micrograph of LiCl treatment. Cells were treated with 10 M LiCl for 4 hours. Note the presence of blebs on the cells and the fibrous material (FM) that connects the coccolith to the external surface of the cell (arrows). Also note that LiCl caused the release of most of the coccoliths from the cell surface. X 6,000

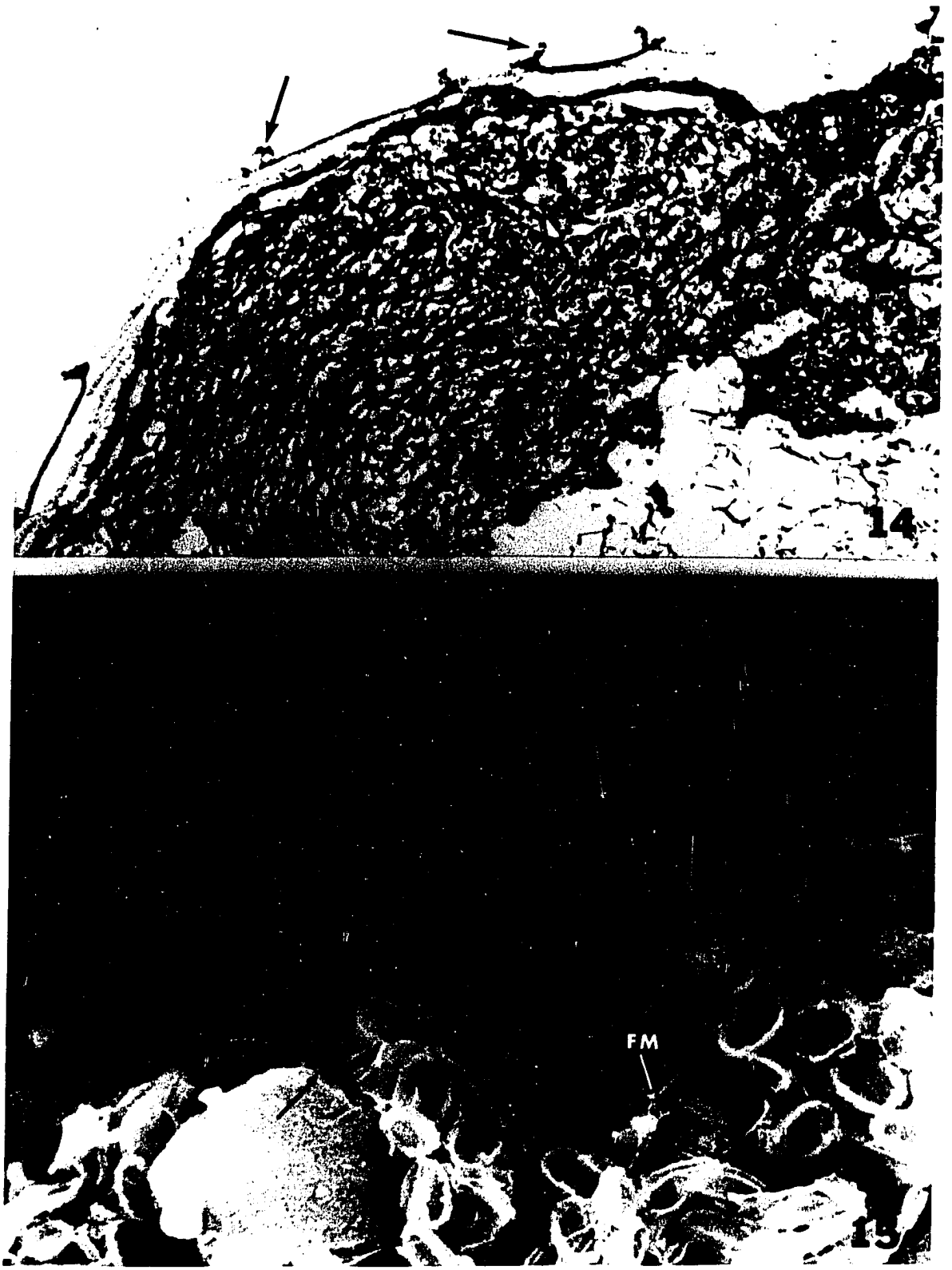
14
FM
13

Figure 16. Effect of different concentrations of LiCl on cell wall solubilization. The most effective concentration of LiCl is 10 M. At this concentration, about 80% of the solubilized component is carbohydrate. Treatment was carried out for 48 hours

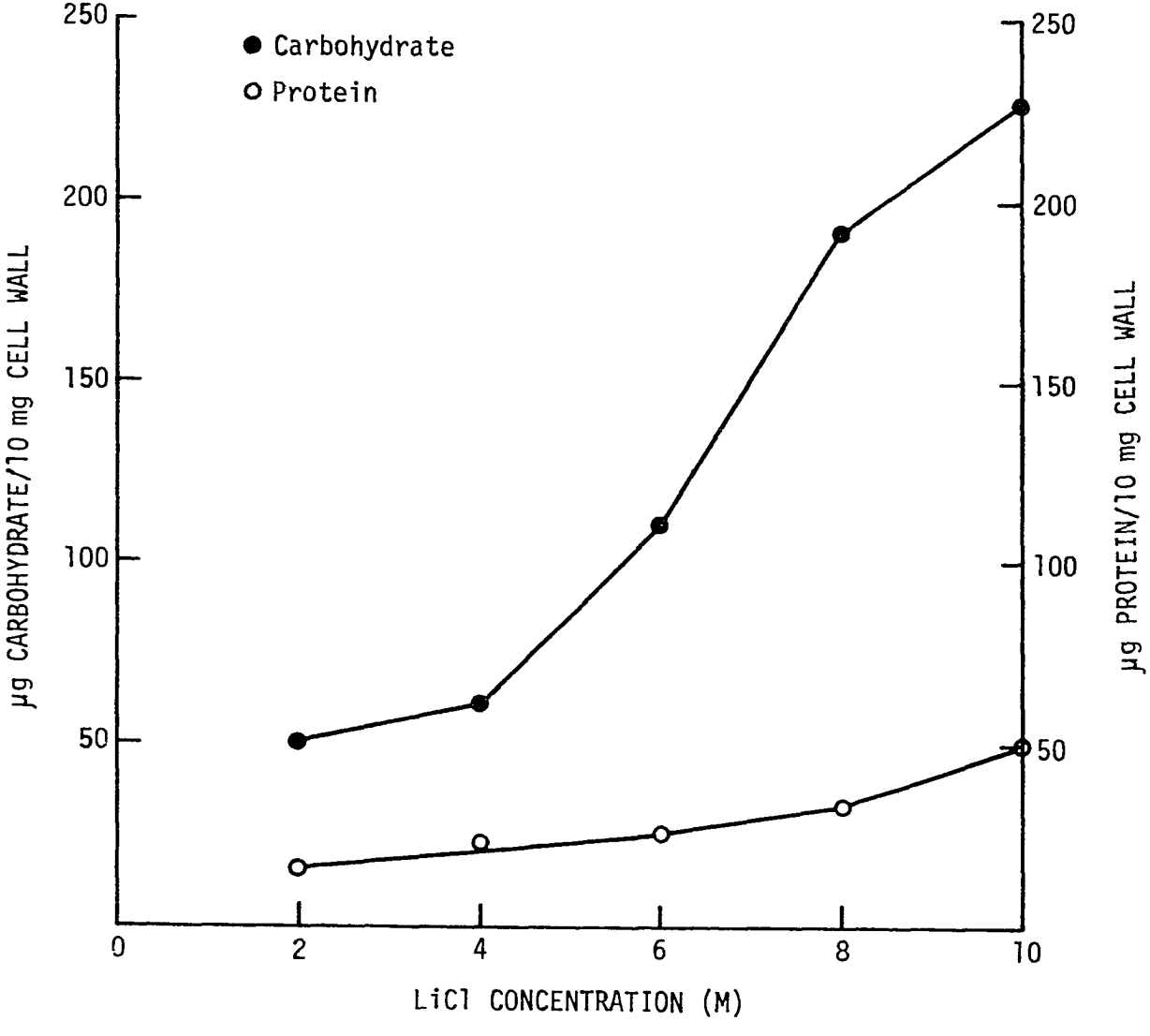
Carbohydrate
Protein
250
200
150
100
50
0
2
4
6
8
10
µg CARBOHYDRATE/10 mg CELL WALL
µg PROTEIN/10 mg CELL WALL
LiCl CONCENTRATION (M)

16

this molarity about 80-85% of the soluble fraction of the wall is carbohydrate and only 2.5-3 mg of soluble fraction can be obtained from 100 mg dry walls. Wall dissociation in the presence of high concentrations of salt is never complete, with insoluble components remaining, which can be removed by centrifugation for 20-30 minutes at 15,000 g. These insoluble fractions consist of coccolith bases, scales, and some fibrous material. The supernatant fluid, after wall dissociation, contains the salt soluble proteins and carbohydrates which will be discussed in a later section.

To find out what has been removed from the wall, the salt insoluble fraction collected by centrifugation was observed with SEM and TEM. Figure 17 shows a scanning electron micrograph of this cell wall after treatment with 10 M LiCl for 4 hours. As also seen before (Figure 14), most components of the wall have been solubilized. In this figure, it is clearly observed that LiCl led to the disorganization of the organic matrix and calcite crystals of the coccolith rim. A more pronounced destructive effect of chaotropic ions is seen in Figure 18. This figure reveals that LiCl treatment for 48 hours removed the matrix of the coccoliths and exposed the expected rhombohedral faces of the calcite crystals. Also, LiCl caused the complete destruction of the calcite crystals in the rim elements in some coccoliths. Figure 19 is a section through the wall extracted by 10 M LiCl for 48 hours showing poor organization of coccolith rims. Other components of the wall, including scales, "glue," and fibrous material, are also present.

Figure 17. SEM micrograph of Hymenomonas ghost treated with 10 M LiCl for 2 hours. Note the LiCl effect on calcite crystals of the coccolith rim (arrows). Also note that most of the "glue" portion of the wall has solubilized. X 17,500

Figure 18. TEM micrograph of Hymenomonas ghost treated with 10 M LiCl for 48 hours. Note the solubilization effect of LiCl on calcite crystals (arrows). X 24,900

Figure 19. TEM micrograph showing a section through Hymenomonas ghost treated with 10 M LiCl for 48 hours. Note the destruction by LiCl on the rim of the coccoliths. Coccolith (C), scales (S), "glue" (G), and fibrous material (FM) are present. X 57,600

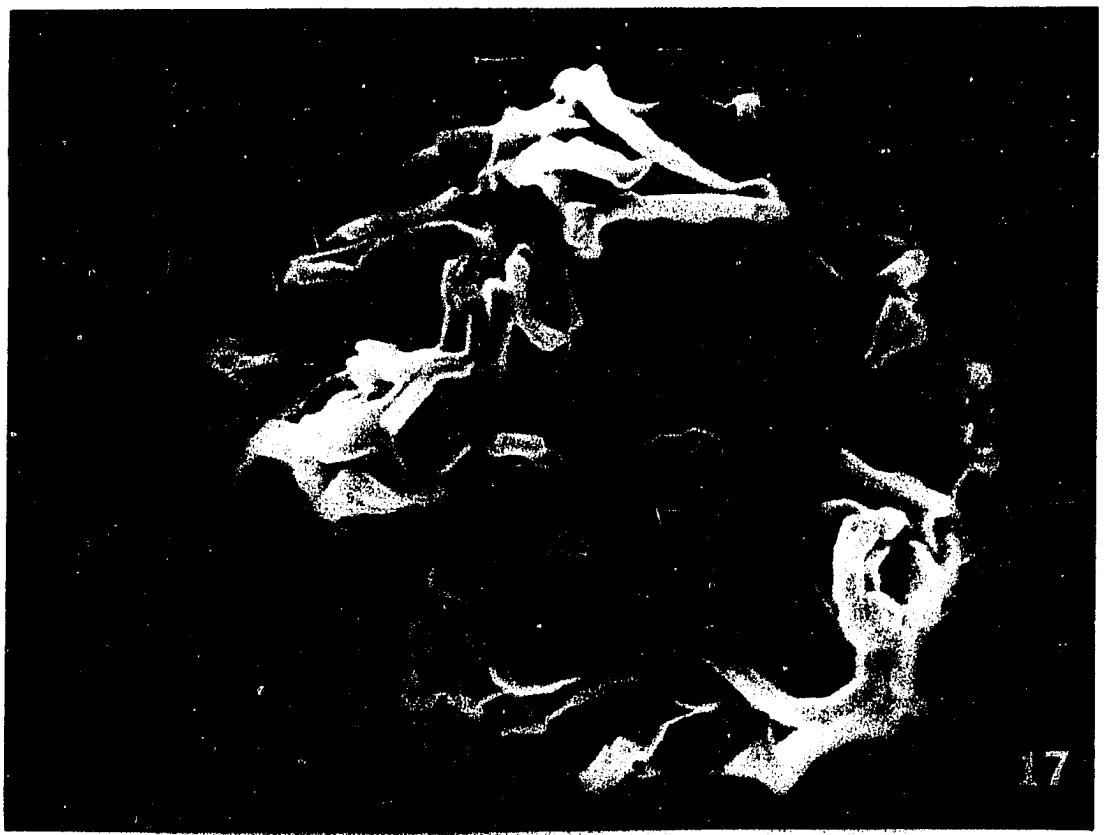
17


18


C
S
C
G
FM
19

LiCl-Soluble Wall Components

Analytical ultracentrifugation of the 10 M LiCl-soluble fraction (LSF) of the wall which was dialyzed against distilled water and 10 mM EDTA shows the presence of one main sedimenting molecule when the solvent is 0.15 M NaCl (Figure 20). The sedimentation coefficient corrected for solvent viscosity and density and solute concentration is 4.51. Some larger components dissociated from the wall are also at the bottom of the ultracentrifuge cell. The same pattern was observed at the presence of 2% SDS (sodium dodecyl sulphate). When the sample was treated with 2% SDS and heated in boiling water for 2 minutes, only one peak with a corrected sedimentation coefficient of 1.55 was observed (Figure 21).

Polyacrylamide gel electrophoresis in the presence of sodium dodecyl sulphate (SDS) of the same sample used for analytical ultracentrifugation is seen in Figure 22. Carbohydrate stain (PAS reagent) revealed three main bands. The result is consistent when the same sample was treated with 2% SDS in 0.15 M NaCl and heated in boiling water for 2, 4, and 6 minutes. Protein stain (Coomassie Blue) showed two main bands along the gel for the same samples (Figure 22). One can compare electrophoretic patterns of LSF (Figure 22) with insoluble fraction (LISF) and the whole wall (Figure 23). Comparison of these samples showed that 1) all the major carbohydrate species in the isolated walls are present in LSF and 2) LiCl has been able to solubilize one of the carbohydrate species completely. (Note the arrow in Figure 23.) Electrophoretic patterns of proteins are similar for whole walls

Figure 20. Schlieren patterns of LiCl solubilized fraction of coccoliths after dialysis against 10 mM EDTA, dH_2O, and 0.15 M NaCl, respectively. The pictures were taken at 16-minute intervals after the rotor reached a speed of 60,000 rpm. The temperature of the run was 21.2° C

Figure 21. Schlieren patterns of LiCl solubilized fraction of coccoliths after dialysis against 10 mM EDTA, dH_2O, and 0.15 M NaCl, respectively. Sample was then treated with 2% SDS and heated in boiling water for 2 minutes. The sample was run at 60,000 rpm and pictures were taken at 16-minute intervals. The temperature of the run was 21.3° C

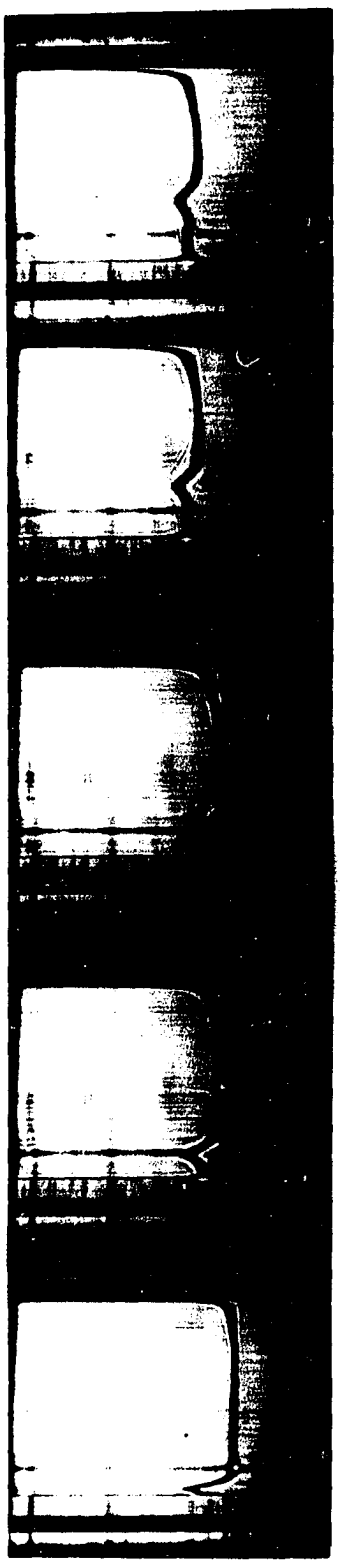

20

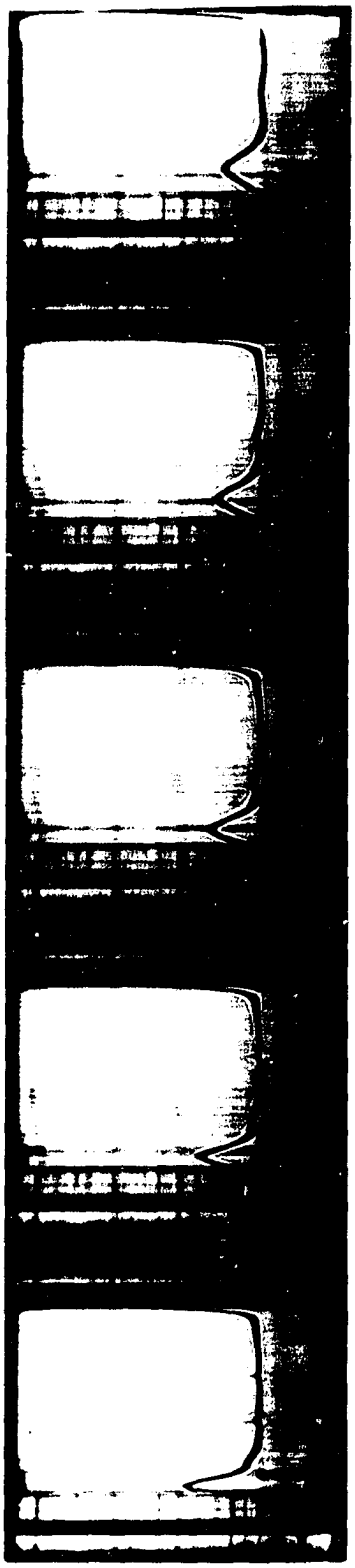

21

Figure 22. SDS polyacrylamide gel electrophoresis of 10 M LiCl-soluble fraction (LSF) from the wall. Samples were the same fraction used for sedimentation analysis. Gels were stained for carbohydrates with PAS reagent and for proteins with Coomassie Blue (CB). Samples were treated with 2% SDS in 0.15 M NaCl and heated in boiling water for 2 minutes (A), 4 minutes (B), and 6 minutes (C) before applying on gels. Note the presence of 3 distinct carbohydrate bands (PAS) and two protein bands (CB)

Figure 23. Comparison of SDS polyacrylamide gel electrophoresis of the cell wall (A) and insoluble fraction of the wall after 10 M LiCl treatment (B). Samples were treated with 2% SDS in 0.15 M NaCl and heated in boiling water for 2 minutes. Gels were stained for proteins with Coomassie Blue (CB) and for carbohydrates with PAS reagent. Note the absence of first carbohydrate band in B

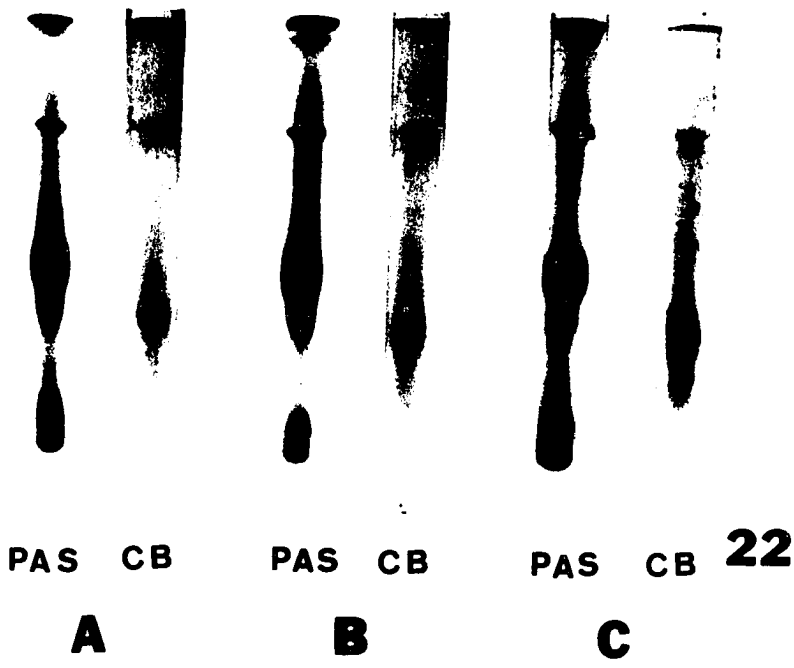
PAS CB
PAS CB
PAS CB
22
A
B
C

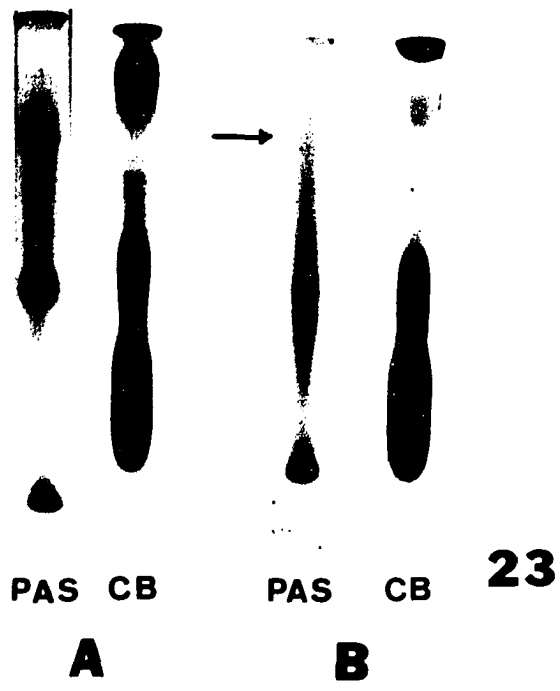
PAS CB
PAS CB
23
A
B

and LISF (three main protein bands can be seen for both samples; see Figure 23) and only two major proteins are present in LSF. The similarity of electrophoretic results for LiCl solubilization and SDS digestion (Figures 22, 23) suggests that LiCl only partially solubilized the wall. This was also indicated by previous morphological data (Figures 16, 17, 18).

EDTA solubilization

Effect of whole cell Cell wall solubilization by EDTA provides data necessary to perceive some chemical interactions among the wall components and in turn with the exterior surface of protoplasts. Scanning electron microscopy of the 10 mM EDTA treated cells (Figure 24) reveals a naked and smooth surface, and also shows some dissociating effects on cell membranes. After EDTA treatment, the coccoliths decalcify, calcite crystals dissociate, and the cell wall is partly degraded. Figure 25 is a section through a cell treated with 10 mM EDTA for 2 hours. Only a remnant of columnar material is present. EDTA had no destructive effect on the interior portion of the cell. Internal coccoliths are intact with a complete calcite rim.

Effect on isolated walls

In order to achieve a better understanding of the structure, chemical nature, and reassembly of some components of cell walls *in vitro*, it was necessary to dissociate the wall into its respective components without denaturation if possible. EDTA appeared to be a suitable compound for this purpose. Dissociation was carried out by using different concentrations of EDTA (1 mM-10 mM) and measuring the

Figure 24. Scanning electron micrograph of cells treated with 10 mM Na_2EDTA for 2 hours. Note the cells have no coccoliths. Some destructive effects on the external surface of cells brought about by EDTA treatment or specimen preparation (fixation, critical point drying). X 68,200

Figure 25. TEM observation of cells treated with 10 mM Na_2EDTA for 2 hours. Cytoplasmic membrane is intact and the columnar material (CM) is present. Internal coccolith (IC), coccolithosomes (Cs), mitochondria (M), and microtubules are also visible. X 91,800

24

25

release of protein and carbohydrate per amount of dry wall. Also, electron microscopic observations of negatively or positively stained preparations and thin sections of walls after EDTA solubilization were studied. Finally, SDS polyacrylamide electrophoretic gels as well as analytical ultracentrifugation patterns of the soluble wall fractions were analyzed. Having demonstrated the capacity to dissociate the wall, a more detailed analysis was undertaken of the conditions necessary for efficient reassembly of EDTA soluble fractions of the wall (ESF). The latter was monitored with light and electron microscopy.

Figure 26 shows the effect of different concentrations of EDTA on dry walls. The experiment was carried out for 48 hours. The most effective concentrations of EDTA for dissociation of the wall was between 10 mM-100 mM. At this range of EDTA concentration, about 80-85% of the ESF is carbohydrate and one can obtain only about 2.8-3.2 mg of soluble nondialyzable fractions of the wall per 100 mg dry walls. Similar to LiCl solubilization of the wall, lower molarities in each case did not achieve complete dissociation and wall dissociation in the presence of high concentrations of EDTA was never complete, with insoluble components remaining, which could be removed by centrifugation for 20-30 minutes at 15,000 x g. These EDTA-insoluble fractions (EISF) are coccolith bases, scales, fibrous material, and some remnants which can be dissociated by repeating the EDTA solubilization experiment or exposing the insoluble components to SDS (see SDS gel electrophoresis of the insoluble fraction of the wall). Some biochemical properties of the ESF will be discussed later.

Figure 26. Cell wall solubilization by EDTA for 48 hours causes the release of protein and carbohydrate. The effect of different concentrations of EDTA is illustrated. Note that there is no significant change in solubilization of the wall at concentrations of 10-100 mM EDTA

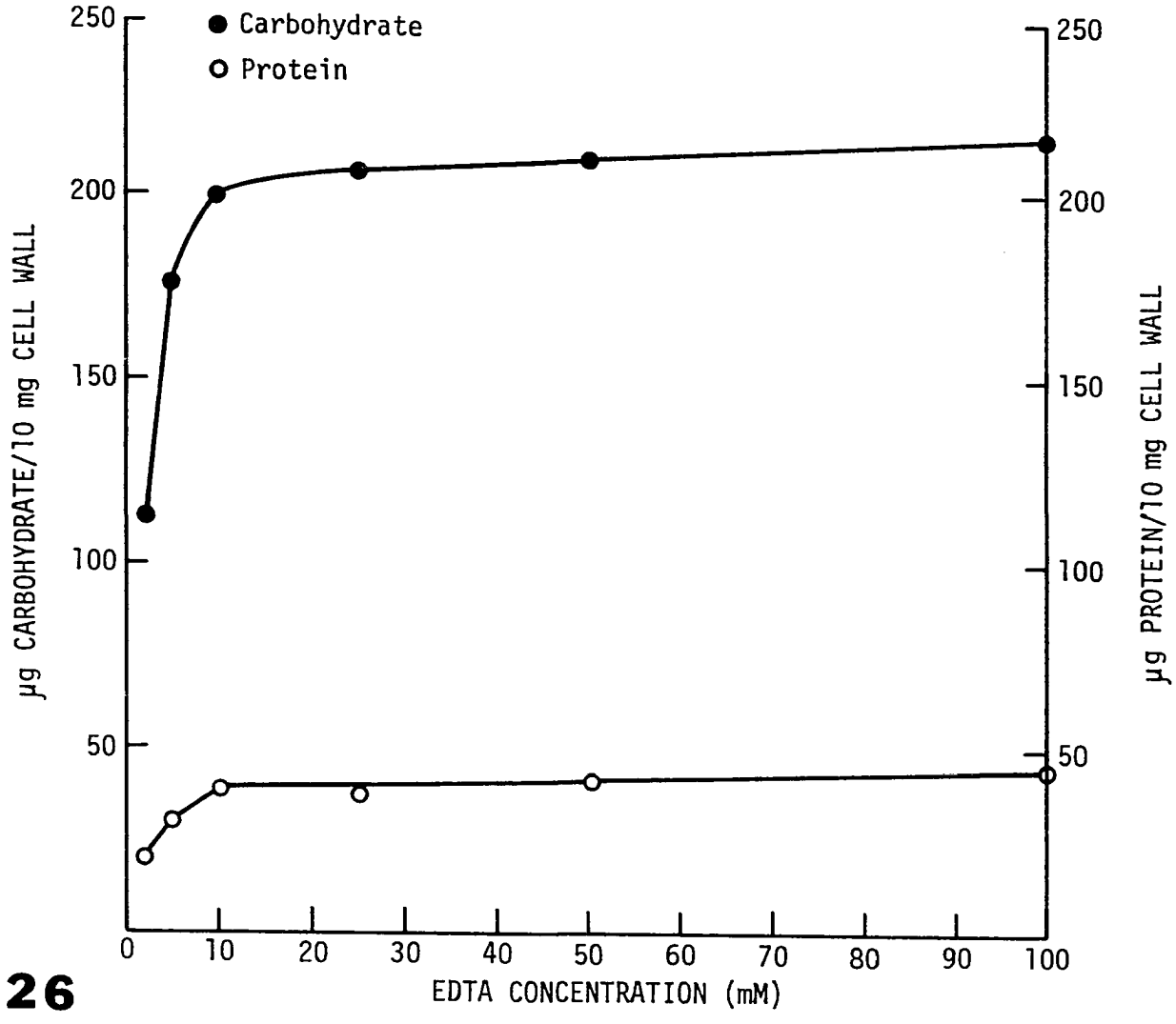
Carbohydrate
Protein
250
200
150
100
50
µg CARBOHYDRATE/10 mg CELL WALL
µg PROTEIN/10 mg CELL WALL
0
10
20
30
40
50
60
70
80
90
100
EDTA CONCENTRATION (mM)

26

The degree of solubilization of the wall by 10 mM EDTA was monitored by TEM. Figures 27-29 are electron micrographs showing the most effective site of EDTA solubilization, the matrix material, and calcite crystals. This degradation effect is due to the chelating property of EDTA, especially for Ca^{++}. The fibrous material connecting the base of coccoliths to the glue fraction of the wall is visible in Figure 27. This figure also shows some amorphous material connecting strands of fibers together. Figure 28 is a thin section through the wall showing that EDTA does not completely solubilize the calcareous rim of the coccolith. There is also a residue of calcite crystals on coccolith bases, even after 48 hours EDTA treatment. Figure 29 shows the decalcified coccoliths and the dissociation effects of EDTA on the wall and especially coccoliths. Some aggregated fibrous components are visible in the margins of coccoliths. These aggregated fibers are apparently coming out of the coccolith edge.

Dissociation of the wall by 10 mM EDTA led to a more detailed morphological analysis of the wall structure. Figures 30-34 are illustrative micrographs showing several components of the wall. Figure 30 shows the morphological detail of the scale. The microfibrillar network of the scale with its radial and concentric components is visible. This micrograph strongly suggests that the glue holds the scales together and in turn stabilizes the cytoskeleton. Figure 31 is a high resolution electron micrograph showing the fibrous nature of glue and its connections to scales. Higher magnification of the glue fraction of the wall is shown in Figure 32. This micrograph shows

Figure 27. Walls obtained from Triton X-100 treatment were solubilized with 10 mM Na_2EDTA for 2 hours. Note the EDTA removed the calcareous rim of the coccolith (C), leaving behind a base with radial microfibrils (Rm). The fibrous material (FM) connecting the base of coccolith to the bulk of "glue" (G) and scales (S) connected to coccolith (C) are also visible. X 37,800

Figure 28. Section through walls treated with 10 mM Na_2EDTA for 48 hours. Coccoliths and scales are released from the glue. Only remnants of matrix material remain on coccolith base (arrows). X 22,000

Figure 29. Walls treated with 10 mM Na_2EDTA for 48 hours. Note the presence of aggregated fibrous material on the edges of decalcified coccoliths. X 24,900

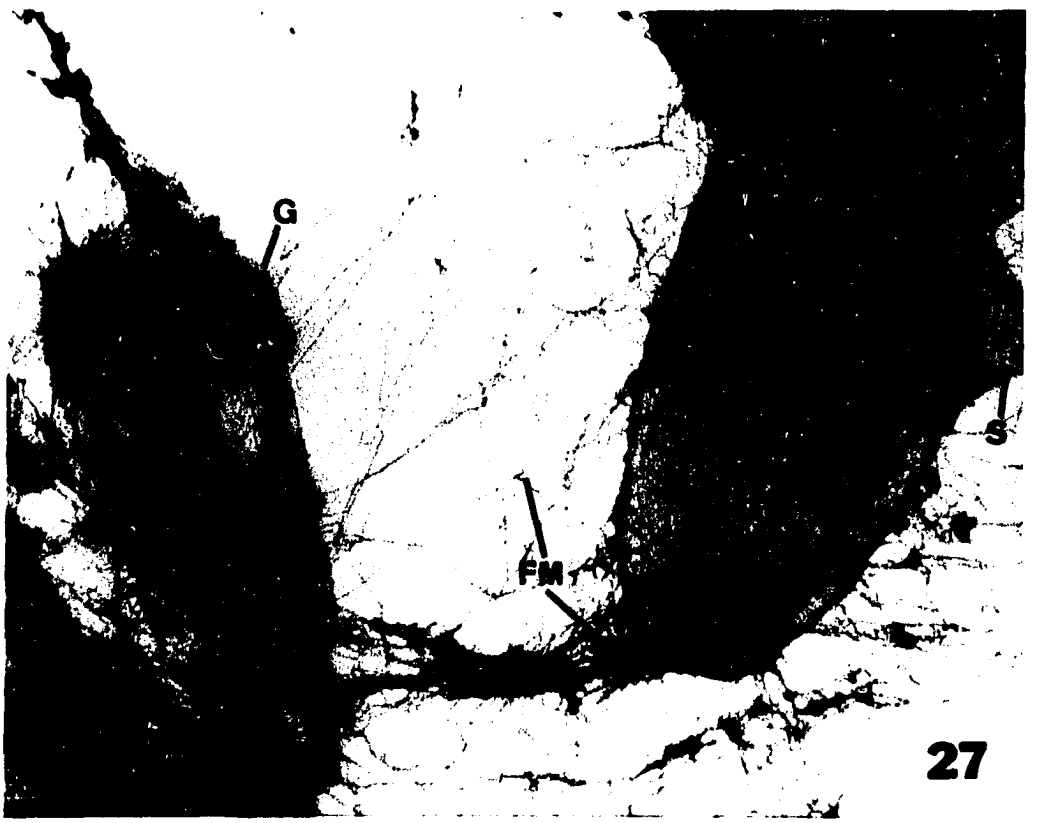

27

28

29

Figure 30. TEM micrograph of scale after dissociation of cell wall with 10 mM EDTA for 2 hours. Fibrous material (FM) attached primarily at the edges of scales. The morphological picture strongly suggests that FM is the "glue" that holds the cytoskeletal elements together. Note the concentric (Cn) and radial (R) microfibrillar network, and the rim of doublet microfibrils of the overlapping scales. X 52,200

Figure 31. High resolution electron micrograph of scale showing fibrous material adhered to the concentric and radial microfibrils in the scale. The scale is curled at the edges. Note the fibrous nature of the "glue" and the presence of small globular bodies (arrows). X 39,600

Figure 32. Higher magnification of "glue" portion of the cell wall. Note the strands of fibrous material (FM) or type A fibers and the presence of small globular bodies (arrows). X 92,600

Figure 33. TEM observation of type B fibers. These fibers are compact and electron dense, with little suggestion of internal organization. X 53,300

Figure 34. TEM micrograph of type C fibers. Note the composites of longitudinally arranged subfibers. X 152,000

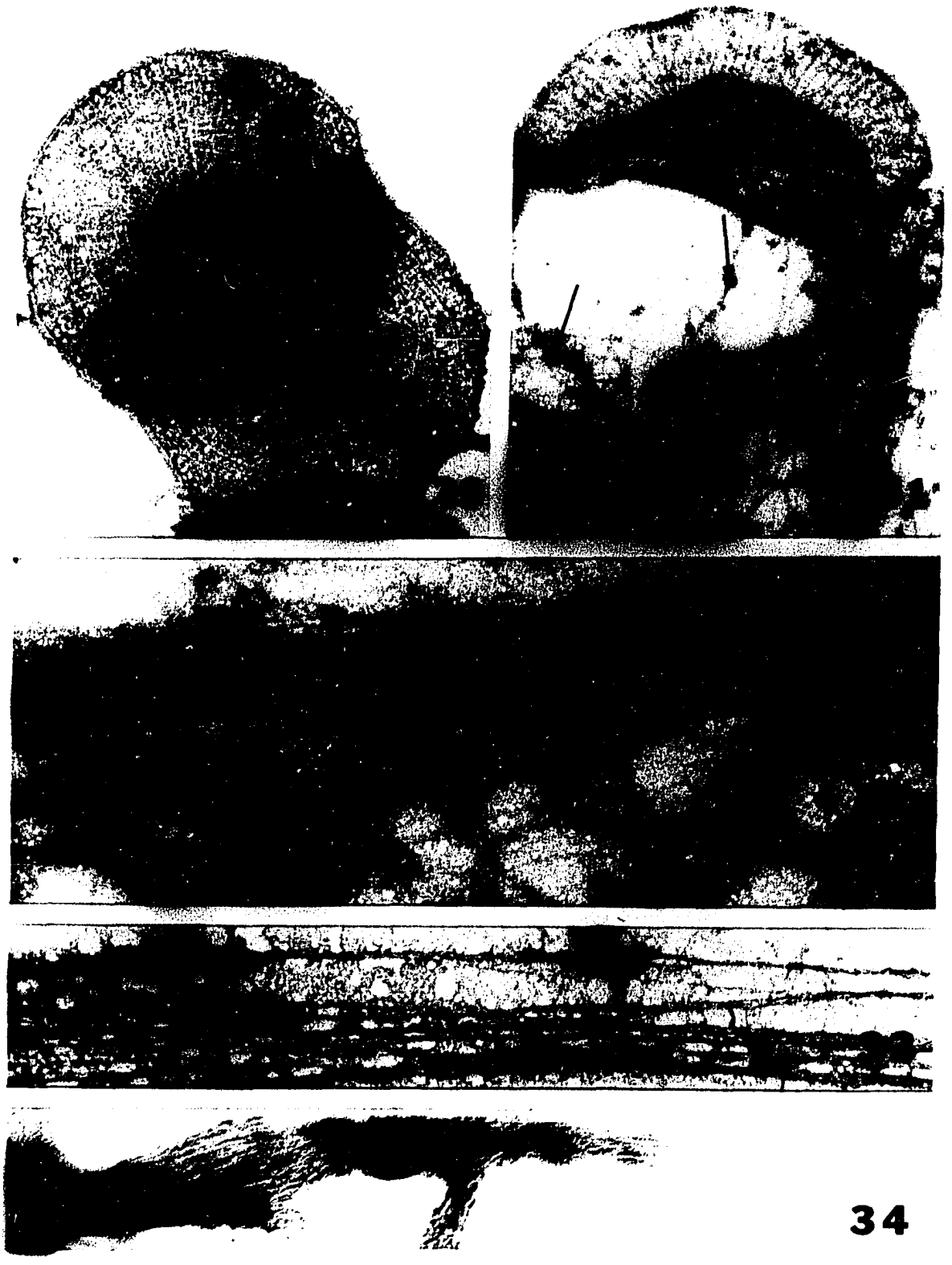

34

that the glue is not a single fraction of the wall but rather is composed of strands of fibrous material (type A fibers) and small globular bodies. In addition to type A fibers, some compact strands with no internal structure, called type B fibers (Figure 33) and some larger strands or type C fibers (Figure 34) with longitudinally arranged subfibers are visible. So the term glue is a descriptive term which probably includes different chemical components

EDTA-Soluble Fraction of Wall (ESF)

Morphology of reassembly

Reassembly of ESF was monitored under controlled conditions. Light and electron microscopic observations of reaggregated components are shown in Figures 35-41. Figure 35 is the light micrograph of ESF after filtration through a 0.22 um millipore filter, dialysis against distilled water and 0.1 M $CaCl_2$. Under light microscopy, one can watch the appearance of nucleation centers which form spontaneously. The time course of complete reassembly under the phase contrast or Normarski differential interferance contrast microscope was between 3-10 minutes. Figure 36 shows that, in addition to the nucleation centers of Figure 35, fibers of different lengths (up to several centimeters) were observed. Air drying of a drop of ESF on a microscope slide revealed folded sheets of reaggregated components. At the electron microscope level, different species of reassembled material were observed. Figures 38 and 39 are TEM micrographs showing the appearance of aggregated centers which can grow in size. Each aggregation center consists of

Figure 35. Nomarski differential interference contrast light micrograph of reaggregation of the EDTA solubilized fraction (ESF) of the wall after dialysis against dH_2O and then 0.3 M $CaCl_2$. By placing a drop of SF on a slide, adding a cover glass, and sealing with melted vaseline or fingernail polish, one can watch the formation of nucleation centers which form spontaneously. X 1,500

Figure 36. Observation of aggregated EDTA solubilized fraction of wall (ESF) by phase contrast microscopy. In addition to nucleation centers, one can see the formation of fibers which may reach lengths of several centimeters. X 1,500

Figure 37. Nomarski differential interference contrast light micrograph of reaggregation of ESF. After placing a drop of SF on a slide and allowing it to air dry, the folded sheets of reaggregated material can be observed. X 1,500

Figure 38. After solubilization with 10 mM EDTA followed by filtration through 0.22 um filter, dialysis against dH_2O, and then dialysis against $CaCl_2$, one obtains small aggregates which seem to grow in size. X 9,500

Figure 39. The higher magnification of aggregates shown in Figure 38, showing sheets of aggregated ESF. X 60,000


37

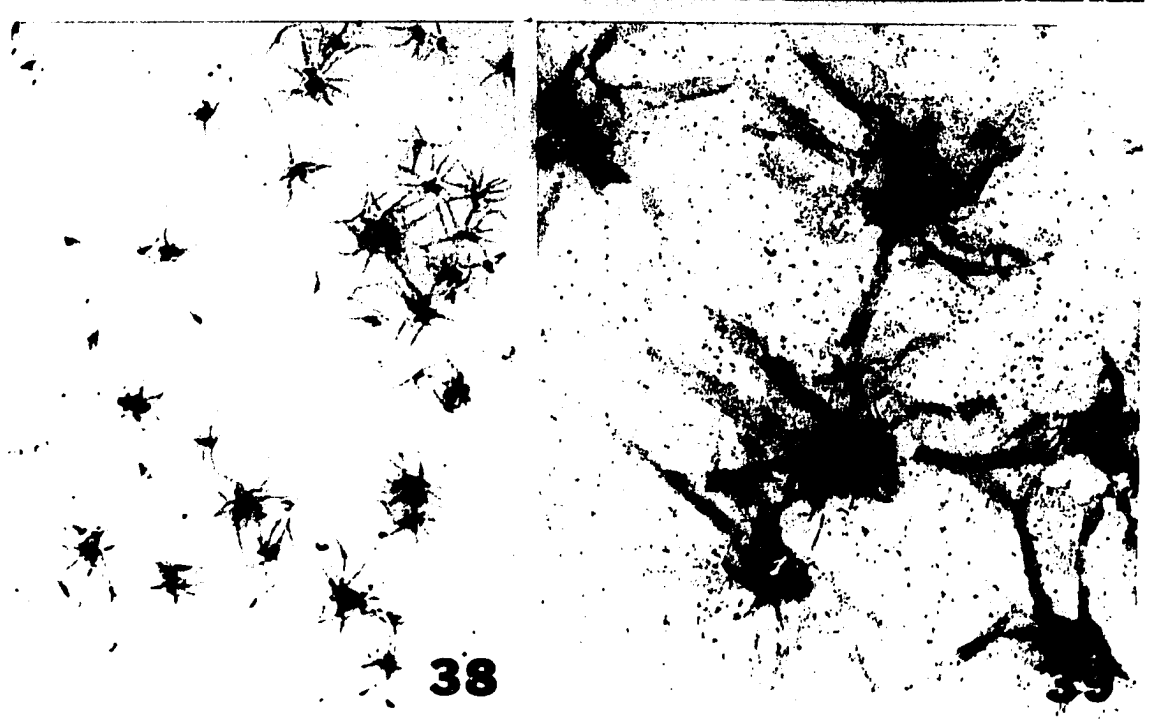
38

Figures 40 and 41. TEM observations of 0.22 µm filtered soluble fraction of 10 mM EDTA (ESF) after dialysis against dH_2O, and then 0.1 M CaCl

40. At the molecular level, ESF often forms microcrystalline arrangements. Preparation was stained with 5% aqueous sodium tungstate adjusted to pH 6.8 with formic acid. X 182,000

41. TEM micrograph of ESF showing molecules with sizes slightly larger than Figure 40. Preparation was stained with 1% uranyl acetate in 50% ethanol. X 100,000

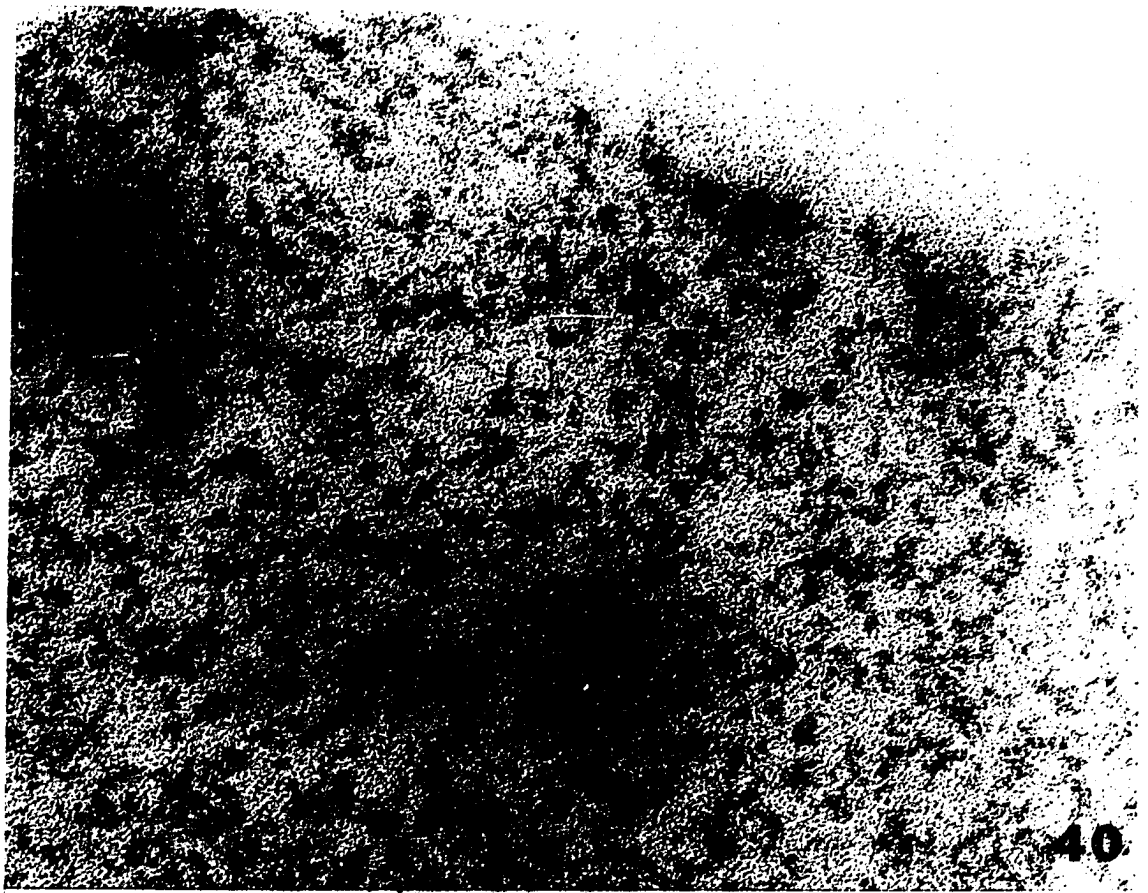

40

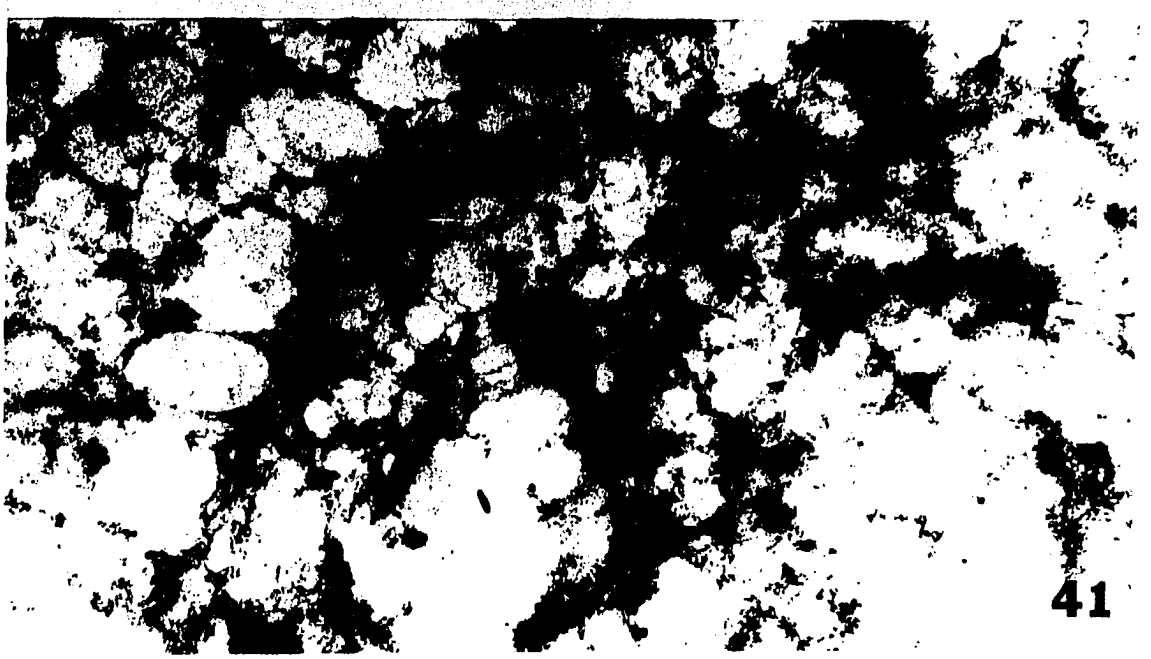

41

several arms of aggregated sheets, along with many smaller components resembling aggregated sheets which are still in solution (Figure 39). At the molecular level, ESF forms a fine structure (Figures 40,41). The presence of a crystalline lattice structure with center to center spacing of about 60-66 Å was frequently seen under TEM (Figure 41). So the conditions necessary for successful reassembly of cell wall components include the solubilization of wall soluble material with EDTA, dialysis against distilled water, which causes the removal of EDTA, and the presence of Ca^{++} which enhances the reaggregation.

Colorimetric determinations

The results of colorimetric determinations carried out with ESF are given in Table 1. It appears that the ESF contains about 15-20% protein and 80-85% carbohydrate. The presence of uronic acid indicates that at least some of this fraction is acidic in nature.

Table 1. Colorimetric determination of some components of ESF

Component	% per ml of ESF[a]
Protein	15-20
Carbohydrate	80-85
Uronic acid	35-40

[a]For assays, see Materials and Methods.

Analytical ultracentrifugation

The ultracentrifugal patterns of the ESF are shown in Figure 42. Two distinct peaks were seen when the solvent was 0.15 M NaCl. The sedimentation coefficients corrected for solvent viscosity and density and solute concentration (See appendix B.) are 1.81 and 4.71 Svedbergs. When this same material was treated with 2% SDS and heated in boiling water for 2 minutes, only one peak with sedimentation coefficient of 1.55 was observed (Figure 43). Adding 2% SDS and omitting the heat from the procedure did not change these ultracentrifugal patterns.

SDS-polyacrylamide gel electrophoresis

Following ultracentrifugation, the same samples were used for SDS gel electrophoresis. These samples were treated with 2% SDS in 0.15 M NaCl and heated for 2, 4, and 6 minutes before applying the samples on the gels. Gels stained with PAS reagent revealed one distinct, and some diffuse carbohydrate bands. No pronounced differences were observed in carbohydrate patterns as a result of different times of heating the samples, except that, in the sample heated for 6 minutes, PAS reagent is more diffused. The protein patterns seem to be different due to different times of heating. Samples heated with 2% SDS for 6 minutes revealed more distinct protein bands (Figure 44).

SDS polyacrylamide gel electrophoresis of the whole wall and the insoluble fraction (EISF) of the wall is shown in Figure 45. Following digestion with 2% SDS at 100^{o} C for 2 minutes and staining for protein and carbohydrate similar electrophoretic patters are observed, for both samples. Three major carbohydrate bands and three different

Figure 42. Schlieren patterns of EDTA solubilized fraction of the cell wall (ESF) in 0.15 M NaCl. The pictures were taken at 16-minute intervals at 60,000 rpm. The temperature of the run was 21° C

Figure 43. Schlieren patterns of the EDTA solubilized fraction of ESF after treating with 2% SDS in 0.15 M NaCl and heating in boiling water for 2 minutes. The pictures were taken at 16-minute intervals after the rotor reached the speed of 60,000 rpm. The temperature of this run was 21.3° C

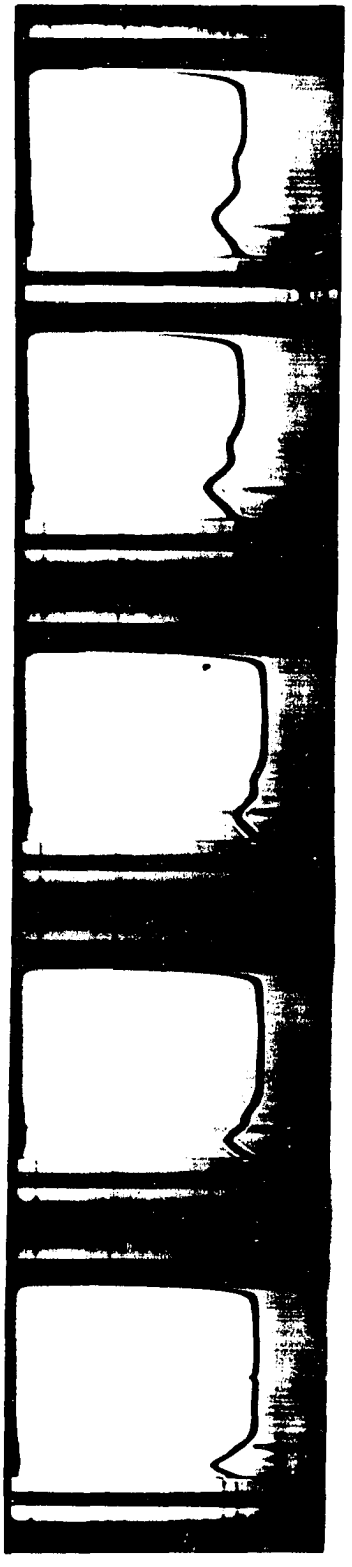

42

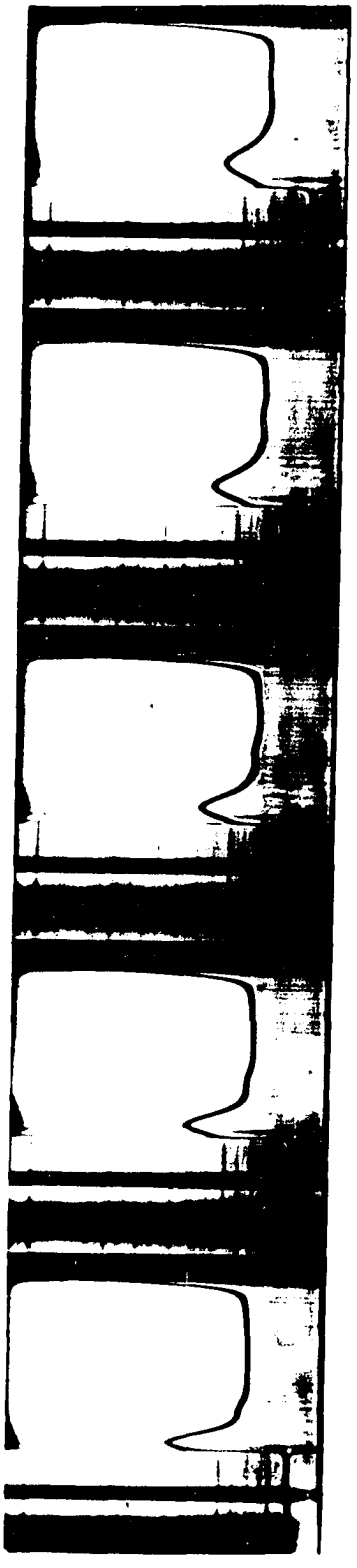

43

Figure 44. SDS polyacrylamide gel electrophoresis of 10 mM EDTA-soluble fraction of wall (ESF). Samples were the same fractions used for ultracentrifugation studies. They were treated with 2% SDS in 0.15 M NaCl and heated in boiling water for 2 minutes (A), 4 minutes (B), and 6 minutes (C) before applying on gels. Gels were stained for proteins (CB) and carbohydrates (PAS)

Figure 45. Comparison of SDS polyacrylamide gel electrophoresis of cell wall (A) and insoluble fraction of wall after 10 mM EDTA (EISF) treatment (B). Samples were treated with 2% SDS in 0.15 M NaCl and heated in boiling water for 2 minutes. Gels were stained for carbohydrates (PAS) and proteins (CB)

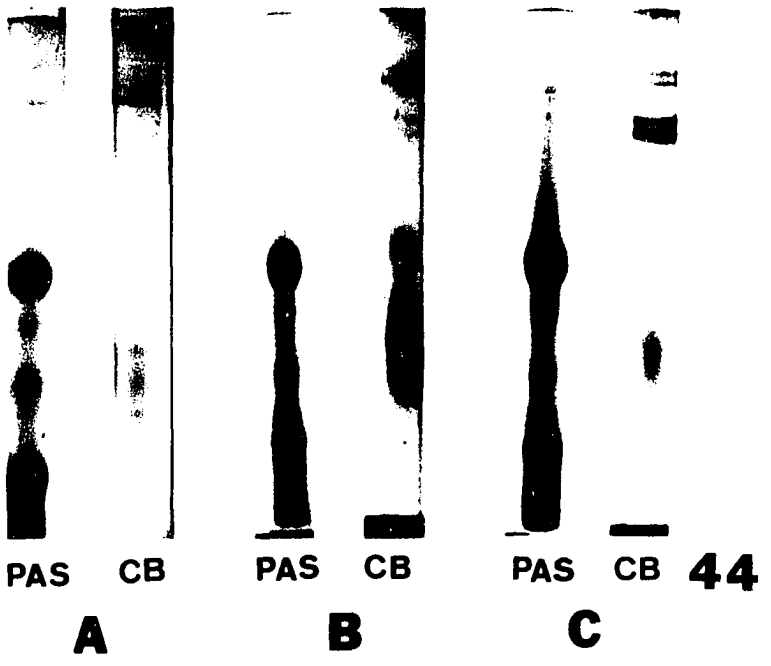
PAS CB
PAS CB
PAS CB
44
A
B
C


PAS CB
PAS CB
45
A
B

protein bands can be seen. Electrophoretic comparison of the three different fractions revealed a great similarity in the carbohydrate patterns, but there are minor differences in the protein patterns (Figures 44,45). Figure 45 shows that the more pronounced effect of SDS digestion is on protein rather than carbohydrate. The similarity of fractions confirms the point of the previous morphological observations (Figures 27-29) that EDTA only causes the partial solubilization of the wall in the absence of SDS.

Figure 46 is a survey electron micrograph showing the effect of SDS digestion on the EDTA insoluble fraction of wall (EISF). Comparing this micrograph with Figures 27, 28, and 29, one concludes that, like EDTA, SDS also partially solubilizes some of the wall components. As is seen in Figure 46, the matrix component of the coccolith is completely digested, and most strands of fibrous material (type A fibers) are missing. Only the residual parts of glue (type B fibers with poor organization, and degraded globular bodies) remain. The effect of SDS, especially on matrix material can be followed after digestion of the whole wall. Figure 47 shows a coccolith with partially degraded matrix material and type A fibers apparently connected to its edges. This micrograph clearly shows the degradation effect of SDS on calcite crystals and matrix material of the coccolith. So electrophoresis data and electron-microscopic results strongly suggest that, like EDTA or LiCl, SDS partially digests the wall and there are many similarities among the solubilized fractions.

Figure 46. After solubilization with 10 mM EDTA for 48 hours followed by 2% SDS for 48 hours, the hydrated or gelatinous state of the "glue" is not visible but type B fibers with small globular bodies are seen (arrows). Also coccolith has completely lost its matrix material. Several scales (S) and one coccolith (C) are present. Note the miniature or haptonemal scales (HS). X 30,000

Figure 47. Digestion of wall with 2% SDS for 48 hours. A coccolith (C) with fibrous material (FM) attached primarily at the edges is visible. The remnants of matrix material remain on the coccolith base (arrows). X 54,000

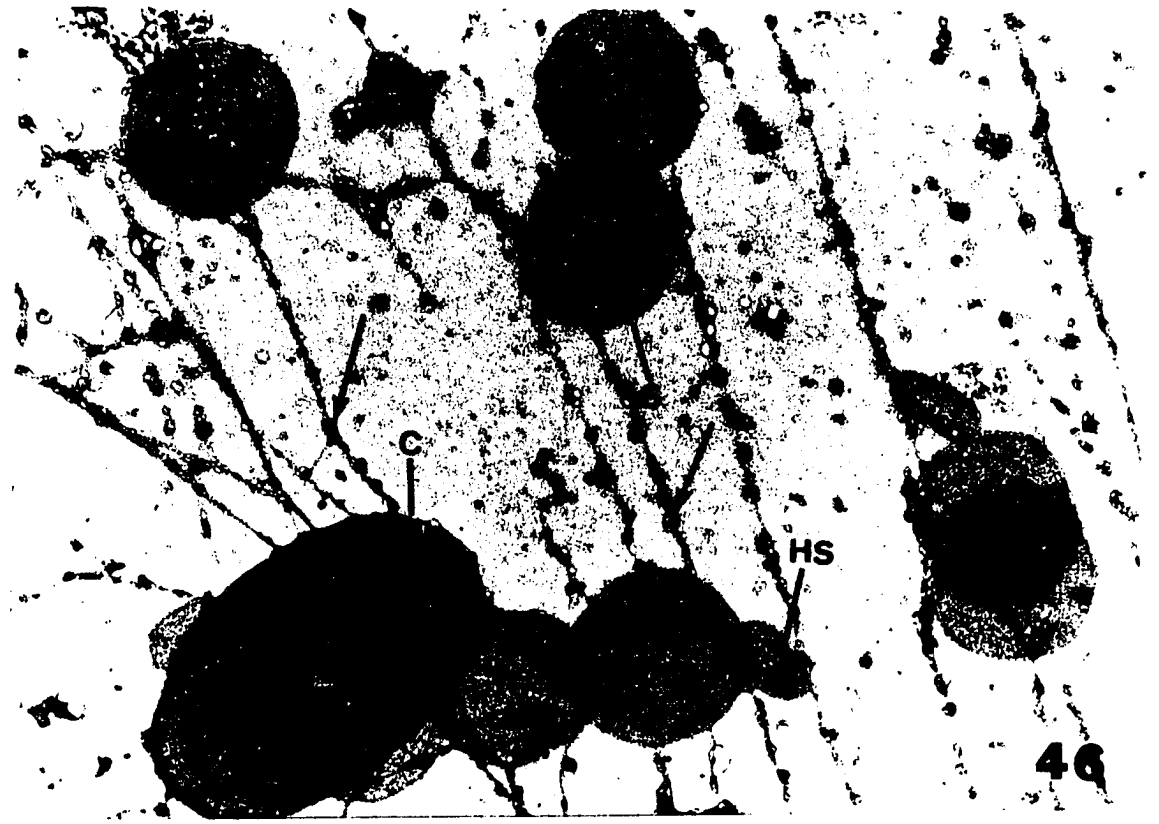
C
HS
46


47

Gel filtration

Results obtained from analytical ultracentrifugation of EDTA-soluble fractions of the wall (ESF) showed the presence of molecules with low sedimentation coefficients. The gel filtration technique was used for isolation and further characterization of these molecules. Figure 48 (A-C) shows the results of gel filtration of ESF applied on Biogel P10, Biogel P60, and Biogel P100 columns and eluted with 0.15 μ NaCl. A single peak was obtained in the void volume of the Biogel P10 column. For Biogel P60 and P100, also the main peak appeared in the void volume of the columns. Similar results were observed when the sample was eluted with distilled water. Ultracentrifugation behavior and SDS gel electrophoresis of the void volume from different columns revealed the same patterns observed in Figures 42 and 44. Electron microscopic examination of the void volume of Biogel P10 is shown in Figure 56. This figure demonstrates the aggregated macromolecular nature of the void volume.

Isolation and Characterization of Acidic Polysacchrides

Polyacrylamide gel electrophoresis

The results of polyacrylamide gel electrophoresis in the absence of SDS are shown in Figure 49. The EDTA-soluble fraction of the wall (A) and the EDTA-soluble coccolith fraction (B) were submitted to polyacrylamide gel electrophoresis and were stained for acidic polysaccharides with Alcian Blue (AB) and for proteins with Coomassie Blue (CB). In this technique, only charged molecules can migrate along the gels. Four carbohydrate bands were observed for ESF (AB) and no protein bands were

Figure 48. Gel filtration

(A) Gel filtration of the EDTA soluble fraction (ESF) from cell wall through Biogel P10. Elution occurred with 0.15 M NaCl at room temperature. Absorbance was measured at 490 nm for phenol sulfuric test

(B) Gel filtration of SF through Biogel P60. Sample was eluted with 0.15 M NaCl

(C) Gel filtration of SF through Biogel P100. Sample was eluted with 0.15 M NaCl

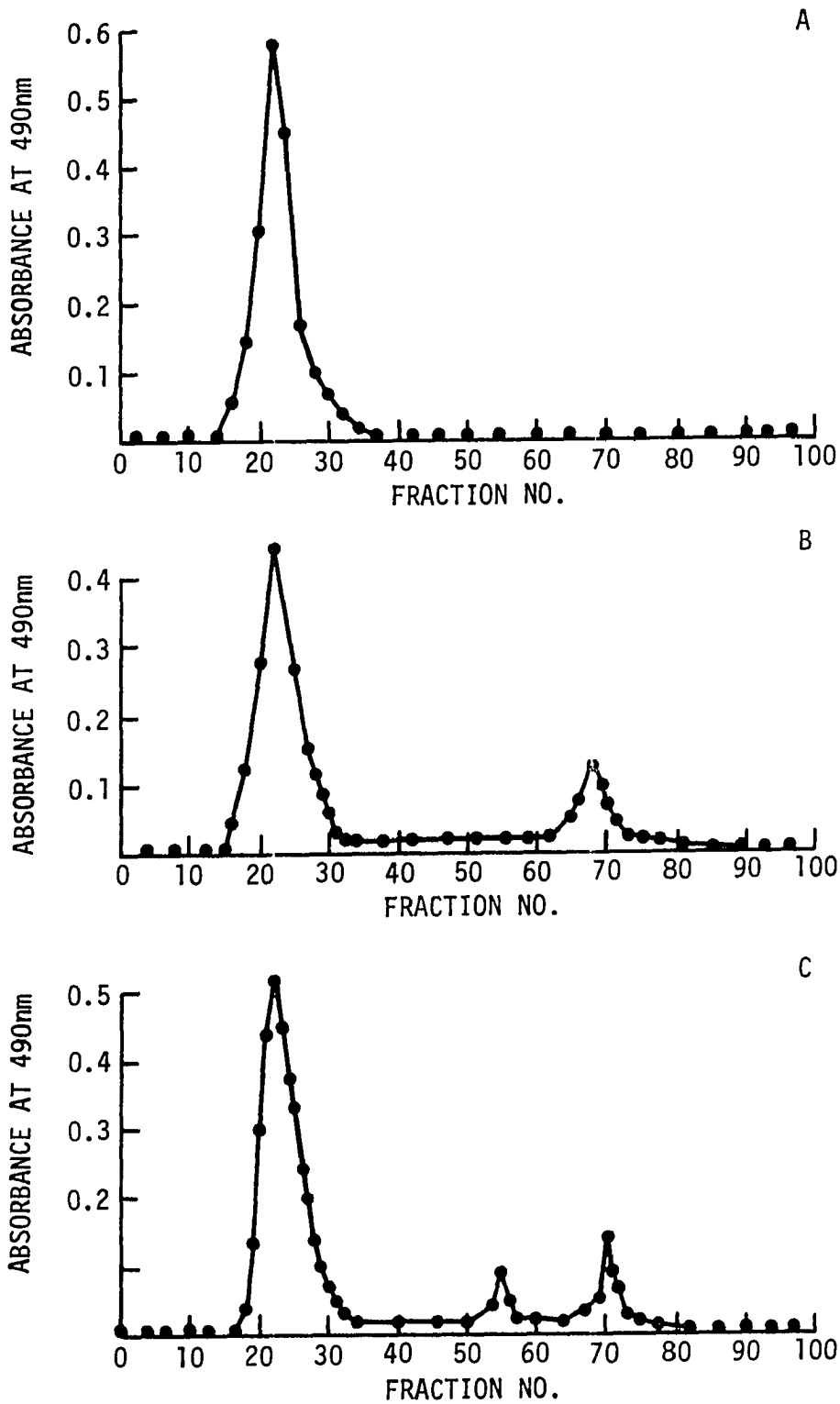
A
ABSORBANCE AT 490nm
0.6
0.5
0.4
0.3
0.2
0.1
0 10 20 30 40 50 60 70 80 90 100
FRACTION NO.
B
ABSORBANCE AT 490nm
0.4
0.3
0.2
0.1
0 10 20 30 40 50 60 70 80 90 100
FRACTION NO.
C
ABSORBANCE AT 490nm
0.5
0.4
0.3
0.2
0 10 20 30 40 50 60 70 80 90 100
FRACTION NO.

48

Figure 49. Polyacrylamide gel electrophoresis of the EDTA-soluble fraction from the whole wall (A) and from coccoliths (B). Walls were prepared by Triton X treatment and free floating coccoliths were collected from the growth cultures. Gels were stained with Alcian Blue (AB) for acidic carbohydrates and with C omassie Blue (CB) for proteins. Only four carbohydrate bands are observed with this technique. Note the similarity between the two samples, (A) and (B)

Figure 50. Polyacrylamide gel electrophoresis of the isolated acidic polysaccharides obtained by cutting and eluting polysaccharides from band no. 4 (a) and band no. 1 (b). After treating (b) with 2% SDS in 0.15 M NaCl for 2 minutes, the dissociation effect of SDS and heat on this molecule can be observed. Gels were stained with Alcian Blue (AB) for acidic carbohydrates and with Coomassie Blue (CB) for proteins. No protein band is observed

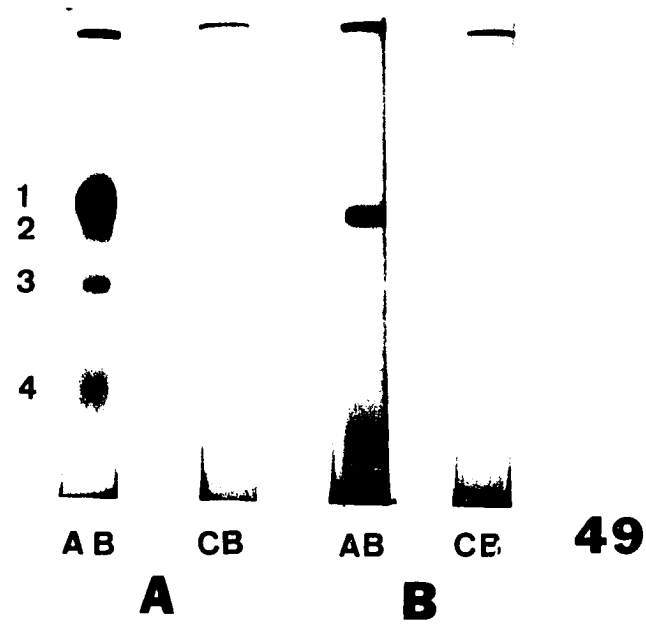

49

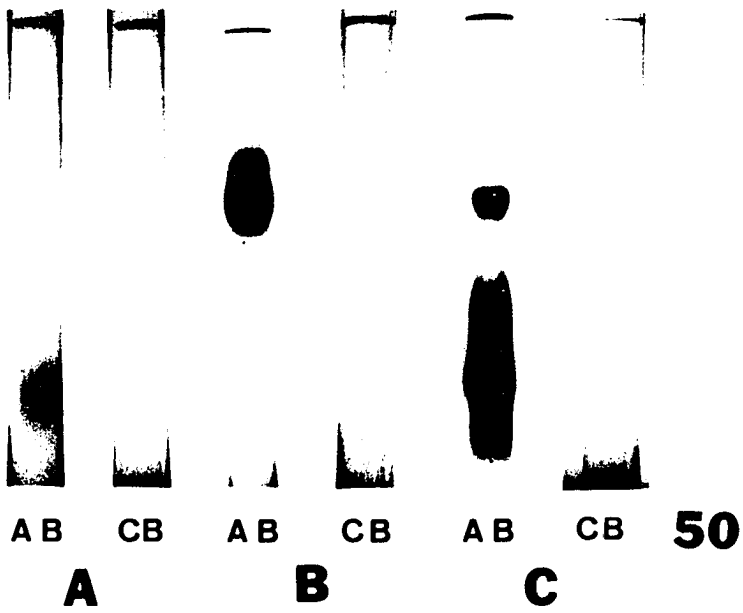

50

visible for the corresponding (CB) gel. The first two carbohydrate bands were very close together and it seemed that two species of molecules must have been mixed. In the coccolith soluble fraction (B), one distinct and two faint carbohydrate bands and no protein bands were observed. The fourth band for both samples appeared very diffused and it seemed to be a highly negatively charged (polyanionic) molecule, since it migrates along the gel with or ahead of the tracking dye. Although there are protein species in these samples (see SDS gel electrophoresis and colorimetric results) in the absence of SDS, these protein molecules do not migrate along the gels. So, this technique could screen the carbohydrate fractions of ESF from the proteins. This allowed the use of a preparative gel electrophoretic technique for polysaccharide isolation, but owing to the small quantity of ESF and the diffusion of components from the gel into the buffer system during the experiment, this method was not very effective. Finally, a suitable technique was found. It was based on cutting, eluting, and lyophylizing a specific polysaccharide band from the polyacrylamide gel (for further details of the technique, see Materials and Methods) and permitted the isolation of different acidic polysaccharides. Figure 50 shows the polyacrylamide gel electrophoresis of polysaccharides obtained from band no. 4 (A) and band no. 1 (B) of ESF.

While previous ultracentrifugal results of ESF (see Figure 42) showed two distinct sedimenting molecules in the absence of SDS and only one prominent peak after treating the ESF with 2% SDS and boiling (see Figure 43), the electrophoretic pattern of the same sample did not reveal such a change (Figure 44). This is probably due to sensitivity of two

techniques to concentration changes of each species of molecules, dependency of electrophoresis to distribution of charges on molecules, and ionic conditions. However, such correlation between electrophoretic results and ultracentrifugation behavior was possible when the isolated (pure form) of the molecules were used. After eluting the first polysaccharide band (Figure 50, B) and treating with 2% SDS at 100^{o} C for 2 minutes, the carbohydrate molecules dissociated into smaller components. Figure 50 (C) shows dissociation effects of SDS and heat and reveals that, under these conditions, partial dissociation of the polysaccharide occurred.

Analytical ultracentrifugation

The ultracentrifugal results of isolated acidic polysaccarides are shown in Figures 51, 52, and 53. Two distinct peaks were observed for the first electrophoretic band when the solvent was 0.15 M NaCl. The sedimentation coefficient corrected for solvent viscosity, density, and solute concentration (see Appendix B) are 4.284 and 1.558 Svedbergs (Figure 51). Figure 52 shows the ultracentrifugal behavior of the third electrophoretic band eluted from gels. The Schlieren pattern illustrates the presence of a low sedimenting molecule similar to the first peak of the first sample (Figure 51). Due to the low concentration of the sample in Figure 52, it was not possible to calculate a sedimentation coefficient. The ultracentrifugal behavior of the fourth electrophoretic band eluted from the gel is seen in Figure 53. A single peak is observed in the presence of 0.15 M NaCl. The sedimentation coefficient corrected for solvent viscosity and density and solute concentration is

Figure 51. Schlieren patterns of acidic polysaccharide (eluted from the first band of polyacrylamide gel) in 0.15 M NaCl. The pictures were taken at 16-minute intervals after rotor reached a speed of 60,000 rpm and the temperature of the run was 21° C

Figure 52. Schlieren patterns of acidic polysaccharide (eluted from the third band of polyacrylamide gel) in 0.15 M NaCl. The pictures were taken at 60,000 rpm, 16-minute intervals, and 20° C

Figure 53. Schlieren patterns of acidic polysaccharide (eluted from the fourth band of polyacrylamide gel) in 0.15 M NaCl. The pictures were taken at 16-minute intervals, 60,000 rpm, and 21° C


51
52
53

1.82 Svedbergs.

Electron microscopic observations

Figures 54 and 55 are high resolution electron micrographs showing the appearance of acidic polysaccharides under the electron microscope when the solvent is 0.15 M NaCl. Figure 54 shows the morphological features of molecules obtained from eluting the first band of gels after electrophoresis. One can find definite examples of order in this figure. Figure 55 shows the aggregated acidic polysaccharide obtained from the fourth band of gels. This molecule is highly negatively charged (in the electrophoretic field and even in the absence of SDS, it moves with or ahead of tracking dye), forming a crystalline lattice with center to center spacing of about 60-66 Å when the molecules are in 0.15 M NaCl.

Enzymatic degradation of wall and uronic acid assay

The effect of pectinase was observed on isolated walls both microscopically and biochemically. Figure 57 is an electron micrograph showing the isolated walls after treating them with 40 mg/l pectinase for 48 hours at 4.5. The degradation effect of pectinase especially on coccoliths is visible. Figure 58 (A) illustrates the effect of different concentrations of pectinase on 10 mg of dry walls. Whole walls were incubated in pectinase for 45-50 hours, the supernatant was collected, and the amount of uronic acid released due to pectinase at different concentrations of enzyme was measured (for details of procedure, see Materials and Methods). One can see that pectinase degrades the wall and releases a considerable amount of uronic acid. From Figure 58 (A), the most effective concentration was 40 mg/ml enzyme. The release of

Figure 54. TEM of the acidic polysaccharide obtained from eluting the first band of a polyacrylamide gel. The molecules were in 0.15 M NaCl. Preparation was stained by 1% uranyl acetate in 50% ethanol. X 73,800

Figure 55. TEM of acidic polysaccharide molecules obtained from the fourth band of a polyacrylamide gel. In 0.15 M NaCl, these molecules often form crystalline latice arrangement with spacing of about 60-66 Å. Preparation was stained with 1% uranyl acetate in 50% ethanol. X 20,800

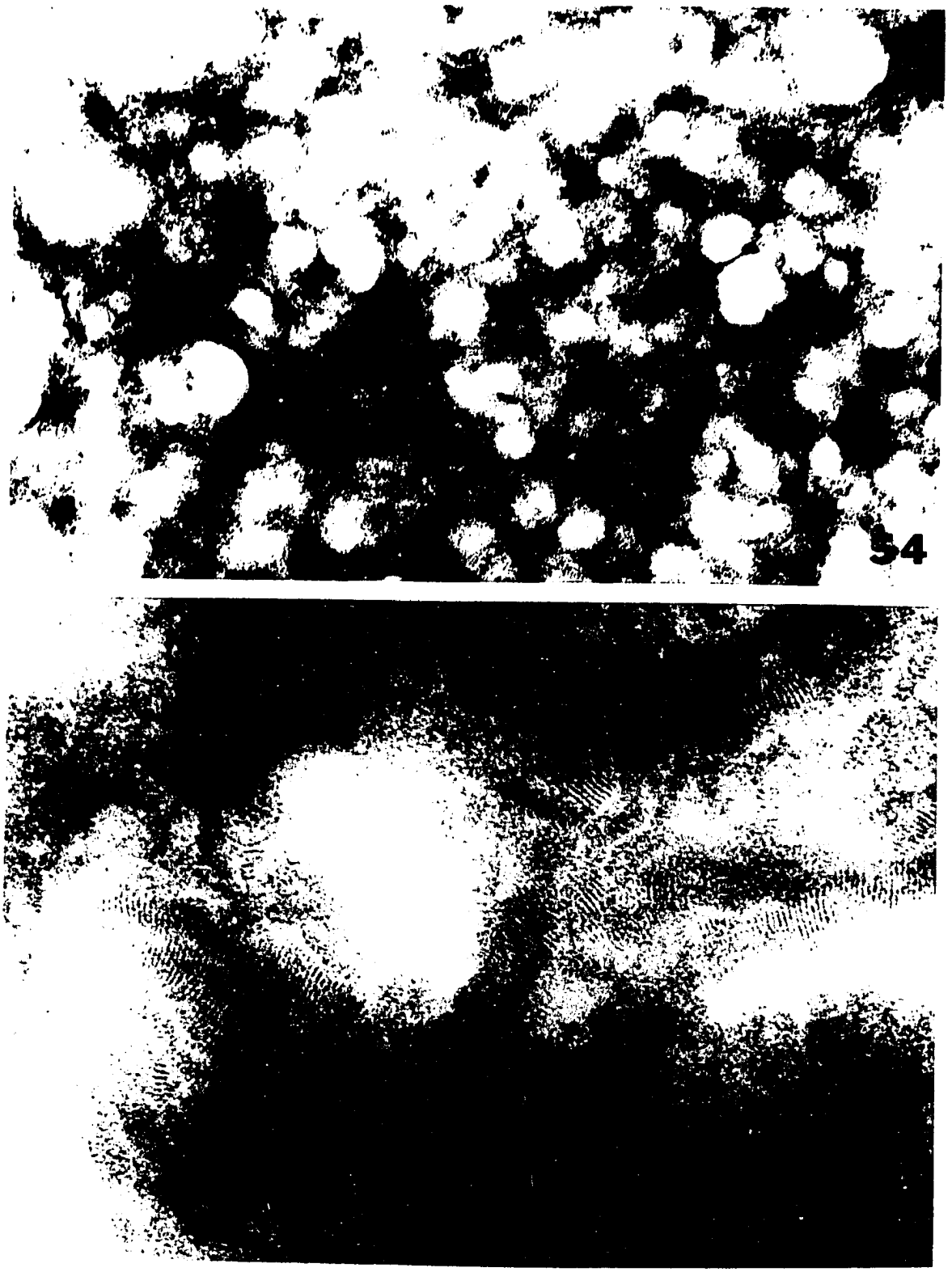
54

Figure 56. TEM observation of the void volume of Biogel P-60 column. Note the different levels of aggregation. X 47,200

Figure 57. Destruction effect of 40 mg/liter pectinase on the wall of H. carterae. X 22,800

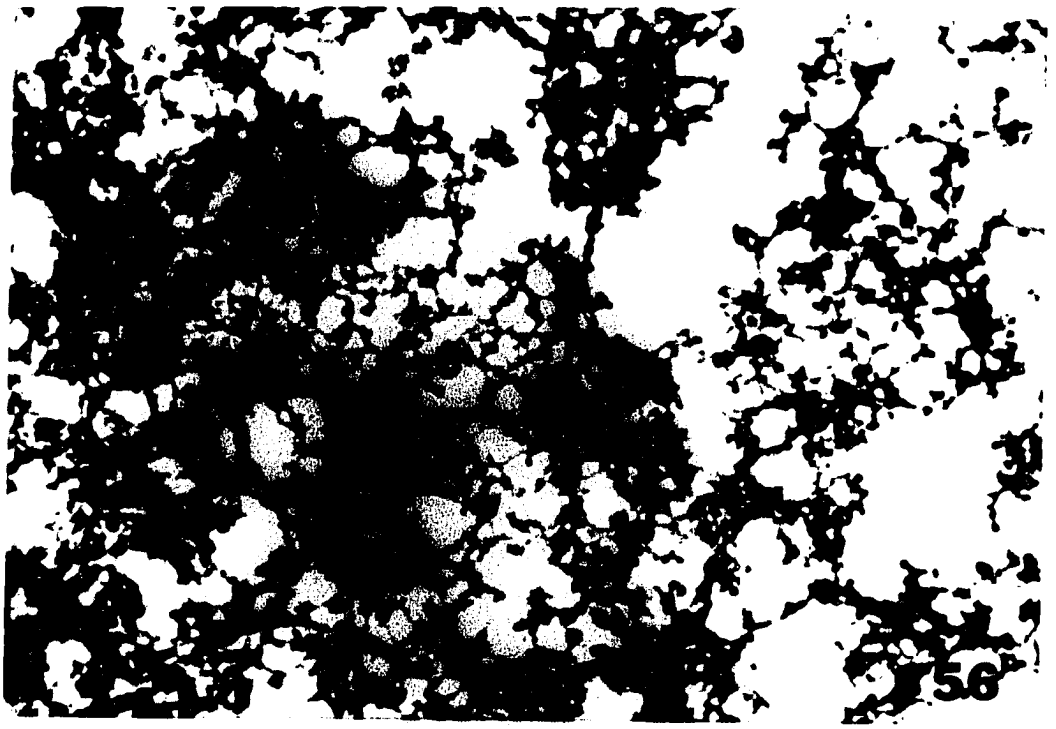
56


57

Figure 58. Cell wall digestion by pectinase

A) The release of uronic acid from the cell wall at different concentrations of pectinase

B) Effect of varying the length of pectinase treatment on release of uronic acid from the cell wall

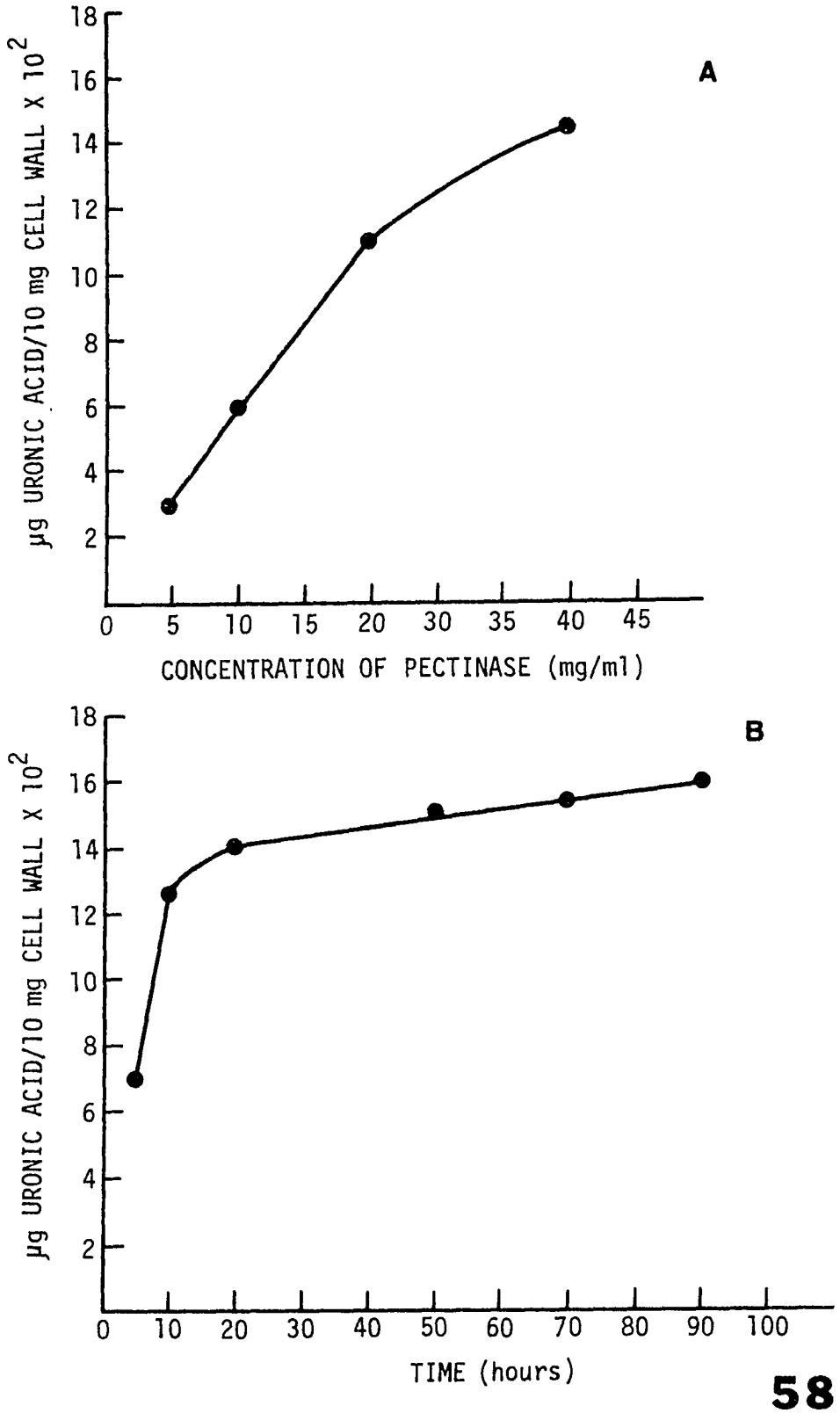
A
µg URONIC ACID/10 mg CELL WALL X 10^2
18
16
14
12
10
8
6
4
2
0 5 10 15 20 30 35 40 45
CONCENTRATION OF PECTINASE (mg/ml)
B
µg URONIC ACID/10 mg CELL WALL X 10^2
18
16
14
12
10
8
6
4
2
0 10 20 30 40 50 60 70 80 90 100
TIME (hours)

58

uronic acid was also assayed when isolated, dry walls were subjected to 40 mg/ml pectinase at different lengths of time. The effect is shown in Figure 59 (B). Apparently, after 10 hours the enzyme has been degraded or the substrate is used up (the plateau portion of Figure 59, B).

Cytochemical Localization of Acidic Polysaccharides and Ionic Interaction of Wall Components

Ruthenium red interactions

The location of negatively charged molecules (polysaccharides) in the cell wall of H. carterae was observed microscopically with ruthenium red and cationized ferritin as electron dense molecules.

Ruthenium red (ammoniated ruthenium oxychloride) is an inorganic, crystalline, synthetically prepared compound which is moderately heavy (atomic number 44). It has been used for a long time in light microscopy as a standard stain for pectins in plant tissues. For electron microscopy, it was introduced by Reimann (1961). Ruthenium red is a hexavalent cation (diameter, 1.13 nm) and reacts with a large number of polyanions. It is a strong oxidant and probably acts as a stain as well as a fixative along with osmium teroxide. The maximum contrast is obtained when ruthenium red and osmium tetroxide are applied together. Chloride free cacodylate buffer was used in this method since it has been considered to be the most ideal one for maximum contrast (Hayat, 1975).

Figure 59 shows the cell wall and subsurface of cells maintained under standard conditions of growth. Fibrillar projections appear on

Figure 59. A thin section through the wall and subsurface of H. carterae. Normal fixation, embedding, sectioning, and staining techniques for TEM do not preserve and stain fibrous projections well. When a saturated solution of ruthenium red in cacodylate buffer is added to OsO_4 and the normal fixation procedure is followed, there is no need to post stain the section. In this micrograph, one can see coccoliths (C) with fibrous projections (FP), scales (S), crystalline vesicles (CV) containing electron dense material (arrows), cell membrane (CM), and a part of a chloroplast (Ch). X 57,600

Figure 60. TEM of the isolated cell wall, coccoliths (C) with fine fibrillar projections (FP) coming from their outer surfaces; scales (S) are present. On the right side of the micrograph, a section through rim elements of a coccolith is observed. X 40,800

60

the upper surface of coccoliths in much higher contrast than normal, apparently owing to the use of the saturated solution of ruthenium red in osmium tetroxide and chloride-free cacodylate buffer. The most interesting feature of this figure is the presence of a large number of single membrane bounded vesicles, "crystalline vesicles" in the cell wall. Some of these vesicles contain the electron dense crystalline component or ruthenium red positive material. Figure 60 is a section through the isolated wall which also shows the deposition of ruthenium red on fine fibrous components on the exterior surface of coccoliths.

Figures 61 and 62 are transverse sections through walls of cells maintained on the normal diurnal cycle. Both figures were prepared by the ruthenium red/osmium/cacodylate procedure. In addition, Figure 61 was also post-stained with uranyl acetate and lead citrate. Both figures show comparable structures of fibers on the top of coccoliths, on columnar material, on the top and bottom of scales, and on the proximal surface of the coccolith base. Post-staining (uranyl acetate and lead citrate) seems to introduce almost too much electron density for sections of this thickness.

Cationized Ferritin Interactions

Cationized ferritin is a polycationic derivative of ferritin used for labeling negatively charged molecules. It is prepared from horse spleen ferritin in which the carboxyl groups are cationized with N,N dimethyl-1,3 propanediamine (Danon, 1972). At a physiological pH range, about 50-60% of the carboxyl groups are cationized and so the molecule can form ionic interactions with negatively charged molecules. The

Figure 61. A section through a cell using a modified fixation procedure; fixed with a ruthenium red-osmium-cacodylate mixture, post-stained with uranyl acetate and lead citrate. X 44,000

Figure 62. TEM showing ruthenium red-osmium attached to columnar material (CM), glue (G), scales (S), and the external surface of coccoliths (arrows). Fixation in 4% glutaraldehyde for 5 hours followed by 1% OsO_4 containing 15 mg/ml ruthenium red for 5-6 hours. The section was not post-stained. X 63,000

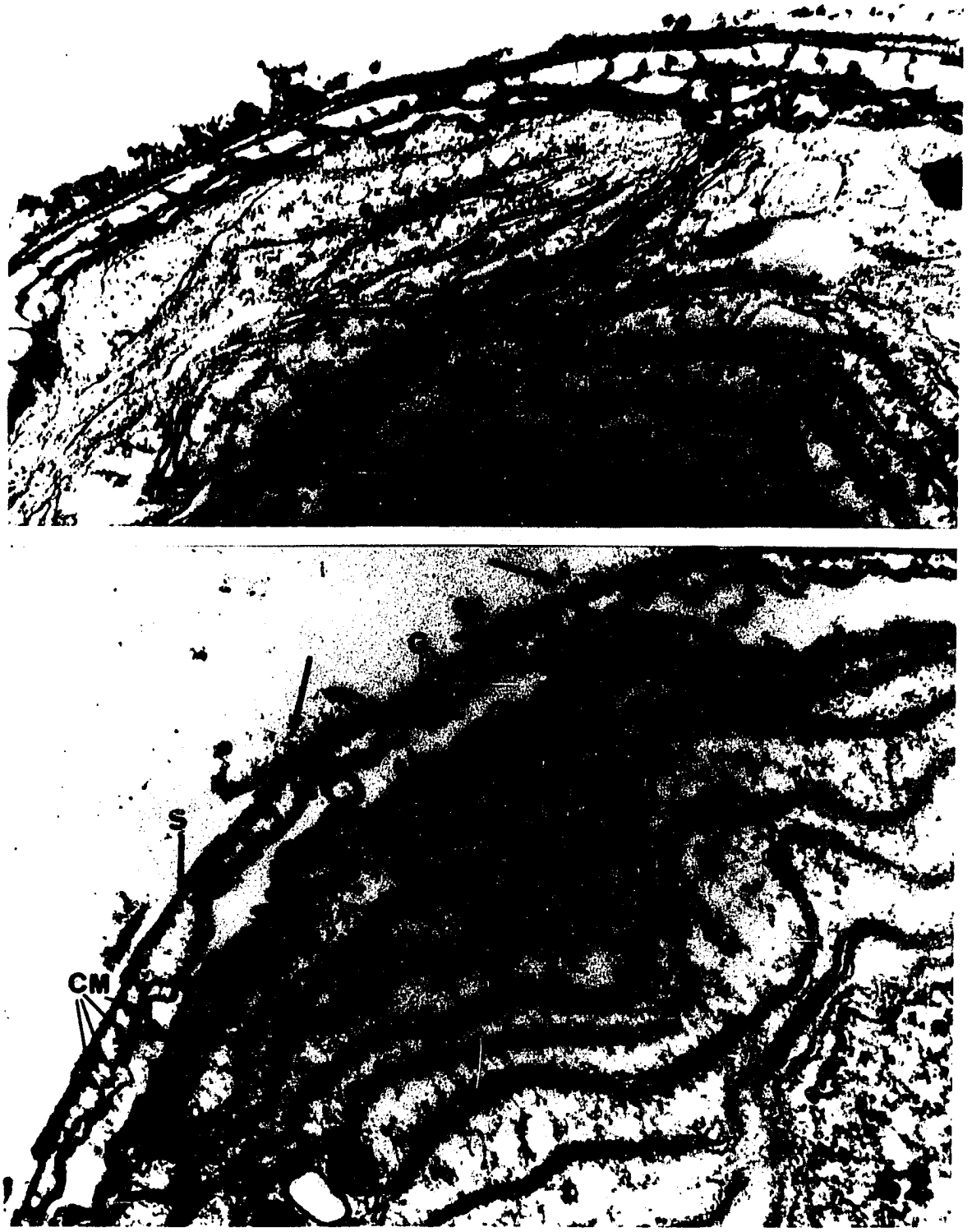
S
CM

molecule is 110 Å in diameter with a molecular weight of 750,000 d. The presence of iron in the molecule provides very useful electron-dense depositions wherever the ferritin label becomes attached.

Electron microscopic observations demonstrated that the labeling of the cell wall with cationized ferritin may take place both before and after fixation with glutaraldehyde at pH 7.5 (Figures 64, 65). Comparison of the control (Figure 63) with cells treated with cationized ferritin before (Figure 64) and after (Figure 65) fixation with glutaraldehyde can be seen in Figures 63, 64, and 65. Labeling with ferritin prior to fixation has the advantage that it can be performed at physiological conditions. Figure 64 shows the granular ferritin depositions on columnar material, the top and bottom of scales, and the bottom of coccolith base in samples treated with cationized ferritin before fixation. Prefixation of Hymenomonas preparations and labeling with cationized ferritin shows a significant difference (Figure 65). Only the outer surface of coccoliths was labeled. It seems that, in prefixed samples, ferritin molecules tend to aggregate along the fibrous projections of the outer surface of coccoliths which were also visible in ruthenium red treated samples (see Figures 61, 62). This can be seen for further evidence in Figure 67. Figures 66 and 67 are sections through the isolated cell walls treated with ferritin before or after fixation with glutaraldehyde. Figure 66 shows similar results obtained when the whole cell was treated with cationized ferritin. No cationized ferritin deposits are seen on the outer surface of coccoliths. Prefixation of isolated walls also illustrats the same results revealed

Figure 63. A thin section through the wall and subsurface of a control cell. Normal fixation, embedding, sectioning, and staining techniques for TEM were carried out. Coccoliths (C), scales (S), columnar material (arrows), and crystalline vesicles (arrowheads) are present. X 44,400

Figure 64. Cells treated with 0.5 mg/ml cationized ferritin in artificial sea water (PMW II) for 30 minutes at standard conditions of growth and normal EM procedures. Note the electron dense granules of ferritin binding to the bottom surface of the coccolith, both sides of scales (arrows) and columnar material (arrowhead). X 49,200

Figure 65. Cationized ferritin treated cell showing the effect of fixation on the cell wall. Preparation was made by using 0.5 mg/ml cationized ferritin in cacodylate buffer for 30 minutes after cells were fixed with 4% glutaraldehyde followed by the normal EM preparative procedures. Note that cationized ferritin was bound only to the external surface of coccoliths and scales (arrows). No binding occurs to the scales embedded inside the wall and columnar material (arrowheads). X 70,200

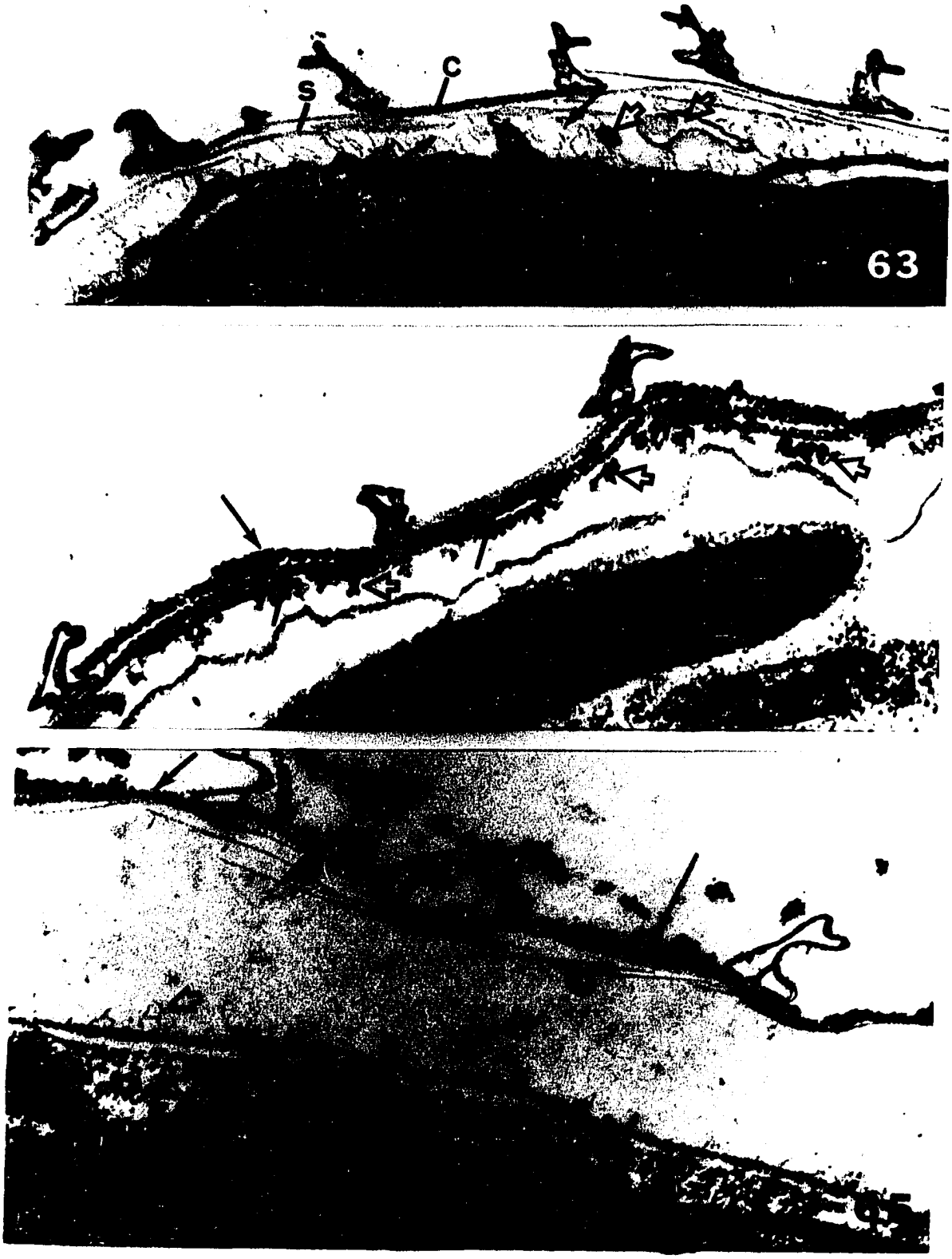
S
C
63

Figure 66. Section through the isolated cell wall treated with 0.5 mg/ml cationized ferritin for 30 minutes before standard fixation procedures. Different components of the wall including coccolith (C), scales (S), glue (G), and columnar material (CM) are represented. The electron dense granules are cationized ferritin. No ferritin binds to the top of the coccoliths. X 35,200

Figure 67. Section through an isolated cell wall. After fixation with 4% glutaraldehyde, pH 7.5, walls were treated with 0.5 mg/ml cationized ferritin for 30 minutes, after which normal EM procedures were followed. Note that cationized ferritin primarily binds to the outer surface of coccoliths (arrowhead). Also one can see the cationized ferritin binding sites inside, and outside, of the rim elements of the coccolith, showing the presence of negatively charged molecules (arrows). X 63,000

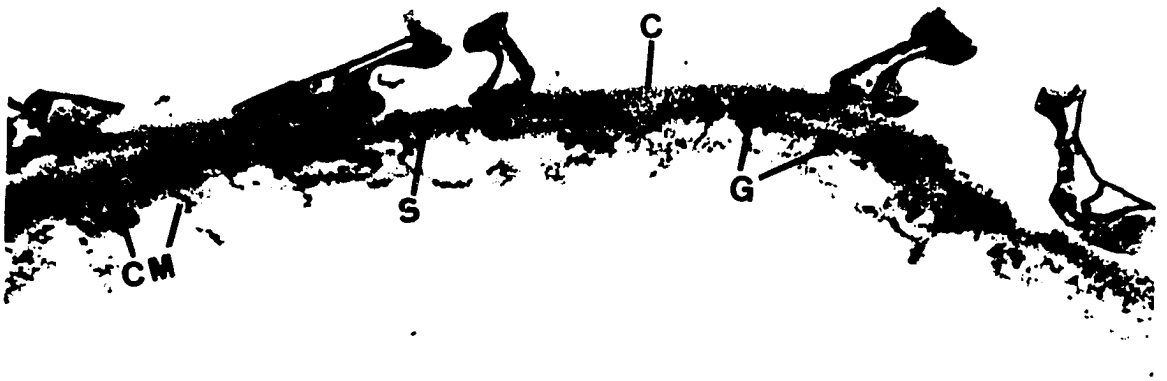

66

for whole cells. The accumulation of ferritin molecules are visible along the fibrous protections of the outer surface of coccoliths. Several layers of cationized ferritin deposits with a regular arrangement can be observed in partitions within the coccolith rim (Figure 67). Also, 2-3 layers of ferritin molecules are present on the outside of the coccolith rims. So cationized ferritin, as a polycation of known size, appears to serve as a good marker for localization of negative charge distribution in the cell wall of Hymenomonas.

Formation of protoplasts

Enzymatic methods have been successful in isolating protoplasts from leaf and other tissues of plants. The technique involves the use of diverse sources of enzymes, such as pectinase and cellulase (Cocking, 1972) usually obtained from fungi. In algal systems, the same method has only been successful on a few species (see Discussion). The following results revealed that the technique involving the use of pectinase and cellulase is also efficient for removing the wall of Hymenomonas, thereby deriving protoplasts. Protoplast isolation was performed for two major purposes: 1) to investigate the regeneration of the wall and the kinetics of wall formation by protoplasts, and 2) to study the chemical inhibition of cell wall formation.

The method involves the utilization of 3% macerozyme and 5% cellulase. These were used as an individual enzyme treatment, as a sequential two-step enzyme sequence, and a mixed one-step enzyme treatment. Table 2 shows different treatments, time of enzyme incubation, and the percentage of protoplast formation by different procedures. The cell

Table 2. The percentage of protoplasts obtained due to different procedures

Enzyme treatment	Time (hours)	% Protoplasts
Macerozyme	2-3	0
Cellulase	2-3, 20	0, 5
Sequential[a]	2, 4-5	98
Mixed (Ca^{++})[b]	4-5	95-98
Mixed (no Ca^{++})[c]	4-5	8-10

[a]Cells were incubated in 3% macerozyme for 2 hours prior to 4-5 hours treatment with 5% cellulase.

[b]Cells were incubated in a mixture of 3% macerozyme and 5% cellulase in the presence of 8 mM $CaCl_2$.

[c]Cells were incubated in a mixture of 3% macerozyme and 5% cellulase in the absence of $CaCl_2$.

concentration used for each experiment was 3-4 x 10^5 organisms/ml of enzyme.

The results presented in Table 2 indicate that the mixed procedure is probably the most efficient one. The percentage of protoplasts obtained when cells were incubated in a mixture of 3% macerozyme and 5% cellulase in the presence of Ca^{++} is almost the same as that of the sequential treatment, but, in this procedure, cells have been exposed to enzyme for a shorter period than cells in sequential treatment. Table 2 also shows that Ca^{++} plays an important role in somehow stabilizing protoplasts during the isolation. In both sequential

and mixed procedures, presence of Ca^{++} is necessary. For sequential treatment, Ca^{++} was added to the macerozyme solution.

The criteria for protoplast formation were based upon 1) Nomarski differential interference contrast observations of the cell surface, 2) the use of calcafluor white M_2R as a stain for cellulose, in which cells with a cell wall absorb the dye and emit a blue fluorescence when exposed to ultraviolet light. The relative number of fluorescent cells in the population was used as a measure of the efficiency of the enzymatic treatment, and 3) TEM and SEM observations.

When cells are placed in an enzyme containing solution, the first thing that can be seen is the shedding of the flagella. The protoplasts tend to "swell-out" of the wall which appears to be rapidly degraded and thus weaker anteriorly. When protoplasts are freed of the cell wall, they round up and form clumps of protoplasts. Figure 68 is a Nomarski light micrograph of protoplasts obtained after sequential treatment of cells with macerozyme and cellulase. Protoplasts tend to stick together presumably owing to charge effects on the now-naked outer membranes, forming clumps of cells. Figure 69 is a scanning electron micrograph of a protoplast showing the absence of the wall components on the surface. Figure 70 is a TEM micrograph of a protoplast obtained from sequential enzyme treatment. This micrograph also shows no structured wall components on the cell surface.

Observations by electron microscopy revealed that the site of enzyme action on the cell wall of H. carterae is primarily the scale. Figure 71 illustrates that, after sequential enzyme treatment,

Figure 68. Nomarski differential interference contrast light micrograph showing protoplasts of H. carterae. The average diameter of protoplast is about 7 um. X 2,752

Figure 69. SEM micrograph of protoplasts obtained after sequential treatment of cells with 3% macerozyme (2 hours) followed by 5% cellulase (4-5 hours). X 10,120

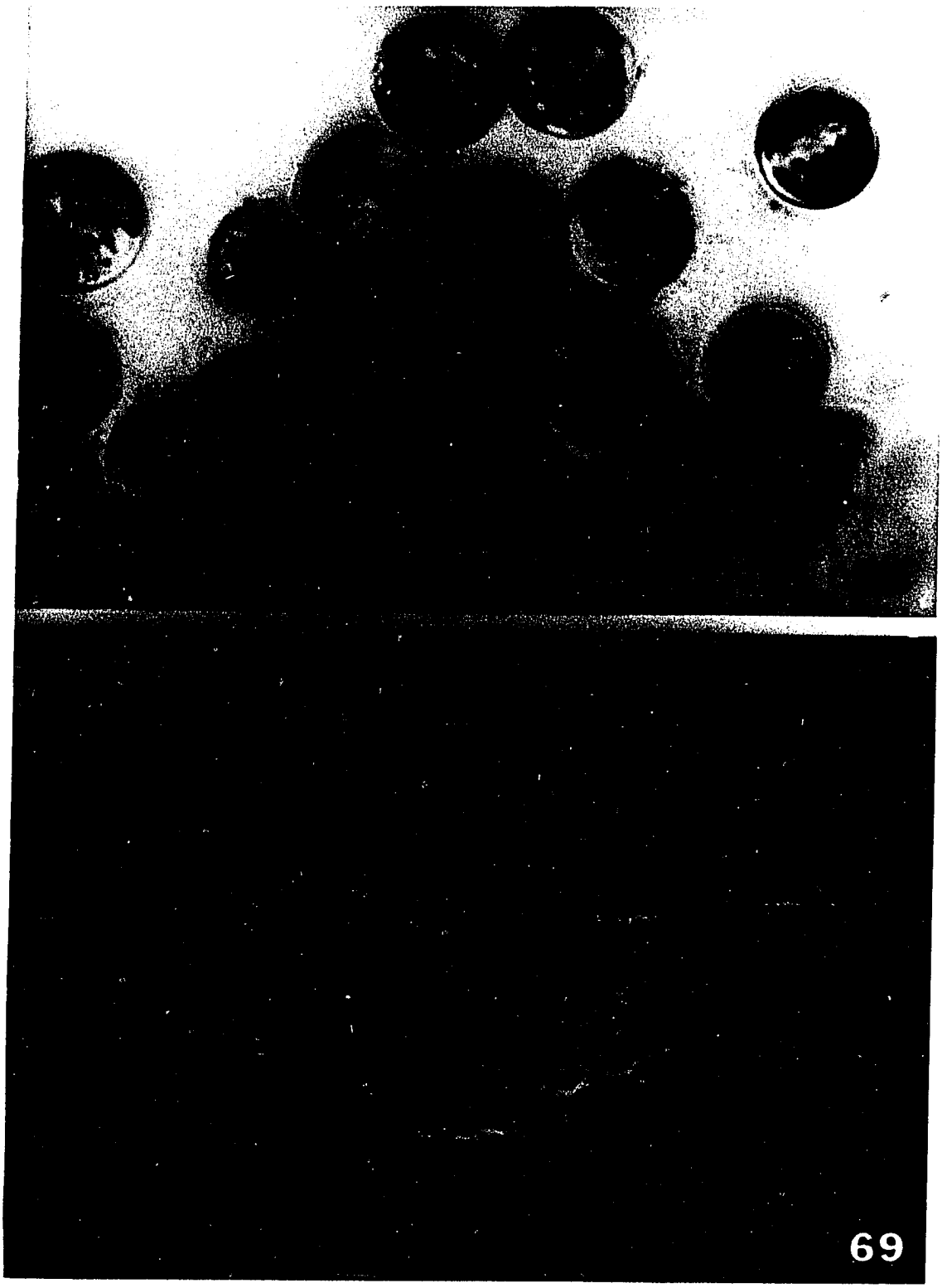
69

Figure 70. TEM micrograph showing a section through a protoplast Visible are the nucleus (N), rough endoplasmic reticulum (RER), mitochondria (M), and a part of a chloroplast (Ch). There are no formed wall structures on the surface. X 30,100

Figure 71. Sequential treatment of cells by macerozyme followed by cellulase causes the degradation of the cell wall. Enzymatic action is most effective on the scale. It is difficult to tell whether radial or concentric microfibrils are degraded more rapidly. X 45,000

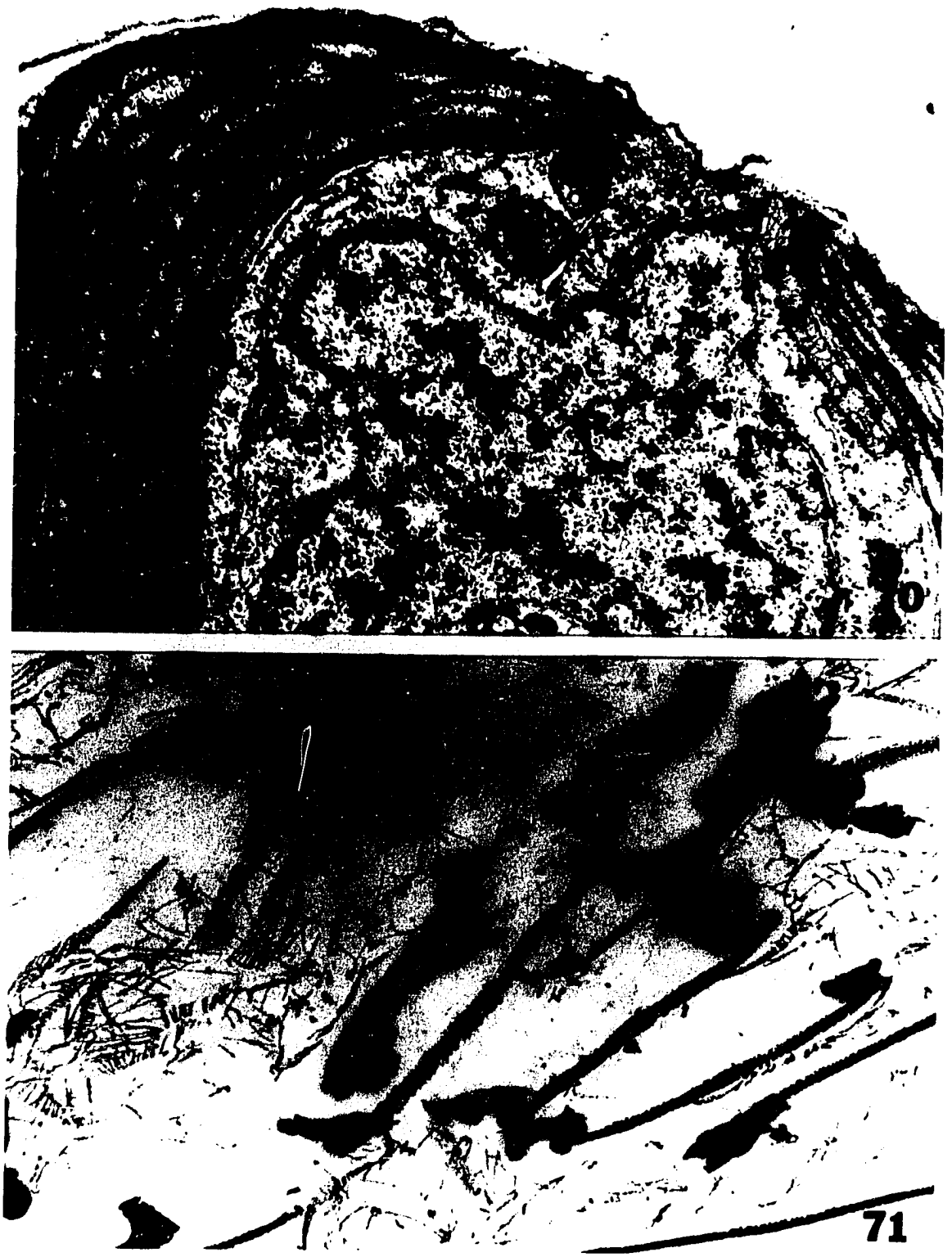
0
71

coccoliths and degraded scales are released into the enzyme mixture. The part of the scale most sensitive to enzyme treatment is the concentric microfibrils. Figure 72 also reveals some biochemical differences between the scale and the base of the coccolith, with the latter being quite resistant to enzymatic degradation. The only visible effect of enzymes on the coccolith is some disorganization of the calcareous coccolith rim.

Growth of protoplasts and Cell Wall Regeneration Under Standard Conditions

Growth study

Comparison of the logarithmic growth of a control sample and protoplasts grown under standard conditions can be seen in Figure 72. Logarithmic growth at a rate of 0.8-1 generation per day was maintained for 5-6 days for the control and at a rate of 0.4-0.5 generation per day for the same period of time for protoplasts. The maximum cell density was 2×10^5 and 1.4×10^4 cells/ml for the control cells and protoplasts, respectively.

The kinetics of wall formation and coccolithogenesis during wall recovery

Following sequential enzyme treatment, cells were kept in PMW II under standard conditions of growth. The percentage of live protoplasts was determined by using fluorescine diacetate or by counting the number of cells which produced flagella. The percentage survival was about 86%. Cells exposed to macerozyme and cellulase sequentially exhibit a coccolith production of 2-2.5 coccoliths per hour during the 25-30

Figure 72. Effect of sequential enzyme treatment on cells, showing that the growth of protoplasts during recovery and under standard conditions is much lower than the control

Figure 73. Coccolithogenic pattern following sequential macerozyme-cellulase treatment. In the control sample, the cells were decalcified according to Williams (1974). The kinetics of coccolith formation for enzyme treated cells and controls were 2-2.5 and 9-10 coccoliths per cell per hour, respectively

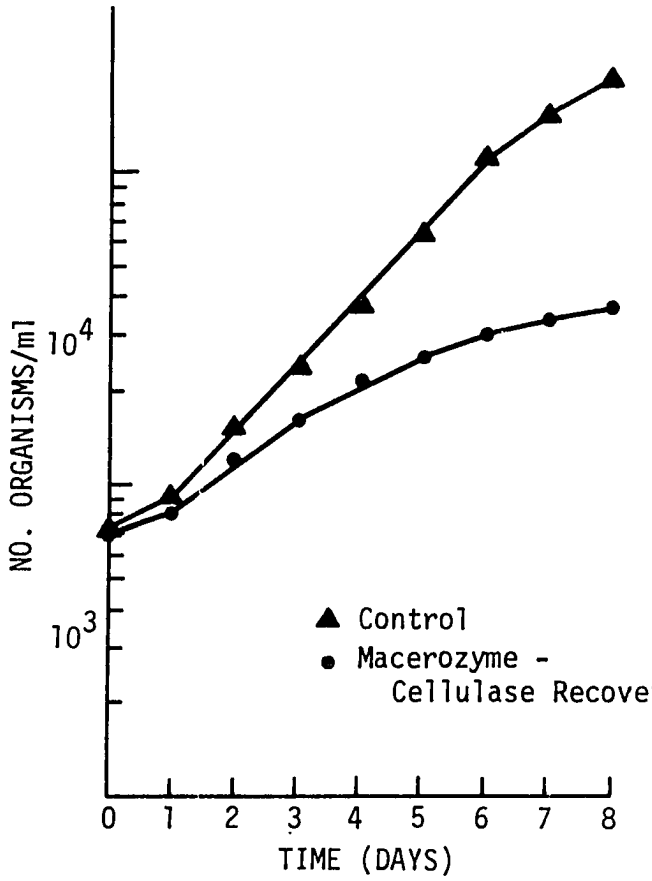
NO. ORGANISMS/ml
10^4
10^3
Control
Macerozyme - Cellulase Recovery
0 1 2 3 4 5 6 7 8
TIME (DAYS)

72

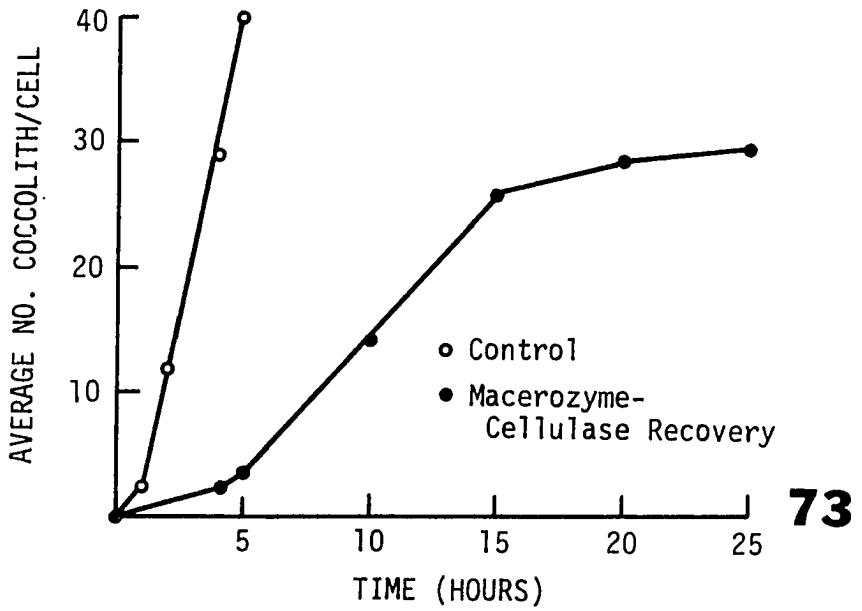
AVERAGE NO. COCCOLITH/CELL
40
30
20
10
Control
Macerozyme- Cellulase Recovery
5 10 15 20 25
TIME (HOURS)

73

hours recovery (Figure 73). This shows a sharp decrease in coccolithogenesis compared to the control with the rate of coccolith production of 8-10 per hour. Light microscope observation of recovery cells showed that, within 30 minutes to 1 hour after transfer to a growth medium, flagella were regenerated and began to beat. The recovery cells were present as singles or clumps, and after 4-5 hours of recovery new coccoliths started to appear on the cell surface. Such new coccoliths were randomly dispersed over the cell surface. The kinetics of coccolithogenesis was monitored by Nomarski light microscopy at different times of recovery. The histogram of recovery from macerozyme-cellulase treatment is presented in Figure 74, which shows the distribution of several groups of cells with different numbers of coccoliths at various times of recovery.

Regeneration of the Cell Wall

Recovery cells at 5, 12, and 24 hours were observed by TEM and SEM. Figure 75 shows a section of a cell at 5 hours recovery. Columnar material is beginning to appear on the cell surface. A number of scales (S) have already extruded from the cell and are present on the external surface. Figure 76 is a section of a cell at 12 hours recovery. For this part of the cell, considerable columnar material is present. Many small, connected, single membrane-bound vesicles, so-called "crystalline vesicles" or "paramural bodies" are present, along with scales and coccoliths, and the wall is approaching a normal appearance. Another example of a cell at 12 hours recovery is shown in Figure 77. The cell has formed scales, columnar material and coccoliths. The fibrous projections

Figure 74. Histogram of recovery from sequential macerozyme-cellulase treatment illustrating the distribution of coccoliths per cell at different times of recovery. The distribution of coccoliths at different times of recovery was found by counting coccoliths per 50 cells in the population

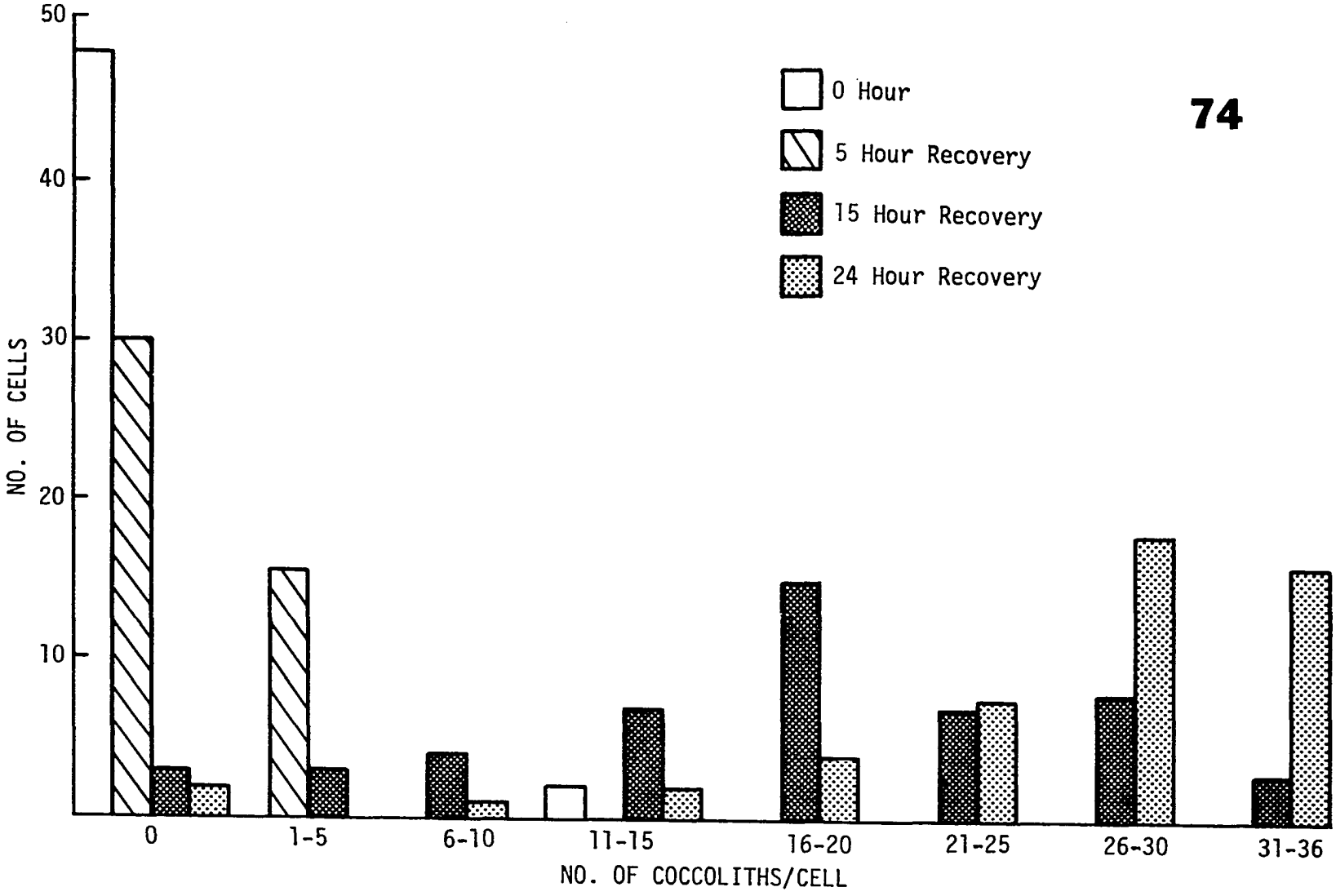
50
40
30
20
10
NO. OF CELLS
0 Hour
5 Hour Recovery
15 Hour Recovery
24 Hour Recovery
0
1-5
6-10
11-15
16-20
21-25
26-30
31-36
NO. OF COCCOLITHS/CELL

74

Figure 75. A thick section of a cell at 5 hours recovery from the sequential macerozyme-cellulase treatment. The appearance of scales (S), columnar material (CM), and electron dense material between the cell membrane (Cm) and chloroplast membrane (arrowheads). Free floating coccolith (FC), residual parts of scales (RS), and the nucleus (N) are visible. X 31,200

Figure 76. A thick section through a cell at 12 hours recovery from sequential macerozyme cellulase treatment. Note the appearance of columnar material (arrows) and strings of single vesicles or crystalline vesicles (arrowheads). X 68,000

Figure 77. A thin section through a cell at 12 hours recovery from sequential enzyme treatment. Coccoliths (C), scales (S), and columnar material (arrowhead) are present. Note the abnormal rim of the coccolith (arrow). The fibrous projections on the top of the coccolith are visible. X 49,200

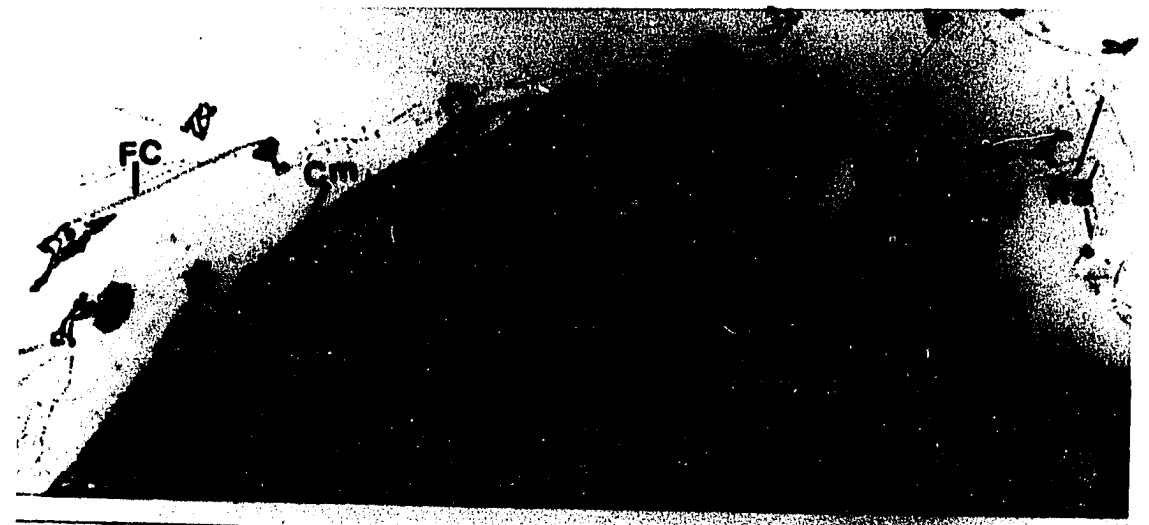
FC
CM


76


77

on the distal surface of the coccolith are nicely visible. Figure 78 is a scanning electron micrograph of cells at 10 hours recovery. The distribution of different classes of cells with various numbers of coccoliths is visible. At this time of recovery, some cells still do not have coccoliths. The strands of fibrous components of the wall (coccolithonets) observed on coccoliths of normal cells grown under standard conditions are not visible yet. Figure 79 is a transmission electron micrograph of a regenerated wall after 24 hours recovery from sequential macerozyme-cellulase treatment. It shows a single layer of scales, columnar material and coccoliths. The coccolith bases are irregularly "wavy" with atypical shapes of the rims. Thus, under standard conditions of growth, protoplasts of H. carterae form a more or less complete and probably functional cell wall in something approximately a 24 hour recovery time. It seems worthy of noting that the building of a new wall in 24 hours is coincident with the time required to build a new wall for a daughter cell under standard conditions.

Chemical Inhibition of Wall Formation in Protoplasts of H. carterae

Coumarin and 2,6-dichlorobenzonitrite are two substances that specifically affect cellulose synthesis in higher plants and Acetobacter xylinum (Hara et al., 1973; Burgess and Linstead, 1976; Meyer and Herth, 1978; Satoh et al., 1976a,b). These compounds reversibly inhibit cell wall formation and, therefore, should be useful in investigating the presence of cell wall formation in protoplasts.

Figure 78. SEM micrograph of cells at 10 hours recovery from sequential macerozyme cellulase treatment. X 4,650

Figure 79. Section of cell at 24 hours recovery from enzymatic treatment. The coccolith on the right shows abnormal A and B rim elements (arrows) and a wavy base while on the left an inverted A element (arrowhead) is present. Present also are scales (S), columnar material (CM), chloroplasts (Ch), and nucleus (N). X 51,000

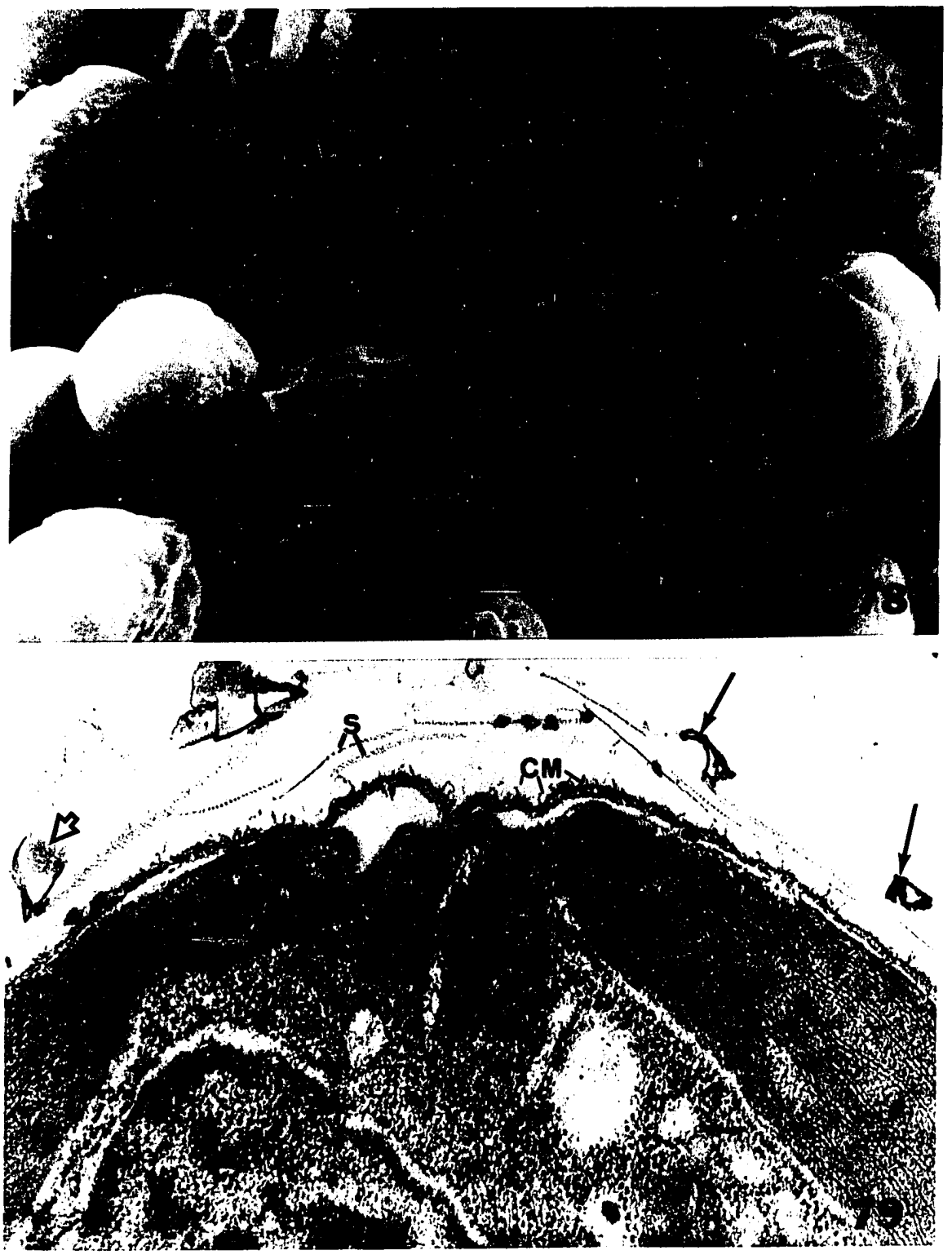
S
CM

Effects of coumarin

Different concentrations of coumarin containing media were used to assess the effect of a continuous treatment with coumarin on isolated protoplasts of H. carterae. In this experiment, 1-2 x 10^5 protoplasts/ml of coumarin-containing medium were used, the cells being kept under otherwise normal conditions of growth. These protoplasts were observed over a time span with Nomarski differential interference contrast microscopy. Concentrations of 10 mg/liter, 50 mg/liter, 100 mg/liter, 150 mg/liter, 200 mg/liter, and 500 mg/liter were used in different experiments. Coumarin at 10-50 mg/liter showed no effect on wall regeneration during 48 hours of frequent observation. Cells had normal flagella with many coccoliths. At 100 mg/liter of coumarin, cells had normal flagella and only some cells with 3-5 coccoliths were observed. At 200 mg/liter, most cells had no flagella and no cells with external coccoliths were observed. At concentrations higher than 200 mg/liter, wall regeneration was totally suppressed. Incubating protoplasts in media containing 250 mg/liter demonstrated a complete inhibition of wall formation and more than 85-90% of the cells had no flagella. Few cells had very small flagella which were able to vibrate without swimming. At 500 mg/liter of coumarin, both cell wall formation and flagella regeneration were completely stopped. Thus, at the concentration range between 200-500 mg of coumarin/liter of PMW II, cell wall formation was totally inhibited.

Viability after coumarin treatment and reversibility of cell wall inhibition

Coumarin affects Hymenomonas by inhibiting cell wall formation. It also causes cells to lose their flagella. Both of these effects are dependent upon the concentration of coumarin and are reversible. The results of coumarin treatment are shown in Table 3.

The results presented in Table 3 show that, in addition to wall inhibition due to 200-500 mg/liter coumarin treatment, flagella formation also stops. At 250 mg/liter coumarin, cytokinesis is completely abolished and, after one week treatment, about 8% of the protoplasts are multinucleated. During this period, no increase in number of protoplasts was observed. When protoplasts from 250 mg/liter coumarin are transferred into PMW II, cell division at a rate of 0.2-0.3 generation per day was monitored for 5-6 days.

Morphology of coumarin treated protoplasts

Samples of protoplasts were treated with 250 mg/liter coumarin for 48 hours or for one week with a 48 hour transfer schedule. Figures 80 and 81 are transmission electron micrographs of protoplasts treated with 250 mg/liter coumarin for 48 hours. Wall formation completely stopped, and columnar material, glue, scales, and coccoliths were present on the cell surface. The nucleus is surrounded by polysomes (Figure 81) and has a distinct nucleolus (Figures 81, 87). The most impressive fact for protoplasts treated with 250 mg/liter coumarin for either 48 hours or seven days is the presence of bundles of microtubules in the cytoplasm (Figures 82, 83).

Figures 80 and 81. TEM observations of protoplasts treated with 250 mg/liter coumarin in PMW II for 48 hours

80. Coumarin prevents wall formation and causes the increase in number of mitochondria (M). X 42,000

81. After coumarin treatment each nucleus (N) shows a prominant nucleolus (Nu). Also a layer of polysomes surrounds the nucleus. X 50,000

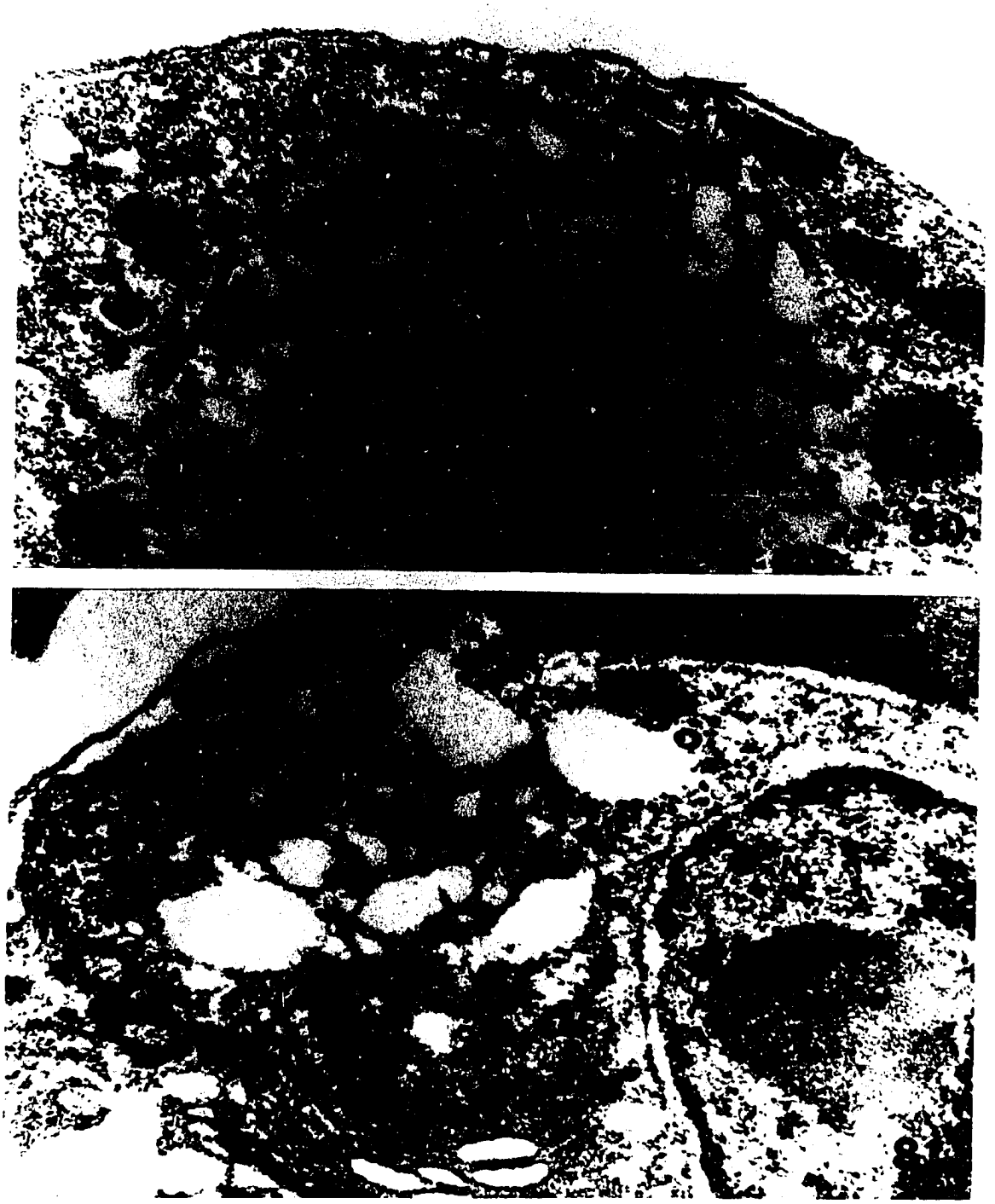

Figure 82. A section through 48 hr, 250 mg/liter coumarin-treated protoplast showing a longitudinal arrangement of microtubules which may be shorter than normal. X 70,700

Figure 83. Some microtubules are also visible in protoplasts treated with 250 mg/liter coumarin for one week. X 33,000

Figure 84. Cross-section through basal bodies of a control protoplast. X 95,400

Figure 85. A section showing an example of the increase in the number of basal bodies presumably owing to 250 mg/liter of coumarin for 48 hours. X 94,400

Figure 86. After treatment of cell with 250 mg/liter coumarin in PMW II, the number of mitochondria increased. Note the "apparently dividing" mitochondria (arrows). X 33,100

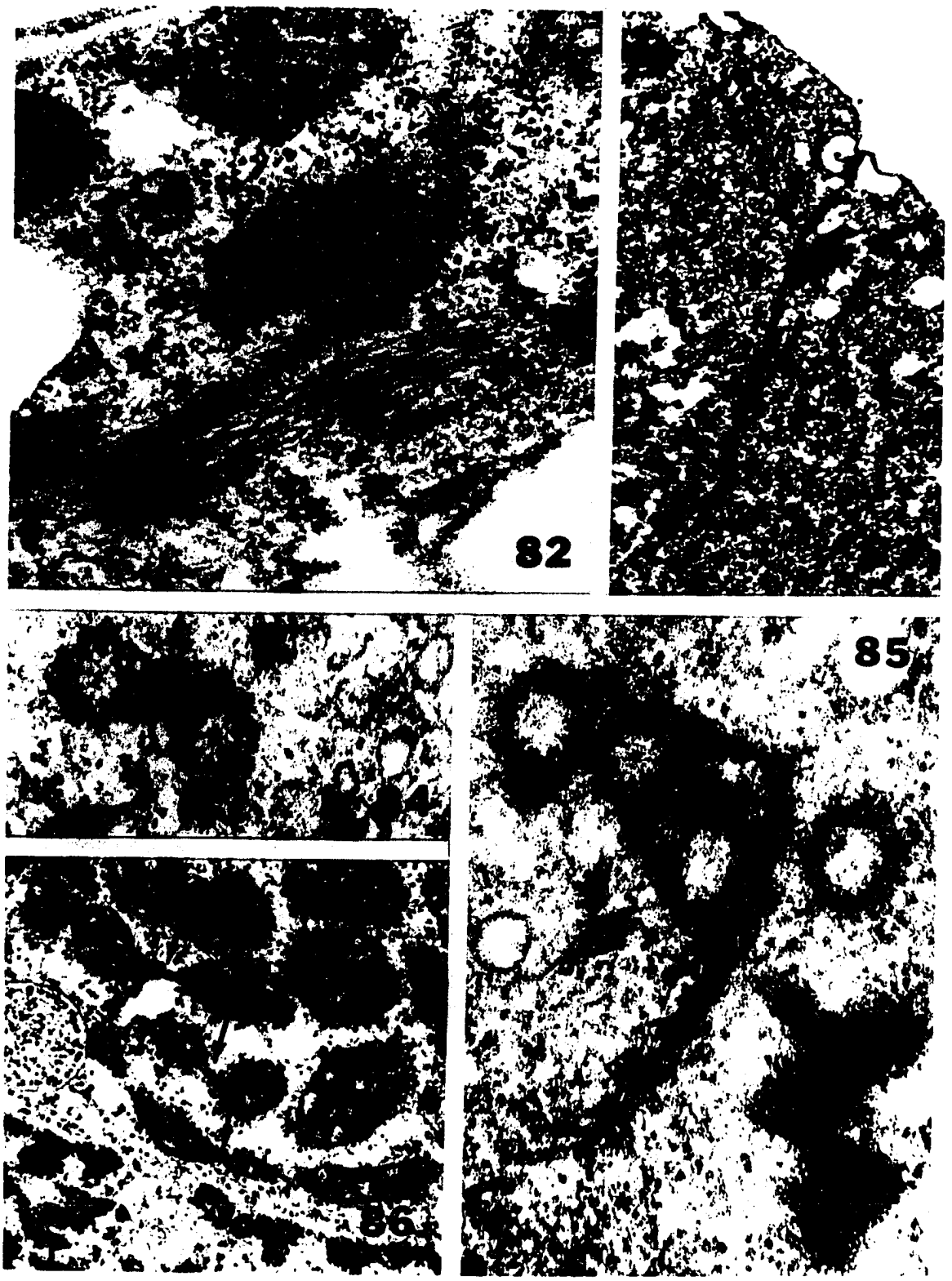
82
85
86

Table 3. The effect of one week treatment with different concentrations of coumarin on cell wall formation, flagella appearance, and reversibility of inhibition under standard conditions of growth

Tested concentration (mg/liter)	Cell wall inhibition[a]	Remarks		Reversibility
		With wall (%)	With flagella (%)	
10	−	100	95-98	+
50	−	100	95-98	+
100	±	25-30	95	+
200[b]	+	0	15-20	+
250[b]	+	0	8-10	+
500	+	0	0	+

[a] + = Presence of wall or flagella in more than 90% of cells; ± = some cells with few coccoliths or some with small flagella; − = absence of coccoliths or flagella.

[b] Flagella which are very small and only capable of vibrating but not propelling.

In Hymenomonas protoplasts, coumarin is not only an inhibitor of cell wall formation, but also affects some other processes. At least some protoplasts cultivated for 48 hours in the presence of 250 mg/liter coumarin have more than two basal bodies. Figures 84 and 85 illustrate the number of basal bodies in normal protoplasts and coumarin-inhibited protoplasts, respectively. Another site of coumarin effect is the mitochondria. Figure 86 reveals that coumarin at a concentration of 250 mg/liter for 48 hours causes an increase in the number of

mitochondria. This figure appears to show the simultaneous division of several mitochondria. Figures 87 and 88 clearly demonstrate that protoplasts cultivated for seven days in the presence of 250 mg/liter coumarin have elongated mitochondria and these mitochondria are located very close to the membranes of other organelles. Figure 87 shows the presence of large vacuoles and a nucleus with a prominent nucleolus. In addition to the above effects, prolonged treatment of protoplasts with coumarin causes the doubling of chloroplasts and increases the number of nuclei (Figure 88). As mentioned before, apparently due to some inhibitory effect of coumarin on mitosis, a low percentage of multinuclear cells was observed. Upon transferring seven-day coumarin-inhibited protoplasts to normal conditions of growth, wall regeneration apparently begins almost immediately and flagella began to appear after 2-3 hours. After 12-15 hours, the first coccoliths begin to appear on the protoplast surface. After 25 hours, most cells had coccoliths. A cell at 40 hours recovery from seven days of treatment with 250 mg/liter coumarin is seen in Figure 89. The wall is complete but the rim of coccoliths is somewhat abnormal.

Effect of 2,6-dichlorobenzonitrile (DBN)

The effect of 2,6-dichlorobenzonitrile has been studied in other systems (Meyer and Herth, 1978; Umetsu et al., 1976). This compound has been found to be the most effective and reversible inhibitor of cell wall formation (Meyer and Herth, 1978). To demonstrate its effects on protoplasts of H. carterae, different concentrations of DBN were used. Table 4 illustrates the effect of one week treatment with

Figure 87. TEM micrograph showing the effect of 250 mg/liter coumarin in PMW II on cells after one week. Note appearance of large vacuoles (V) and the presence of unusual long and narrow mitochondria (M). Nucleus (N) with a large and distinct nucleolus (Nu) is also visible. X 15,040

Figure 88. A section of a cell treated with 250 mg/liter coumarin in PMW II for one week. Coumarin caused the doubling of most organelles. Present are two chloroplasts (Ch), two long and narrow mitochondria (M) adjacent to the chloroplasts, and two nuclei (N). X 18,490

87

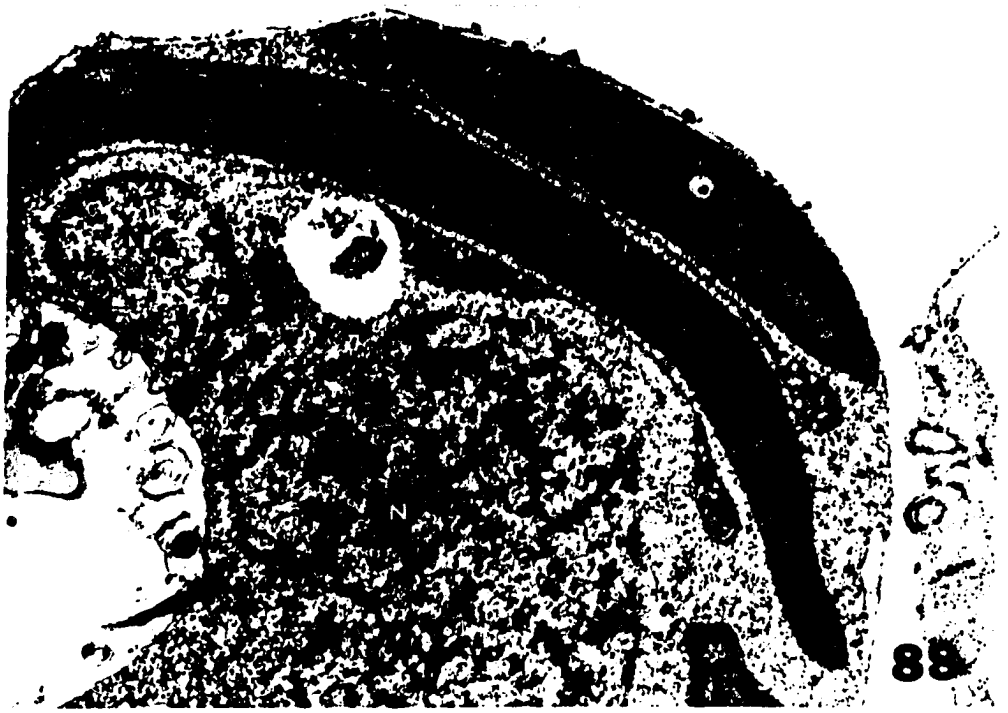

88

Figure 89. A cell at 40 hours recovery from coumarin treatment. Cell wall is complete at this time. The rim of coccoliths look abnormal (arrows). X 58,800

Figure 90. TEM micrograph showing a section of a cell after treating with 10 mg/liter 2,6-dichlorobenzonitrile. Note the presence of a coccolith with no calcareous rim (arrow), scales (S), columnar material (CM), chloroplast (Ch), microtubules (MT), and mitochondria (M) are visible. An apparent accumulation of polysomes in the cytoplasm is also noticeable (arrowhead). X 34,000

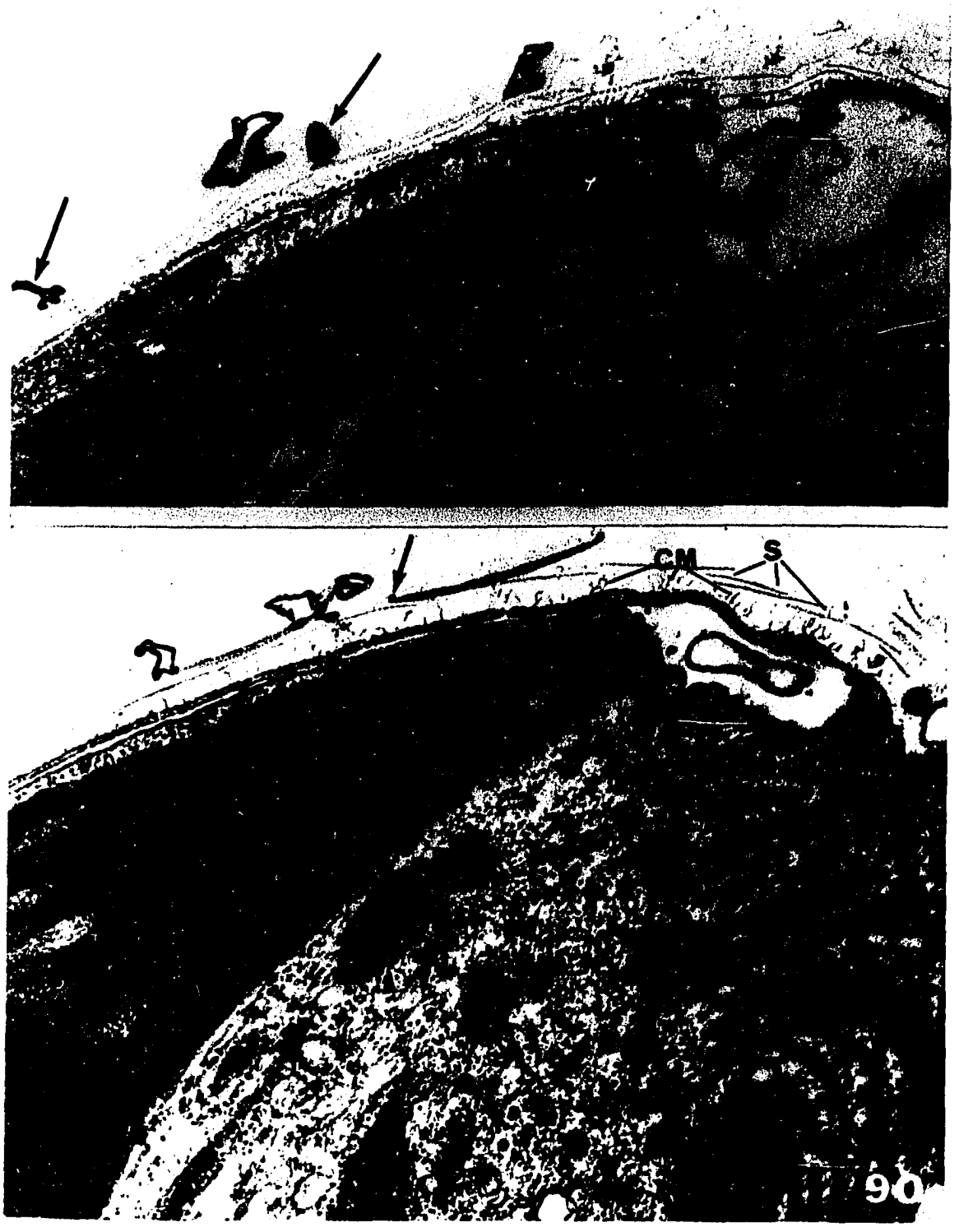
CM
S
90

Table 4. The effect of one week treatment with different concentrations of DBN on cell wall formation, flagella appearance, and reversibility of inhibition under standard conditions of growth

Tested concentration (mg/liter)	Cell wall inhibition[a]	Remarks		Reversibility
		With wall (%)	With flagella (%)	
0.1	−	100	95-98	+
0.5	−	100	95-98	+
1	−	95-98	95-98	+
2	−	95	95-98	+
5	−	90-95	90-95	+
10	±	65-70	90-95	+
20	+	0	80-85	+
40	+	0	2-5	+

[a] − = No effect was observed; ± = 30-35% of cells were susceptible; + = positive effect was detected.

different concentrations of DBN (0.1-40 mg/liter) on cell wall inhibition, flagella formation and reversibility of the inhibitor under normal conditions of growth.

The results presented in Table 4 reveal that, after one week treatment with 10 mg/liter DBN, only 30-35% of the protoplasts have no wall, whereas, at concentrations of 20 mg/liter DBN and 40 mg/liter DBN, cell wall formation was completely stopped. The interesting effect is that, although at 20 mg/liter DBN, cell wall formation was

completely suppressed, about 85% of protoplasts had normal flagella. It seems that at higher concentrations of DBN (i.e., 40 mg/liter), flagella formation also stops. Table 4 also shows that, after transferring one week DBN treated protoplasts to PMW II and normal conditions of growth, reversibility was apparent. Nomarski light microscope observations revealed that, at 10-15 hours recovery, coccoliths had started to appear on the cell surface and that the cell wall was gradually completed thereafter.

Morphology of DBN treated protoplasts

As Nomarski light microscope observations revealed, the majority of protoplasts treated with 10 mg/liter DBN produced coccoliths. TEM observations of these cells showed that all components of the wall are present. A distinct effect of the inhibitor at this concentration is seen on calcite formation of some coccoliths. The absence of notches on the edges of coccoliths are shown in Figures 90 and 94. As a result, no calcified rim is visible in such coccoliths. The most impressive effect of DBN at a concentration of 10-20 mg/liter for one week is the existence of several nuclei in protoplasts. This is presumably due to the interference of the drug with the mechanism of cytokinesis but not karyokinesis. Increases in numbers of nuclei are observed in Figures 91-96. Figure 91 is a light micrograph showing a protoplast cultivated for 4 days in the presence of 10 mg/liter DBN. Most cells at this concentration have several nuclei and some cells have more than two flagella. Figure 92 shows two nuclei (a dividing nucleus in one plane of the section). Nuclei are still connected via the nuclear envelope. At seven days

Figure 91. Nomarski differential interference light micrograph showing an optical section of a cell treated with 10 mg/liter 2,6-dichlorobenzonitrile (DBN) for 4 days. Visible are four flagella, a haptonema (arrow), and three nuclei. The major and minor diameter of the cell are 12 um and 15 um, respectively. X 1,790

Figure 92. TEM of DBN treated cell showing the dividing nucleus (N). Two nuclei are connected by the nuclear envelope. At concentration of 10 mg/liter DBN, cells still produce cell wall components which are generally abnormal. Visible are chloroplasts (Ch) and mitochondria (M). X 10,500

Figure 93. Nomarski micrograph of a cell treated with 10 mg/liter DBN for 7 days. Note the presence of 6 nuclei and two flagella. The major and minor diameters of this cell are 15 um and 17 um, respectively. X 1,792

Figure 94. TEM showing nuclear division and inhibition of cytokinesis by 10 mg/liter DBN in PMW II, after 8 days. Present are nuclei (N), chloroplasts (Ch), mitochondria (M), distinct rough endoplasmic reticulum (RER), Golgi apparatus (G), coccolithosomes (Co), coccoliths (C), and scales (S). Note the absence of notch on one coccolith (arrow). X 10,575


91
92
C
S
93
94

treatment (10 mg/liter DBN), the majority of cells were multinucleated (Figure 93) and about 40% of the cells had 4-6 flagella. Figure 94 is a section through a protoplast at seven days inhibition with 10 mg/liter DBN. Two nuclei are visible at this plane of the section. The endoplasmic reticulum forms a layer of somewhat distinct cisternae parallel to the nuclear envelope. The stack of Golgi cisternae shows the normal general ultrastructure (Figure 94). As previously mentioned, DBN at 20 mg/liter or more stopped cell wall formation. Ultrastructural studies of these protoplasts revealed that, after one week continuous treatment with 20 mg/liter DBN, the only visible component of the cell wall was columnar material (Figures 98-100). Usually, under standard conditions, Hymenomonas makes about 8-10 coccoliths per hour. The coccolith is sequentially assembled in different Golgi cisternae from two precursors, a single base and multiple granular elements called coccolithosomes and are extruded through the membrane by exocytosis. Upon exposing protoplasts to 20 mg/liter DBN, sequential coccolithogenesis is completely suppressed (Figure 98). Figure 98 illustrates the absence of the base of coccoliths and the presence of many coccolithosomes in the Golgi cisternae in such protoplasts. It seems that, in addition to the inhibition of coccolith base formation, calcification is also stopped. Figure 97 shows the contribution of coccolithosomes to form the outer rim matrix, and the subsequent filling of the area enclosed by the matrix by $CaCO_3$ (see Outka and Williams, 1971). Such a contribution is not visible in DBN inhibited protoplasts. DBN not only causes cell wall inhibition but also affects cytokinesis, the

Figures 95 and 96. Nomarski differential interference contrast light micrograph and TEM micrograph of protoplasts treated with 20 mg/liter DBN, showing the increase in number of nuclei after one treatment

95. Optical section of a protoplast showing four nuclei, no wall, and no flagella. Diameter of cell is 13-14 μm. X 1,790

96. Presence of three nuclei (N) in one plane of section. Note that none of the components of the wall are present. Rather, present are a large vacuole (V), chloroplasts (Ch) with a distinct pyrenoid (P), mitochondria (M), and rough endoplasmic reticulum (RER). X 18,100

95

96

Figure 97. A section through a portion of a cell grown under standard conditions. Note a forming coccolith (FC) in a Golgi cisternae. Many coccolithosomes (Co) are also present in the same Golgi cisternae. A forming scale is also visible in another Golgi vesicle (arrow). X 48,600

Figure 98. After treating cells with 20 mg/liter DBN for 7 days, coccolithogenesis stops but coccolithosomes are synthesized. Note the absence of the coccolith and presence of many coccolithosomes in the Golgi cisternae (arrows). Also note the appearance of columnar material (arrowheads) on cell surface. Present are chloroplasts (Ch), microtubules (MT), nucleus (N), a distinct nucleolus (Nu), a prominent rough endoplasmic reticulum (RER) around the nucleus, and free polysomes (FP). X 32,400


97


N
Nu
98

morphology of the endoplasmic reticulum and polysomes. Figures 95 and 96 illustrate that DBN suppressed cytokinesis and provided multinuclear protoplasts. The nuclei were closely associated and had an irregular, lobed shape. At a proper plane of section, the nucleus shows a prominent nucleolus (Figure 98). An increase in the number of nuclei per 100 protoplasts due to 20 mg/liter DBN was monitored with Nomarski light microscopy for one week. Nuclear division at a rate of 0.4 generation per day, at a population density of 1-2 x 10^5 cells/ml on a 48-hour transfer schedule, and under 16 hours of light/8 hours of dark was observed. Cultures continuously treated with 20 mg/liter DBN and no transfer for one week, exhibited a decrease in the rate of nuclear division after 4-5 days (after day five, nuclear division occurred at a rate of 0.12-0.15 nuclei/cell/day). Protoplasts under normal conditions of growth show division at a rate of 0.4-0.5 generation per day for 4-5 days. A decline in division rate is visible after this period. The endoplasmic reticulum in DBN inhibited protoplasts shows a distinct appearance (Figures 96, 98). These protoplasts show many free polysomes which they sometimes accumulate. Illustrated are a mass of polysomes in the cytoplasm (Figures 98, 99). It seems that DBN, at least at the concentrations used in this report, did not affect the appearance of microtubules. Protoplasts cultivated for seven days in the presence of 20 mg/liter DBN often showed microtubular bundles (Figures 98, 100) and microtubular sheets (Figure 100).

Another interesting effect of DBN on protoplasts was the induction of a remarkable cell swelling in one-week inhibited cultures. Usually

Figure 99. TEM micrograph showing the accumulation of polysomes due to treating cells with 20 mg/liter DBN for 7 days (arrows). X 31,800

Figure 100. Section through a cell treated with 20 mg/liter DBN for 7 days, illustrating the microtubular sheet (MS) and bundles of microtubules (BM) in cross sectional view. X 43,200

Figure 101. A cell at 40 hours recovery from 20 mg/liter DBN treatment for 7 days. A complete cell wall is present. Note the "wavy" base and inverted arrangement of A elements on the base (arrowhead). X 2,330

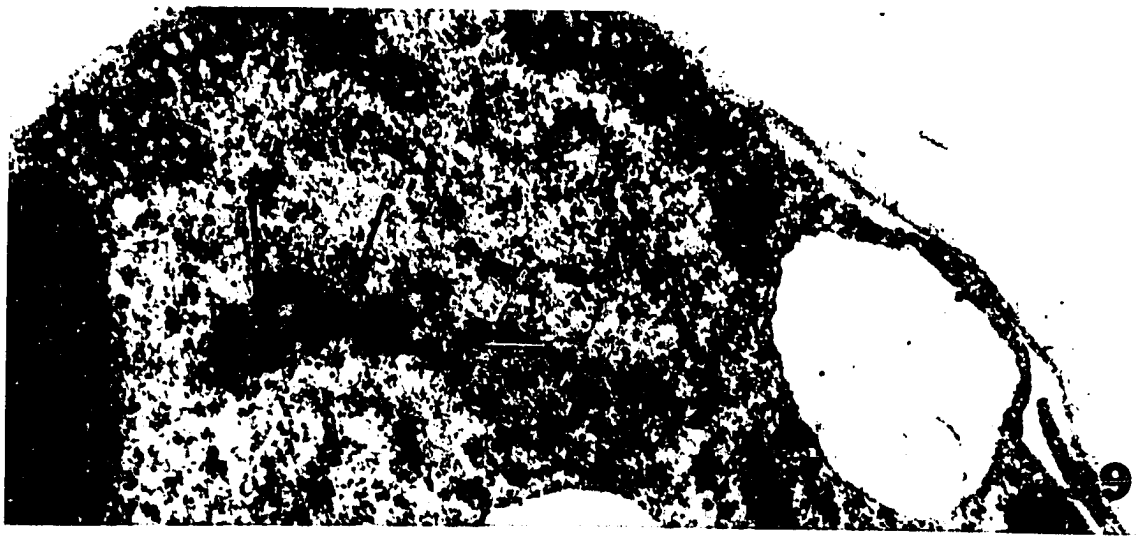
9


M
10


101

normal cells under standard conditions are about 12 um in diameter, and the isolated protoplasts have a diameter of about 7 um (Figure 69). After 7 days inhibition with 10 mg/liter DBN, cells were 15-17 um in diameter. During the same length of time, 20 mg/liter DBN treated cells increased in diameter from 7 um to 13-14 um (Figure 95). As mentioned earlier (Table 4), DBN is a potent inhibitor of wall formation and an important property is its reversibility under normal conditions of growth. Coccoliths start to appear on the cell surface after 12-15 hours recovery and the cell wall is gradually completed. Ultrastructure of cells at 40 hours recovery from 20 mg/liter DBN treatment for one week is shown in Figure 101. All components of the cell wall are present. The only visible effect of DBN treatment on the wall of these cells is the presence of coccoliths with "wavy" bases and atypical rim elements (Figure 101).

DISCUSSION

While there has been extensive investigations and growing interest in the structure of the cell wall in different plant systems, there is no comprehensive set of results about the molecular architecture and the spacial arrangement of the different components of the wall in any complete single system or species. This in part is owing to the chemical complexity and morphological diversity of cell walls in the plant kingdom. One of the problems regarding the correlation of ultrastructure and the chemical nature of the cell wall is the difficulties involved with assigning a specific component to a proper part of the wall. However, various ultrastructural, biochemical, cytochemical, and autoradiographic procedures have been employed to at least partially characterize the cell wall in some systems. A common feature of most plant cell walls is the presence of cellulose which can be synthesized either intracellularly in the Golgi cisternae (see Brown and Romanovicz, 1976) or extracellularly on the plasmalemma (see Brown and Montezinos, 1976; Willison and Brown, 1977). The nice thing about Hymenomonas is that it has a presumably primitive form of higher plant cell wall which consists of discrete units. Under controlled conditions, one can follow the sequential development of scales and coccoliths in different Golgi cisternae with the electron microscope. Although there are differences between the cell wall of Hymenomonas and higher plants, there are also many similarities. The chemical nature of the base of the coccolith and scale is somewhat similar to the cell wall of higher plants by virtue of (1) having cellulosic concentric microfibrils and pectic

radial microfibrils embedded in an amorphous carbohydrate component, which is in turn connected to a hydroxyproline rich protein, and (2) the enzymatic technique which has been successful in digesting cell walls of higher plants also removes the Hymenomonas cell wall. This suggests that the organism possesses cellulose, pectin, and perhaps hemicellulose just as higher plant cells do. The enzymatic method permits the isolation of Hymenomonas protoplasts which offers an excellent starting point for the study of cell wall assembly in vivo. Thus, one can obtain information about the timing of the sequential morphogenesis of the cell wall which in turn may reveal something about the kinetics of wall secretion.

Ultrastructure of the Cell Wall in Different Stages of the Life Cycle

The ultrastructure of the two prominent stages of the life cycle of Hymenomonas with particular reference to the cell wall structure is presented here. Noncoccolith-bearing cells are larger than coccolith-bearing cells and have smooth surfaces as revealed by scanning electron microscopy (Figure 1). The cell wall at this stage consists of several layers of scales embedded in an electron transparent component (Figure 2). Brown and his co-workers (Brown and Romanovicz, 1976; Brown et al. 1973) also reported the presence of a multilayer of scales around the Pleurochrysis cells. These authors did not visualize the small electron dense dots which were arranged in a regular fashion along the radial microfibrils (Figure 2). The coccolith-bearing stage also possesses a multilayered cell wall which is composed of several components, namely,

coccoliths, scales, "glue", and columnar material (Figures 3-6). The transition from one life cycle stage to another can be followed under certain conditions (Brown and Romanovicz, 1976; Safa, 1977). This alternation must be under a precise genetic control which not only determines the ability of the organism to turn coccolith formation on and off but also to determine which stage is to be formed at a particular time under particular environmental conditions.

Cell Wall Chemistry

The data reported here clearly demonstrated that a procedure based upon the use of Triton X-100 in salt solution is an appropriate method for isolation of the cell wall of Hymenomonas. Cell walls obtained by this technique were pure and contained different fractions of the intact wall as seen in whole cell preparations (Figures 7, 8, 9, 10). The nonionic detergent Triton X-100 which was used for preparation of the cell walls apparently solubilizes membrane lipoproteins (Vernon and Shaw, 1969) and has been used in various systems to isolate components without denaturation. Indeed, treatment of hepatocyte plasmamembranes with Triton X-100 has led to the isolation of gap junctions (Goodenough and Stoeckenius, 1972). An intact network of spectrin and monomeric actin has been recovered as a spherical basket of interconnected filaments from erythrocyte ghosts treated with Triton X-100. While there are many other examples of solubilization effects of Triton X-100 on some components of the cell, no evidence of degradation of cell walls or especially calcite crystals were seen (Figures 9, 10). Prolonged exposure of cell walls to this detergent tends to release

some of the coccolithonets from the surface of coccoliths.

The most difficult problem related to work with the Hymenomonas cell wall was that of obtaining a sufficient quantity of walls needed for chemical and physical analysis. As stated earlier, under the conditions used here, the yield of cell walls was only about 1 g per 90 liters of culture after 2 to 3 weeks and upon EDTA or LiCl solubilization of such amounts of wall only 30-35 mg soluble nondialyzable fraction was obtained. Therefore, the yield of the soluble fraction of walls was not sufficient for different analytical procedures, and it would be difficult to establish the complete analysis of different soluble fractions. Therefore, the approach used to study cell wall chemistry was to selectively solubilize some components of the cell wall using a chaotropic agent (LiCl) and an ion chelating compound (EDTA). These compounds do not have drastic effects on cell walls and one can obtain molecules and cell wall fractions without breaking covalent bonding. Chaotropic compounds like LiCl interrupt hydrogen bonding and hydrophobic interactions (Hills et al., 1975), while EDTA chelates different ions especially Ca^{++} and Mg^{++}, thereby breaking up ionic interactions among the wall components. A more drastic solubilization of the wall was carried out by SDS. As Makino et al. (1973) described, SDS binds to nonspecific low affinity sites on the protein. Its binding is cooperative and accompanied by a major conformational change in the protein. High concentrations of LiCl have been used for solubilization of glycoprotein molecules of the cell wall of Chlamydomonas (Hills, 1973; Hills et al., 1975). Chaotropic

solubilization performed on whole cells of Hymenomonas showed the ability of LiCl to destabilize and dissolve cell membranes (Figure 14). This supports other reports on different systems (see the review by Hatefi and Hanstein, 1974). It also disrupted the coccolith rim and dissociated the columnar material and "glue" fractions of the walls. Chaotropic dissociation of the whole cell released coccoliths and scales from the cell surface (Figure 15) and showed that these components of the wall are connected to the cell surface and maintained there by coccolithonets probably through hydrophobic interactions, hydrogen bonding, and ionic interactions (also see EDTA solubilization and cationized ferritin interactions in a later part of this discussion).

Chaotropic solubilization of isolated walls revealed that as in Chlamydomonas (Hills, 1973; Hills et al., 1975), high concentrations of LiCl (10 M) dissociates the cell wall of Hymenomonas into soluble and insoluble fractions. Ultrastructural visualization of the insoluble fraction showed partial degradation of the matrix and calcite crystals (Figures 18, 19).

The analytical ultracentrifugation results of LiCl soluble fraction of wall (LSF) showed the presence of molecules with low sedimentation coefficient (see Figure 20). Addition of SDS and heating the sample dissociated the sedimenting molecule to smaller sedimenting species (Figure 21). These sedimentation patterns resemble Kuratana's data (1974) on fraction(s) of coccoliths. However, the sedimentation coefficient of this material is considerably lower than that of Isenberg et al. (1976).

While analytical ultracentrifugation results revealed the presence of only one distinct sedimenting molecule with low sedimentation coefficient in the presence of SDS and some components with very high sedimentation coefficient which sediment very fast at the bottom of the centrifuging cell, the SDS gel electrophoresis procedure showed different results. (Three main carbohydrate bands and two main protein bands were seen, see Figure 22.)

The results of colorimetric determinations suggested, in fact, that the LSF contains much more carbohydrate than protein (Figure 16). In such a case, the application of the gel electrophoresis method for molecular weight determination is not very useful. The difficulties involved with correlating sedimentation results and SDS gel electrophoresis data might be due to the presence of molecules with different charge distributions (because of their molecular structure, ionic conditions, and pH of the solvent) which probably have the same or very similar sedimentation coefficients.

Ultrastructural and biochemical data presented in this report provided a significant conclusion, namely, that LiCl only partially solubilized the cell wall in the absence of SDS.

EDTA Solubilization

In order to have a better understanding of the chemical nature and in turn interactions among the wall components, EDTA extraction was performed. EDTA decalcified the cells leaving behind a naked and smooth surface (Figures 24, 25). In a similar experiment using shorter times of treatment, Flesch (1977) showed that EDTA decalcified

the coccolith rim while the coccolith base was still connected to the cell. This also resembles the results of Williams (1972, 1974), who used an acidic pH of 5.5 for decalcification. The removal of the whole cell wall by EDTA treatment suggests the presence of ionic interactions among the wall components (see later discussion concerning cationized ferritin and ruthenium red interactions with wall material) and supports the cell wall model proposed by Flesch (1977) in which different components of the wall are held together by ionic interactions.

As with LiCl, EDTA also dissociates the isolated walls into EDTA-soluble and EDTA-insoluble fractions (ESF, EISF). A significant portion of ESF is carbohydrate (Figure 26) and some carbohydrates of this fraction are acidic in nature (Table 1). Ultrastructural studies on EISF revealed that the most effective site of EDTA solubilization was the matrix material and calcite crystals owing to the chelating properties of EDTA. As concluded for LiCl dissociation, various ultrastructural observations (Figures 27-29) combined with SDS gel electrophoresis data (Figures 44, 45) revealed that EDTA also partially solubilizes the cell wall in the absence of SDS.

Dissociation of the cell wall with EDTA also provided some detailed ultrastructural information about the nature of the "glue" fraction of the wall. "Glue" is composed of three types of fibrous material (type A, B, and C fibers, see Figures 31-34) and small globular bodies (Figure 32). Therefore, from the complexity of the morphological structure of the "glue", one would suspect a considerable biochemical complexity as well, which in turn would require the application of

more sophisticated preparative procedures for their more complete characterization.

Reassembly of the EDTA-soluble Fraction (ESF)

Most studies on self-assembly processes have been performed on relatively small and simple structures such as viruses (Kellenberger and Edgar, 1971), bacterial flagella (Bouch and Brown, 1976), and microtubules (Borisy et al., 1974; Bouch and Brown, 1976). The self-assembly of cell wall glycoproteins and the first case in which a plant cell wall (in Chlamydomonas) has been reassembled in vitro (Hills, 1973; Hills et al., 1975) shows that very large cellular structures can also be built by the self-assembly process. The advantage of the Chlamydomonas and Hymenomonas wall systems is that insofar as resolution permits the assembly process can be observed in the light microscope. ESF also reaggregates under certain experimental conditions as described earlier (Figures 35-41). In this system, as in Chlamydomonas, the self-assembly of some components of the wall can be monitored with both light and electron microscopes. The important factors involved here are the presence of ESF which has been dialyzed against distilled water to remove the EDTA from the soluble fraction and subsequent subjecting of the fraction to proper ionic conditions. The role of calcium is significant for enhancing the rate of reassociation but even in the absence of Ca^{++} some reaggregation occurs. This in fact can be seen in Figures 54, 55, and 56, wherein reaggregation occurred even in the absence of any ions (Figure 56). Also crystalline lattice formation took place at 0.15 M NaCl (Figure 55). Except for the Chlamydomonas

cell wall (Hills et al., 1975), many other self-assembly systems seem to be dependent on the presence of specific cations, particularly the divalent ones, Ca^{++} and Mg^{++}. In Chlamydomonas, cell wall reassembly takes place normally even in the presence of 0.05 M EDTA or 0.05 M EGTA. The only report concerning reassociation of wall material from Hymenomonas is from Flesch (1977). His approach involved the chaotropic extraction of cells or walls and reassociation of soluble material under controlled conditions. His reaggregated material was amorphous and electron transparent, from which he deduced that it might correspond to "glue". Unlike Chlamydomonas (Hills et al., 1975), the reaggregation of this material was Ca^{++} and pH dependent. The requirement of Ca^{++} or Mg^{++} for reaggregation of alginate of brown algae (Haug, 1974) shows similarity to the behavior of cell wall components of Hymenomonas. The carrageenan of red algae requires monovalent cations for gel formation and is not affected by divalent cations (Haug, 1974). As the results demonstrated (Figures 54, 55) and will be discussed later, at least two species of reaggregated products from the Hymenomonas cell wall are acidic polysaccharides, and, although these molecules are chemically different from the reaggregated, high molecular weight glycoproteins of Chlamydomonas (Catt et al., 1976; Hills, 1973; Hills et al., 1975; Roberts and Hills, 1976), they do provide crystalline structures (Figure 55) similar to but not identical with Chlamydomonas. These crystalline lattice structures show definite periodicity, allowing the determination of center-to-center spacings.

As colorimetric data showed (Table 1), most of the ESF is carbohydrate and about half of the carbohydrate moiety is acidic in nature. Also 15-20% of this fraction is protein. Isenberg et al. (1966) and Kuratana (1974) also reported the presence of protein and carbohydrate in soluble fractions of isolated coccoliths of Hymenomonas. In contrast, the EDTA soluble fraction of isolated coccoliths of C. huxleyi (DeJong et al., 1976; Fichtinger-Schipman et al., 1979; Westbroek et al., 1973) did not contain protein. Westbroek et al. (1973) reported that 99% of this fraction was carbohydrate and acidic in nature, with no amino sugars. The absence of protein in the report of Westbroek et al. (1973) should be due to their coccolith isolation technique in which they treated coccoliths with chloroform-methanol, pronase, and a strong oxidizing agent to remove all nonintracrystalline organic material before EDTA solubilization. The protein in the coccolith fraction of Hymenomonas studied by Isenberg et al. (1966) and Kuratana (1974) either belongs to the external matrix (extracrystalline matrix) of the coccoliths or it is a contaminant from other components of the cell wall. Cell walls in most systems are known to contain hydroxyproline-rich glycoproteins (Hills et al., 1975; Lamport, 1970, 1974, 1977).

Analytical ultracentrifugation results of ESF illustrated two prominant sedimenting species with low sedimentation coefficients when the solvent was 0.15 M NaCl (Figure 42). Adding SDS and heating the sample yielded only a single peak. The sedimentation coefficient in SDS is lower than that of the major peak in salt solution (Figure 43). This might be due to either dissociation or unfolding of the molecules.

Similar results have been observed for fraction (b) of coccoliths (Kuratana, 1974). The sedimentation data reported here and by Kuratana (1974) is considerably different from what Isenberg et al. (1966) reported for the F-1 fraction of the coccolith. It is very difficult to evaluate the work of Isenberg et al. (1966).

SDS-polyacrylamide gel electrophoresis of ESF showed one distinct and some diffuse carbohydrate bands. Corresponding gels stained for proteins revealed different patterns in the presence of SDS and different boiling times (Figure 44). Although some species of these molecules seem to be glycoproteins, as also reported by Kuratana (1974), further investigation (see later part of discussion) proved in fact that these molecules were mostly acidic polysaccharides. Protein bands were more distinct when ESF was treated with SDS and heated for 6 minutes. This might have been because there was a more complete dissociation of polymers and adequate charge distributions on molecules which allowed them to migrate in more discrete bands.

Ultrastructural observations (Figures 27-29) and the similarity of electrophoretic patterns of the ESF, EISF, and the whole isolated wall (Figures 44, 45) made it clear that EDTA partially solubilized the cell wall in the absence of SDS. This result resembled the conclusion arrived at by Kuratana (1974) working with isolated coccoliths.

The lack of information about the shape and partial specific volume of sedimenting molecules did not allow meaningful values for molecular weights to be obtained by the sedimentation procedure. Also the application of SDS polyacrylamide gel electrophoresis method for

molecular weight determination in this case was not useful because this technique cannot be correctly applied to molecules containing more than 10% carbohydrate. Previous results showed that the ESF contained about 85% carbohydrate with a high proportion of acidic groups (Table 1). Therefore, to obtain molecules in pure form and have some data about molecular weights, the method of gel filtration was applied. However, owing to the aggregation properties of ESF, this technique was also inappropriate, since the ESF, when applied to different biogel columns (Figure 49, A-C) was seen in void volume of each column. TEM observations of void volumes (Figure 56) showed the presence of aggregated molecules. Westbroek et al. (1973) also found that, when the ESF of coccoliths from C. huxleyi was applied to a Sephadex G-50 column, it appeared in the void volume of the column.

While there has been extensive investigations on chemical and physical properties of the ESF of isolated coccoliths of C. huxleyi (DeJong et al., 1976; Fichtinger-Schipman et al., 1979; Westbroek et al., 1973), no data about molecular weights have been reported. The reaggregation of ESF would seem to exclude such molecular weight determinations, if attempted.

Polyacrylamide gel electrophoresis in the absence of SDS led to further characterization and purification of ESF. In this technique, Alcian Blue was used for staining acidic polysaccharides since several biochemical and ultrastructural investigations have shown that this cationic dye binds to such molecules (Brown et al., 1970; DeJong et al., 1976; Mathews and Decker, 1971; Parker and Diboll, 1966; Westbroek et

al., 1973). Alcian blue staining revealed that only carbohydrate molecules migrate along the gels (Figure 49), therefore, the procedure screens the carbohydrate fraction of ESF from the proteins. This result apparently showed that the SDS electrophoretic patterns observed in Fig. 44 was because of coincident migration of protein fractions which were separate molecules and independent from their corresponding carbohydrate molecules (compare Figures 44 and 50). Since Coomassie blue (CB) staining did not reveal any protein bands in gel electrophoresis without SDS (Figure 50), one can conclude the following: 1) proteins of ESF were probably not charged molecules, or, if charged, were too big to migrate along the gel and 2) SDS and heat dissociates protein polymers to smaller fractions (monomers) thereby providing proper charges for such molecules such that they could move in an electrophoretic field. Staining with alcian blue showed four acidic polysaccharide bands. These results were similar for 2-3 bands seen for the coccolith soluble fraction (Figure 49). The first two bands appear to be mixed and the fourth band moves with and ahead of the tracking dye, and therefore is a highly negatively charged (polyanionic) molecule. Other investigators have also reported the presence of polyanionic polysaccharides from isolated coccoliths of C. huxleyi. They have postulated that this molecule serves as a heterogeneous matrix for calcite crystallization (DeJong et al., 1976; Fichtinger-Schipman et al., 1979; Westbroek et al., 1973).

The isolation of different acidic polysaccharides was carried out by cutting, eluting, and lyophylizing individual bands from the

gel. Molecules obtained by this method were reasonably pure as judged by electrophoresis (Figure 50). Sedimentation analysis of the polysaccharides of the first electrophoretic band revealed two distinct peaks with sedimentation coefficients of 4.284 and 1.558 Svedberg units, similar to the molecules which were thought to be glycoproteins (Kuratana, 1974). The molecule with the larger sedimentation coefficient might be a polymer of the smaller one. However, the two species should have similar charge distributions on their molecular structure to appear as a mixed electrophoretic band. The acidic polysaccharide from the fourth electrophoretic band which is a polyanionic molecule possesses a sedimentation coefficient of 1.82 Svedbergs. It, therefore, seems that the two low sedimenting species (i.e., 1.558 Svedbergs and 1.82 Svedbergs) are probably different molecules with different charge distributions which could move to two positions through the gel, but, since their sedimentation coefficients were similar, only one peak was seen in sedimentation experiments. Such an explanation would make a significant correlation between previous electrophoretic and ultracentrifugation results for both ESF and LSF. An alternative and equally theoretical explanation would be that both of the low sedimenting molecules were degradation products of the original molecule having a larger sedimentation coefficient (i.e., 4.284 Svedbergs).

The ultrastructural feature of these molecules revealed definite examples of order and some similarities between different fractions which also support the above explanations. The crystalline lattice structure observed for the acidic polysaccharide of the fourth

electrophoretic band is similar but not identical to reaggregated glycoproteins of the cell wall of Chlamydomonas (Hills, 1973; Hills et al., 1975).

The foregoing discussion presents conclusive information concerning some wall components. Although their mode of action is different, both LiCl and EDTA partially solubilize the cell wall. Both compounds solubulize proteins and carbohydrates of the wall, some of which must have belonged to coccoliths. These ultrastructural observations, sedimentation data, and electrophoretic results of the cell wall and coccoliths when compared with those of Kuratana (1974) revealed that the low sedimenting molecules are more likely to constitute a part of the coccoliths. The fact that these molecules are indeed acidic polysaccharides with self-assembly characteristics suggests their probable involvement in calcification of rim elements. The most interesting contribution made by Outka and Williams (1971) to the understanding of the matrix structure of H. carterae was describing the multiple granular elements called coccolithosomes and the contribution of granular material by coccolithosomes to form the matrix of the coccolith rim. They concluded that coccolithosomes each contain 12 or fewer opaque, granular subunits about 70 Å in size with a relatively constant center-to-center spacing of about 85 Å. They also showed that subunits were present but poorly defined in unstained sections and had a strong affinity for lead citrate. Their data suggested that preparative treatments of decalcified material showed about a 12% increase in coccolithosome size and the center-to-center spacing between subunits. As discussed

earlier, polyanionic polysaccharides from coccoliths of Hymenomonas under certain conditions provided reaggregated products with a crystalline-latice appearance and with center-to-center spacing of about 65 Å. Considering the fact that Outka and Williams (1971) used a double staining procedure (uranyl acetate and lead citrate) and they also found 12% increase in size due to preparative treatments reveals the possibility that both coccolithosomes and polyanionic molecules (with self-assembly properties) are the same. As noted before, the involvement of coccolithosomes in matrix construction of H. carterae (Outka and Williams, 1971) and the contribution of an acidic polysaccharide as a heterogeneous matrix in coccolith formation in C. huxleyi (DeJong et al., 1976; Westbroek et al., 1973) supports this hypothesis. Concerning the chemical nature of the matrix of mineralized cells, macromolecular polyanions invariably seem to be present. In animals, these are usually predominantly proteins, whereas the matrix of diatoms is rich in highly basic polyamines and polyuronic acid (see review by Eastoe, 1968). Therefore, the similarity of the matrix components of diatoms and coccolithophorids is evolutionarily significant.

To have some knowledge of the chemical nature of the wall macromolecules and in turn the interactions of such molecules to form the whole wall structure, the location of negatively charged molecules was observed by ruthenium red and cationized ferritin. Ruthenium red has been used as a standard stain for pectin. The reagent has been used as an electron stain by Luft (1964) in animal histology to reveal a variety of extracellular materials (glycocalyx), the majority of which

seems to be acid mucopolysaccharides. The intensity of the ruthenium red reaction depends primarily upon the number of ionizable carboxyl groups available, provided that the molecular weight of the carrier molecule is sufficiently high. The binding of ruthenium red to its substrate occurs electrostatically (salt linkage)(Hayat, 1975). In Hymenomonas, ruthenium red positive material (supposedly acidic polysaccharides) were observed in columnar material, glue, periphery of scales, and fibrous projections on the proximal surface of coccoliths. This observation plus the ability to remove different wall components with EDTA (Figures 24, 25) and also the qualitative biochemical tests used by Brown et al. (1970), with which they were able to demonstrate that after EDTA treatment the cell wall of Pleurochrysis did not give a further positive reaction with alcian blue or with ruthenium red, suggested that a pectin-like polysaccharide could be associated with the cell wall of H. carterae. This has also been suggested by enzymatic digestion of isolated walls with pectinase and the subsequent determination of the uranic acid (the major monomer of pectin) released upon pectinase treatment (Figure 59, A, B). The results of Romanovicz and Brown (1976) established the presence of both sulfate and carboxyl groups in the acidic polysaccharide (S) of the Pleurochrysis wall.

Ultrastructural localization of acidic molecules (polysaccharides) were also demonstrated by cationized ferritin. The labeling of cell wall components with ferritin may take place both before and after fixation with glutaraldehyde at pH 7.5. The EDTA solubilization data (Figures 24, 25), the ruthenium red staining, and the cationized ferritin

binding prior to fixation which occurs preferentially to the columnar material, the periphery of scales and upper surface of coccoliths (Figures 65, 67) suggest that the cell wall of Hymenomonas is built up primarily by ionic interactions of its components. The results for cationized ferritin binding (prior to fixation) to the wall components is identical to those of Flesch (1977) for Hymenomonas and also Brown and Romanovicz (1976) for Pleurochrysis. The chelation of Ca^{++} by COO^{-} anions and donor groups such as OH from polysaccharides or NH from proteins in Nitella (Wuytack and Gillet, 1978) also suggests ionic interactions similar to those in the Hymenomonas wall. Labeling with cationized ferritin prior to fixation with glutaraldehyde has the advantage that it can be performed under approximate physiological conditions. The labeling of cells after short fixation with glutaraldehyde (Figures 65, 67) showed completely different results. Only the accumulation of ferritin molecules were visible along the fibrous projections of the outer surface of the coccoliths. This might be due to the following: 1) fixation stabilizes the cell wall to rather a rigid structure which does not permit the passage of molecules as big as ferritin (110 Å in diameter); therefore, no binding to other components of the wall occurs, and 2) since the binding of cationized ferritin to the proximal surface of coccoliths only occurred after cells were fixed with glutaraldehyde, there has to be some modifications on the upper surface of the coccoliths as a result to the action of the fixative, which results in exposing or modifying acidic molecules to allow them to interact with cationized ferritin. The binding of

ferritin to different partitions inside of the rim elements (Figure 67) indicates the presence of intracrystalline acidic molecules discussed earlier.

In addition to different structural components of the wall described here, the wall of Hymenomonas possesses a number of single-membrane-bounded vesicles, which contain crystalline ruthenium red positive material and were named "crystalline vesicles" (Figure 59). Marchant and Robards (1968) have described similar membranous or vesicular structures associated with the cell wall of different plants under the general term paramural bodies regardless of their origin. These paramural bodies are subdivided into two classes according to their derivation. Lomasomes originate from cytoplasmic membranes, while plasmalemmasomes are derived from the plasmalemma. These vesicles may be involved in wall synthesis, either as a transitory stage during the incorporation of wall precursors or as the site of incorporation of enzymes for extracellular synthesis. The possible functional significance of paramural bodies, especially regarding wall secretion, has been extensively discussed (Cox and Juniper, 1973; Marchant and Robards, 1968; Mesquita, 1974). There is autoradiographic evidence that this group of organelles may be carriers of wall-matrix polysaccharide materials (Cox and Juniper, 1973). Morphological observation in Hymenomonas suggests that "crystalline vesicles" may have the same function in this case as carriers of the "glue" component of the wall.

Enzymatic Digestion of the Cell Wall and Protoplast Formation

During the past few years, there have been extensive investigations on the isolation of protoplasts of higher plants for various purposes including somatic hybridization (Gamborg, 1976), cell wall regeneration (Burgess and Linstead, 1976, 1979; Willison and Grout, 1978), and inhibition (Burgess and Linstead, 1977; Meyer and Herth, 1978), and also studies in genetics and virology (for more information, see Cocking, 1972; Gamborg and Miller, 1973; Peberdy, 1979; Takebe, 1975). The enzymes such as cellulase, pectinase, and hemicellulase have been employed extensively in obtaining protoplasts from higher plants (Cocking, 1972). The same enzymatic procedure used for isolation of protoplasts from higher plants is capable of digesting the cell wall of H. carterae. The data showed that macerozyme and cellulase used as a sequential two-step treatment or as a one-step procedure would digest the wall completely and provide more than 95% protoplasts.

The site of action of enzymes on the cell wall is primarily the scale (Figure 71). Upon degradation of scales, the cell wall falls apart and the connections between scales, glue, and columnar material are removed, thereby allowing the cell wall and the plasma membrane to become separated. The sensitivity of scales to enzymatic digestion indicated that, although there are some similarities between the scales and the bases of coccoliths, these two wall components are not chemically identical. This was also revealed by differential distribution of attachment of cationized ferritin to the surface of scales and coccoliths (Figures 64, 66).

One of the problems involved with enzymatic digestion of the wall in different systems is the impurity of enzymes which in turn can cause drastic effects on whole cells. These impurities are usually ammonium sulfate (which is used for enzyme isolation), some proteolytic enzymes, and perhaps other degradative enzymes such as lipases. These impurities affect the growth and some other physiological processes of cells. With the enzymatic procedure used here, the normal growth and coccolithogenic rate were sharply decreased (see Figures 72, 73). These changes as well as the production of coccoliths with wavy bases and inverted rim elements can be explained as a result of 1) enzyme impurities and 2) experimental conditions such as pH, temperature, duration of enzyme treatment, and concentrations of enzymes used. One may reduce some of these effects by optimizing the procedures.

TEM observations revealed that the sequential regeneration of the wall begins during the first hours of recovery and after 24 hours a more or less complete wall appears. The time sequence for wall regeneration appears to be similar to that reported by Flesch (1977) for regeneration of the wall on pronase treated Hymenomonas. The only other algae from which protoplasts have been released by enzymatic digestion of their walls are the chlorophytes, Chlorella (Braun and Aach, 1975) and Uronema (Gabriel, 1970), the red alga Porphyridium (Clement-Metral, 1976) and the filamentous green algae Mongeotia, Stigeoclonium, Ulothrix, and Klebsormidium (Marchant and Fawke, 1977). Schlosser et al. (1976) could also remove the cell wall of Chlamydomonas reinhardii by using the species specific cell wall autolysin which is produced by gametes

of this alga. Recently Flesch (1977) reported the successful use of pronase to remove the cell wall of H. carterae. Pronase seems to have various effects on general morphology and wall regeneration of this organism.

Inhibition of Cell Wall Formation

Cell wall formation in protoplasts of Hymenomonas was inhibited by two common inhibitors of cellulose biosynthesis, coumarin and 1,2-dichlorobenzonitrile (DBN).

Coumarin (1,2-benzopyrone) at concentrations of 200 mg/liter or more, completely inhibited cell wall formation in Hymenomonas and induced some other side effects such as inhibition of flagella formation, an increase in the number as well as the elongation of mitochondria, an increase in the number of basal bodies, and chloroplasts. Other investigators have concluded that coumarin inhibits cellulose biosynthesis in higher plants and Acetobacter xylinum (Satoh et al., 1976a, b; Hara et al., 1973; Hopp et al., 1978) as well as preventing microfibrillar deposition on the surface of regenerating tobacco leaf protoplasts (Burgess and Linstead, 1977; Meyer and Herth, 1978). An interesting observation is that even after one-week treatment with coumarin, cells have bundles of microtubules (Figure 83). This observation supports the report of Harada et al. (1972), Meyer and Herth (1978), and Itoh (1976), which conclude that coumarin does not affect the cortical microtubules of plant cells. My observation revealed that at 250 mg/liter coumarin, cytokinesis was completely abolished but only 8% of protoplasts were multinucleated after one week treatment.

The antimitotic effect of coumarin in tobacco protoplasts also inhibited nuclear division, therefore, only a low percentage of the protoplasts became multinuclear (Meyer and Herth, 1978). Similar cytological changes including multinuclear cells and a possible interference of coumarin with the mechanism of cytokinesis have also been observed in Euglena gracilis (Vannini et al., 1977). The data presented here reveals that cytokinesis in Hymenomonas protoplasts is not necessarily linked to nuclear division. Similar observations have been reported for Euglena (Vannini et al., 1977), tobacco mesophyll protoplasts (Meyer and Herth, 1978), Petunia protoplasts (Frearson et al., 1973) and for rose suspension culture cells (Pearce and Cocking, 1973).

DBN has also been introduced as an inhibitor of cellulose biosynthesis in higher plants (Hugetsu et al., 1974). In Hymenomonas, 20 mg/liter DBN completely abolished cell wall formation as well as inducing some other cytoplasmic rearrangements. Comparison of different effects of DBN and coumarin (see Tables 3, 4) revealed that DBN is more effective and less toxic (especially regarding nuclear division and flagella formation). Using different inhibitors on tobacco protoplasts, Meyer and Herth (1978) also concluded that DBN is the most effective and reversible inhibitor of cell wall formation. As in Hymenomonas, DBN also causes cell swelling and characteristic modifications in suspension cultured soybean cells (Umetsu et al., 1976). These findings support the assumption of Hara et al. (1973) that inhibition of cellulose biosynthesis in plant cells brings about changes in cell wall properties and causes cell swelling and modification of cell form.

The cell swelling in Hymenomonas is most likely due to accumulation of cell organelles because of inhibition of cytokinesis (Figures 91-96). As in Hymenomonas, recently Meyer and Herth (1978) reported that in tobacco protoplasts DBN is an inhibitor of cell wall formation and also stops cytokynesis but does not affect nuclear division. These authors also presented similar results regarding the presence of free polysomes on the endoplasmic reticulum (Figures 96, 98). The abundance of polysomes might be due to active protein synthesis in inhibited protoplasts. Presence of a prominant nucleolus (Figure 98) also supports this presumption. It seems that the inhibition of the wall assembly is not related to the microtubular system since microtubular bundles and microtubular sheets are visible in DBN-inhibited protoplasts of Hymenomonas as well as normal cells. This resembles other systems (bean epicotyl sections, in a report of Hugetsu et al., 1974, and in the protoplasts of tobacco, Meyer and Herth, 1978).

The interesting point about these inhibitors is that both DBN and coumarin inhibited protoplasts behave similarly to higher plant protoplasts with respect to three cellular processes, namely cell wall assembly, nuclear division, and cytokinesis. The advantage of using Hymenomonas is that it is much easier to work with than higher plant systems owing to ease of culturing, handling, and response to precisely defined conditions.

Model of the Cell Wall of Hymenomonas carterae

Based on morphological observations, biochemical data, and cytochemical evidence, a model for the cell wall of H. carterae is presented

in Figure 102. This model is basically similar to a hypothetical model of Flesch (1977) and emphasizes ionic interactions between the wall components. In addition to such interactions, chaotropic solubilization of the cell wall resulted in evidence that hydrogen bonds and hydrophobic links are also involved in holding the wall fractions together. The ionic charges of these molecules could be visualized by the preferential binding of ruthenium red and cationized ferritin. Although such cationic molecules do not discriminate among different negatively charged groups, so that both proteins and carbohydrates can link to these molecules, nevertheless the results obtained by EDTA extraction, colorimetric determinations, pectinase digestion, and uronic acid assay strongly suggested the presence of pectin-like acidic polysaccharides in the cell wall (which binds to ferritin or ruthenium red). The qualitative biochemical studies of Brown et al. (1970) also suggested that the alcian blue or ruthenium red positive components of the wall of Pleurochrysis could be pectin-like material. In fact, alcian blue staining of Pleurochrysis (Romanovicz and Brown, 1976) indicated that both sulfate and carbohydrate groups were present in such molecules.

The model illustrates that at the plasma membrane the columnar material with its characteristic fibrous appearance is present and is probably synthesized from precursors which are released from "crystalline vesicles" or lomasomes. The enzymes required for such synthesis may also be released from the same vesicles or they could be bound to cytoplasmic membranes. According to Flesch (1977), columnar material should be glycoprotein. A newly synthesized scale with some acidic

Figure 102. Model of the cell wall of H. carterae. Different cell wall components are illustrated and the relative size of each fraction as compared to the cell membrane is given on the right side of the figure. The abbreviations used here are: C = coccolith, CM = columnar material, CV(L) = crystalline vesicle or lomasome, G = glue, GB = globular bodies, PM = plasma membrane, TA = type A fibers, TB = type B fibers, TC = type C fibers. The open circles around the rim elements of the coccolith are representative of the external matrix and the solid round circles inside the rim elements illustrate the so-called intracrystalline matrix

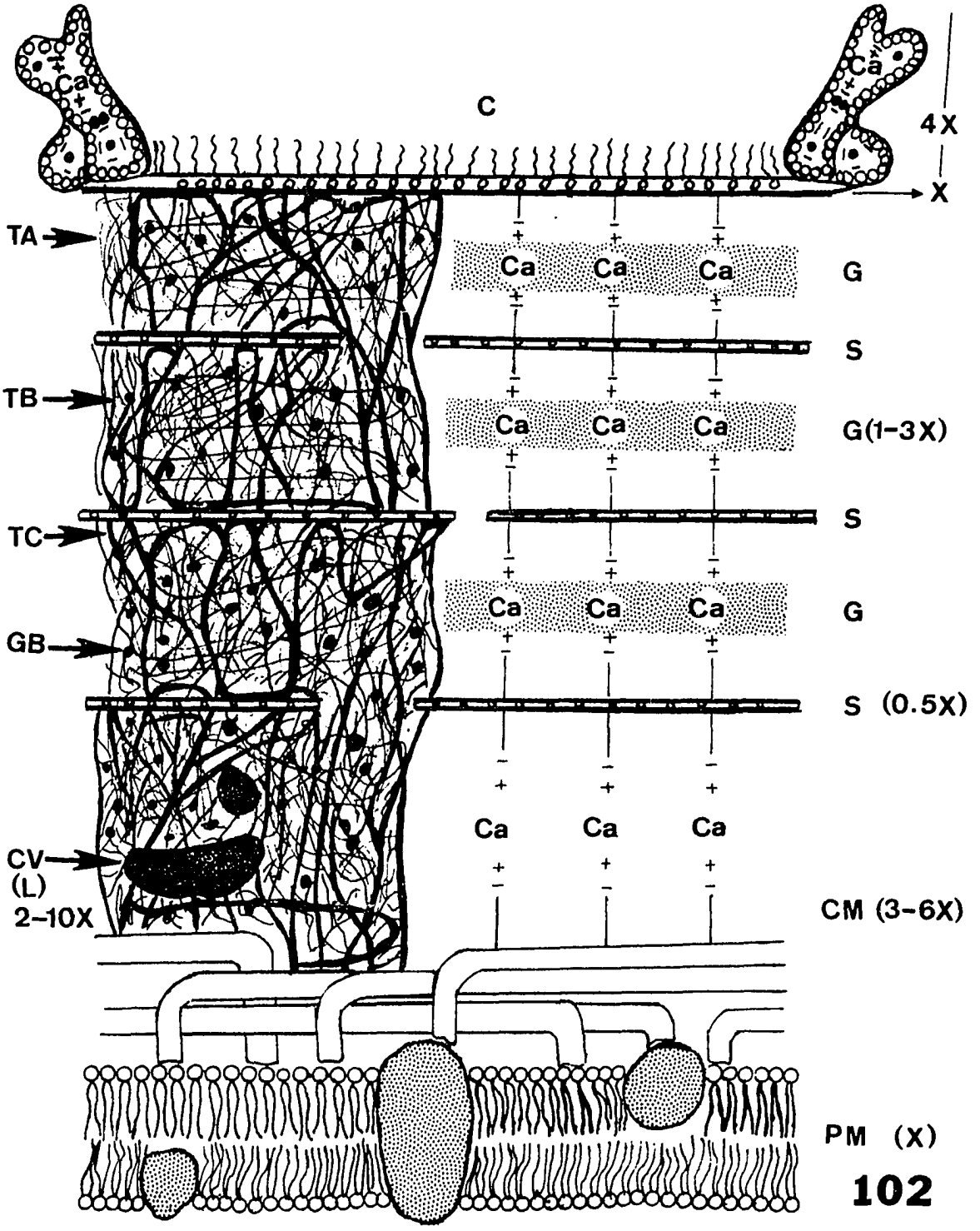
C
4X
X
TA
TB
TC
GB
CV
(L)
2-10X
Ca
G
S
G(1-3X)
S
G
S (0.5X)
CM (3-6X)
PM (X)
102

polysaccharide is secreted and becomes linked to columnar material primarily by several calcium linkages. Such a scale is also attached to several calcium polysaccharide bridges which are provided by the glue fraction of the wall. The glue is an acidic fraction of wall composed of three types of fibers with different diameters (type A, 50 Å; type B, 100 Å; and type C, 250-400 Å) along with globular bodies and amorphous acidic molecule(s). Type C fibers are branched with subfibrillar organization and most likely originate from the columnar material. The coccolith also attaches to the cell via calcium polysaccharide bridges derived from the glue and outer scale layer. Hydrogen bonding and hydrophobic interactions also help to maintain coccoliths and scales on the cell. Each coccolith is composed of a base, rim elements, and fibrous projections (with an acidic nature) on the proximal surface. Cationized ferritin binding to both internal and external portions of the rim elements revealed the presence of acidic molecules as extracrystalline and possibly intracrystalline matrix components. Several reports have indicated that the extracrystalline component is glycoprotein and the results presented here and also for C. huxleyi (Westbroek et al., 1973) suggest that the intracrystalline component is an acidic polysaccharide. The concept of multiple intracrystalline matrices adds complexity to the mechanism of single calcite crystal formation as established by electron diffraction studies by Watabe (1967) and Outka (unpublished data, Department of Biochemistry and Biophysics, Iowa State University, 1974). In this model, other divalent cations such as Mg^{++} could also be involved.

CONCLUSION

The combined morphological and biochemical investigations provided additional knowledge about the structure, chemical nature, and self-assembly of some wall components, along with interactions of these components in the assembly of the wall. The detailed morphology of different wall components was presented and conclusive information indicated that the cell wall of Hymenomonas is formed primarily by ionic interactions of its components probably along with the presence of hydrophobic and hydrogen bonding in the wall. The enzymatic digestion, EDTA solubilization, and cytochemical studies suggested that pectin-like acidic molecules were used in the construction of the cell wall of Hymenomonas. Comparison of morphological and biochemical observations revealed that polyanionic molecules (acidic polysaccharides) obtained from isolated walls or free floating coccoliths were also a constitutive part of the coccoliths and in all likelihood also participated in calcification. Enzymatic digestion of the cell wall, protoplast formation, and inhibition of wall assembly provided additional similarities between H. carterae and higher plants and in turn revealed some information concerning the sequence and kinetics of wall secretion.

LITERATURE CITED

Albersheim, P. 1974. The primary cell wall and control of elongation growth. Pages 145-164 in J. B. Pridham, ed. Plant carbohydrate chemistry. Academic Press, New York.

Albersheim, P. 1975. The walls of growing plant cells. Sci. Am. 232:80-95.

Albersheim, P. 1976. The primary cell wall. Pages 225-274 in J. Bonner and J. E. Varner, eds. Plant biochemistry. Academic Press, New York.

Baddiley, J. 1975. Mechanism and control of cell wall synthesis in bacteria. Pure Appl. Chem. 42:417-429.

Bateman, D. F., and H. G. Basham. 1976. Degradation of plant cell walls and membranes by microbial enzymes. Pages 316-355 in R. Heitifuss and P. H. Williams, eds. Physiological plant pathology. Volume 4. Encyclopedia of Plant Physiology. Springer-Verlag, Berlin.

Baumann, G., H. D. Isenberg, and J. Gennaro, Jr. 1978. The inverse relationship between nutritional nitrogen concentration and coccolith calcification in culture of the coccolithophorid Hymenomonas sp. J. Protozool. 25(2):253-256.

Bauer, W. D., K. W. Talmadge, K. Keegstra, and P. Albersheim. 1973. The structure of plant cell walls. II. The hemicellulose of the walls of suspension-cultured sycamore cells. Plant Physiol. 51:174-187.

Blackwelder, P. L., R. E. Weiss, and K. M. Wilbur. 1976. Effects of calcium, strontium, and magnesium on the coccolithophorid Cricosphaera (Hymenomonas) carterae. I. Calcification. Mar. Biol. 34:11-16.

Blackwelder, P. L., L. E. Brand, and R. L. Guillard. 1979. Coccolith morphology and paleoclimatology. II. Cell ultrastructure and formation of coccoliths in Cyclococcolithina leptopora (Murray and Blackman) Wilcoxon and Gephyrocapsa oceanica Kamptner. Scanning Electron Microscopy 11:417-420.

Blankenship, M. L., and K. M. Wilbur. 1975. Cobalt effects on cell division and calcium uptake in the coccolithophorid Cricosphaera carterae (Haptophyceae). J. Phycol. 11:211-219.

Blankley, W. 1971. Auxotrophic and heterotrophic growth and calcification of coccolithophorids. Ph.D. Thesis. University of California, San Diego (Lib. Congr. Card No. Mic. 71-22,618). 186 pp. Univ. Microfilms, Ann Arbor, Michigan.

Borisy, G. G., J. B. Almstad, J. M. Marcum, and C. Allen. 1974. Microtubule assembly in vitro. Fed. Proc. Fed. Amer. Soc. Exp. Biol. 33:167-174.

Bouch, G. B., and D. L. Brown. 1976. Self-assembly in development. Ann. Rev. Plant Physiol. 27:71-94.

Braun, E., and H. G. Aach. 1975. Enzymatic degradation of the cell wall of Chlorella. Planta 126:181-185.

Brown, R. G., and W. C. Kimmins. 1977. Glycoproteins. Pages 183-209 in D. H. Northcote, ed. International Rev. of Biochem. Plant Biochemistry II. Vol. 13. University Park Press, Baltimore.

Brown, R. M., Jr. 1969. Observations on the relationships of the Golgi apparatus in the marine chrysophycean alga, Pleurochysis scherffelii Pringsheim. J. Cell Biol. 41:109-123.

Brown, R. M., Jr. 1975. Pleurochrysis scherffelii (Chrysophyceae) negative development. Encyclopedia Cinematographica E1682.

Brown, R. M., Jr., and D. Montezinos. 1976. Cellulose microfibril: Visualization of biosynthesis and orienting complexes in association with the plasma membrane. Proc. Natl. Acad. Sci. USA 73: 143-147.

Brown, R. M., Jr., and D. K. Romanovicz. 1976. Biogenesis and structure of Golgi derived cellulosic scales in Pleurochrysis. I. Role of the endomembrane system in scale assembly and exocytosis. Appl. Poly. Symp. 28:587-610.

Brown, R. M., Jr., W. W. Franke, H. Kleinig, H. Falk, and P. Sitte. 1969. A cellulosic wall component produced by the Golgi apparatus of Pleurochrysis scherffelii. Science (Washington) 166:894.

Brown, R. M., Jr., W. W. Franke, H. Kleinig, H. Falk, and P. Sitte. 1970. Scale formation in chrysophycean algae I. Cellulosic and noncellulosic wall components made by the Golgi apparatus. J. Cell Biol. 45:246-271.

Brown, R. M., Jr., W. Herth, W. W. Franke, and D. Romanovicz. 1973. The role of the Golgi apparatus in the biosynthesis and secretion of a cellulosic glycoprotein in Pleurochrysis: A model system for the synthesis of structural polysaccharides. Pages 207-257 in F. Loewus, ed. Biogenesis of plant cell wall polysaccharides. Academic Press, New York.

Brown, R. M., Jr., J. H. M. Willison, and C. L. Richardson. 1976. Cellulose biosynthesis in Acetobacter xylinum: Visualization of the site of synthesis and direct measurement of the in vivo process. Proc. Natl. Acad. Sci. USA 73:4565-4569.

Burgess, J., and P. J. Linstead. 1976. Scanning electron microscopy of cell wall formation around isolated plant protoplasts. Planta 131:173-178.

Burgess, J., and P. J. Linstead. 1977. Caumarin inhibition of microfibril formation at the surface of cultured protoplasts. Planta 133:267-273.

Burgess, J., and P. J Linstead. 1979. Structure and association of wall fibrils produced by regenerating tobacco protoplasts. Planta 146:203-210.

Burgess, J., P. J. Linstead, and V. E. Bonsall. 1978. Observations on the time course of wall development at surface of isolated protoplasts. Planta 139:85-91.

Catt, J. W., G. J. Hills, and K. Roberts. 1976. A structural glycoprogein, containing hydroxyproline, isolated from the cell wall of Chlamydomonas reinhardii. Planta 131:165-171.

Catt, J. W., G. J. Hills, and K. Roberts. 1978. Cell wall glycoproteins from Chlamydomonas reinhardii and their self assembly. Planta 138:91-98.

Clement-Metral, J. D. 1976. Preparation and some properties of protoplasts from the red alga Porphyridium cruentum. J. Microsc. Biol. Cell. 26:167-172.

Cocking, E. C. 1972. Plant cell protoplasts. Isolation and development. Ann. Rev. Plant Physiol. 23:29-50.

Colvin, J. R., and G. G. Leppard. 1976. The biosynthesis of cellulose by Acetobacter xylinum and Acetobacter acetigenus. Can. J. Microbiol. 23:701-709.

Colvin, J. R., L. Chene, L. C. Sawden, and M. Takai. 1977. Purification and properties of a soluble polymer of glucose from cultures of Acetobacter xylinum. Can. J. Biochem. 55:1057-1063.

Cox, G., and B. Juniper. 1973. Autoradiographic evidence for paramural body function. Nature New Biol. 243:116-117.

Craigie, J. S., and C. Leigh. 1978. Carrageenans and agars. Pages 145-164 in J. A. Hellebust and J. S. Craigie, eds. Handbook of phycological methods. Physiological and biochemical methods. Cambridge University Press, Cambridge.

Crawford, R. M., and P. F. Heap. 1978. Transmission electron microscopy X-ray microanalysis of two algae of the genera Scenedesmus and Silerocelis. Protoplasma 96:361-367.

Crenshaw, M. 1964. Coccolith form by two marine coccolithophorids, Coccolithus huxleyi and Hymenomonas. Ph.D. Thesis. Duke Univ. (Lib. Congr. Card No. Mic. 65-3972). 74 pp. Univ. Microfilms, Ann Arbor, Michigan.

Danon, D. 1972. Use of cationized ferritin as a label of negative charges on cell surfaces. Ultrastruct. Res. 38:500-510.

Darvill, A., M. McNeil, and P. Albersheim. 1978. Structure of plant cell walls: Fractionation and characterization of the pectic polymers. Plant Physiol. 59(6):17.

Davies, D. R., and V. Lyall. 1973. The assembly of a highly ordered component of the cell wall: The role of heritable factors and of physical structure. Mol. Gen. Genet. 124:21-34.

DeJong, E. W., L. Bosch, and P. Westbrock. 1976. Isolation and characterization of a Ca^{2+}-binding polysaccharide associated with coccoliths of Emiliania huxleyi (Lohmann) Kamptner. Eur. J. Biochem. 7:611-621.

Dische, Z. 1947. A new specific color reaction of hexuronic acids. J. Biol. Chem. 167:189-198.

Domozych, D. S., and J. S. Cantral. 1978. Selected area electron diffraction: A technique for comparative cell wall studies in the Chorophyta. J. Phycol. 14:35.

Domozych, D. S., K. R. Mattox, and K. D. Stewart. 1978. A comparative study of the cell walls of selected green algae. J. Phycol. 14:35.

Dorigan, J. L., and K. M. Wilbur. 1973. Calcification and its inhibition in coccolithophorids. J. Phycol. 9:450-456.

Eastoe, J. E. 1968. Chemical aspects of the matrix concept in calcified tissue organization. Calc. Tiss. Res. 2:1-19.

Ebersold, W. T. 1963. Heterozygous diploid strains of Chlamydomonas reinhardii. Genetics 48:888.

Ebersold, W. T. 1967. Chlamydomonas reinhardii heterozygous diploid strains. Science 157:447-449.

Elder, J. H., C. A. Lembi, L. Anderson, and D. J. Morre. 1971. Scale calcification in a Chrysophycean alga. A test system for the effects of DDT on biological calcification. Proc. Indiana Acad. Sci. 81:106-113.

Elias, H. G. 1977. Macromolecules II. (Translated from German by J. W. Stafford). Plenum Press, New York. Chapter 31, Polysaccharides. 1067-1101.

Esquierré-Tugayé, M. T., and D. T. A. Lamport. 1979. Cell surfaces in plant - microorganism interactions. Plant Physiol. 64:314-319.

Esquierré-Tugayé, M. T., C. Lafitte, D. Mazan, A. Toppan, and A. Ţanzé. 1979. Cell surface in plant-microorganism interactions. Plant Physiol. 64:320-326.

Evans, L. L., and M. E. Callow. 1976. Secretory processes in seaweeds. Pages 487-499 in N. Sunderland, ed. Perspectives in experimental biology. Vol. 2. Botany. Pergamon Press, Oxford.

Fichtinger-Schipman, J. P., J. Kamerling, F. G. Vliegenthart, E. W. DeJong, L. Bosch, and P. Westbrock. 1979. Composition of methylated, acidic polysaccharide associated with coccoliths of Emiliania huxleyi (Lohmann) Kamptner. Carbohydrate Res. 69:181-184.

Flesch, D. 1977. The in vivo and in vitro assembly of cell walls in the marine coccolithophorid, Hymenomonas carterae. Ph.D. Thesis. Iowa State University. 190 pp.

Frearson, E. M., J. B. Power, and E. C. Cocking. 1973. The isolation, culture, and regeneration of Petunia leaf protoplasts. Dev. Biol. 33:130-137.

Gabriel, M. 1970. Formation, growth, and regeneration of protoplasts of the green alga, Uronema gigas. Protoplasma 70:135-138.

Gamborg, O. L. 1976. Plant protoplast isolation culture and fusion. Pages 107-127 in D. Dudits, G. L. Farkas, and P. Maliga, eds. Cell genetics in higher plants. Publishing House of the Hungarian Academy, Budapest.

Gamborg, O. L., and R. A. Miller. 1973. Esolation, culture and uses of plant protoplasts. Can. J. Bot. 51:1795-1799.

Gartner, S. 1978. Coccolithophores--Their evolution through time. J. Phycol. 14:36.

Good, B. H., and R. L. Chapman. 1978. The ultrastructure of the green alga Phycopeltis (Chroolepidaceae: Chlorophyta). I. Sporopollenin in the cell walls. Amer. J. Bot. 65(1):27-33.

Goodenough, D. A., and W. Stoeckenius. 1972. The isolation of mouse hepatocyte gap junctions. J. Cell Biol. 45:646-656.

Green, J. C., and D. H. Jennings. 1967. A physical and chemical investigation of the scales produced by the Golgi apparatus within and found on the surface of the cells of Chrysochromulina chiton Parke et Manton. J. Exp. Bot. 18:359-370.

Grimm, I., H. Sachs, and D. G. Robinson. 1976. Structure, synthesis, and orientation of microfibrils. II. The effect of colchicine on the wall of Oocystis solitaria. Cytobiology 14:61-74.

Grout, B. W. W. 1975. Cellulose microfibril deposition at the plasmalemma surface of regenerating tobacco mesophyll protoplasts: A deep-etch study. Planta 123:275-282.

Hara, M., N. Umetsu, C. Miyamoto, and K. Tamari. 1973. Inhibition of the synthesis of plant cell wall materials, especially cellulose biosynthesis by coumarin. Plant Cell Physiol. 14:11-28.

Harada, H., K. Ohyama, and J. Cheruel. 1972. Effects of coumarin and other factors on the modification of form and growth of isolated mesophyll cells. Z. Pflanzenphysiol. 66:307-324.

Hatefi, Y., and W. G. Hanstein. 1974. Destabilization of membranes with castropic ions. Methods in Enzymology 31:770-790.

Haug, A. 1974. Chemistry and biochemistry of algal cell-wall polysaccharides. Pages 51-88 in D. H. Northcote, ed. MTP International Review of Science. Biochemistry Series One. Volume 11. Plant Biochemistry. University Park Press, Baltimore.

Hayat, M. A. 1975. Positive staining for electron microscopy. Pages 162-176 in M. A. Hayat, ed. Positive staining for electron microscopy. Reinhold Company, New York.

Hegnauer, H., and H. R. Hohl. 1978. Cell-wall architecture of sporangia, chlamydospores, oogonia, and oospores in Phytophthora. Exper. Mycol. 2(3):216-233.

Herth, W., W. W. Franke, J. Stadler, H. Bittiger, G. Keilich, and R. M. Brown. 1972. Further characterization of the alkali-stable material from the scales of Pleurochrysis scherffelii: A cellulosic glycoprotein. Planta 105:79-92.

Herth, W., A. Kuppel, W. W. Franke, and R. M. Brown. 1975. The ultrastructures of the scale cellulose from Pleurochrysis scherffelii under various experimental conditions. Cytobiology 10:268-284.

Hills, G. J. 1973. Cell wall assembly in vitro from Chlamydomonas reinhardii. Planta 115:17-23.

Hills, G. J., J. M. Phillips, M. R. Gay, and K. Roberts. 1975. Self-assembly of a plant cell wall in vitro. J. Mol. Biol. 96:431-441.

Hodge, J. E., and B. T. Hofreiter. 1962. Determination of reducing sugars and carbohydrates. Meth. Carbohydr. Chem. 1:380.

Hogetsu, T., H. Shihaaka, and M. Shimokoriyama. 1974. Involvement of cellulose synthesis in action of gibberellin and kinetin on cell expansion. 2,6-dichlorobenzonitrite as a new cellulose-synthesis inhibitor. Plant Cell Physiol. 15:389-393.

Homor, R. B., and K. Roberts. 1979. Glycoprotein conformation in plant cell walls, circular dichroism reveals a polyprolline II structure. Planta 146:217-222.

Hopp, H. E., P. A. Romero, and R. Pont Lezica. 1978. On inhibition of cellulose biosynthesis by coumarin. FEBS Letters 86:259-262.

Hugetsu, T., H. Shibaoka, and M. Shimokariyama. 1974. Involvement of cellulose synthesis in actions of giberellin and kinetin on cell expansion. 2,6-dichlorobenzonitrite as a new cellulose-synthesis inhibitor. Plant Cell Physiol. 15:389-393.

Huizing, H. J., H. Rietema, and J. H. Sietsma. 1979. Cell wall constituents of several siphoneous green algae in relation to morphology and taxonomy. Br. Phycol. J. 14:25-32.

Isenberg, H. D., and L. S. Lavine. 1973. Protozoan calcification. Pages 649-686 in I. Zipkin, ed. Biological mineralization. John Wiley and Sons, Inc., New York.

Isenberg, H. D., L. S. Lavine, M. L. Moss, D. Kupferstein, and P. E. Lear. 1963a. Calcification in a marine coccolithophorid. Ann. N. Y. Acad. Sci. 109:49-64.

Isenberg, H. D., L. S. Lavine, and H. Weissfellner. 1963b. The suppression of mineralization in a coccolithophorid by an inhibitor of carbonic anhydrase. J. Protozool. 10(4):531-534.

Isenberg, H. D., L. S. Lavine, H. Weissfellner, and A. Spotnitz. 1965. The influence of age and heterotrophic nutrition on Ca deposition in a marine coccolithophorid protozoan. Trans. N. Y. Acad. Sci. II 27:530-545.

Isenberg, H. D., S. D. Douglas, L. S. Lavine, S. S. Spicer, and H. Weissfellner. 1966. A protozoan model of hard tissue formation. Ann. N. Y. Acad. Sci. 136:155-170.

Isenberg, H. D., L. S. Lavine, H. Weissfellner, and A. Spotnitz. 1967. Laboratory studies with coccolithophorid protozoans. Am. Zool. 9:759.

Itoh, T. 1976. Microfibrillar orientation of radially enlarged cells of coumarin- and calchicine-treated pine seedlings. Plant Cell Physiol. 17:385-398.

Kaji, A., and T. Sahelsi. 1975. Endo-arabanase from Bacillus subtilis F-11. Biochim. Biophys. Acta 410:354-360.

Karr, A. L. 1976. Cell wall biosynthesis. Pages 405-426 in J. Bonner and J. E. Varner, eds. Plant biochemistry. 3rd ed. Academic Press, New York.

Keegstra, K., K. W. Talmadge, W. D. Bauer, and P. Albersheim. 1973. The structure of plant cell walls. III. A model of the walls of suspension-cultured sycamore cells based on the interconnections of the macromolecular components. Plant Physiol. 51:188-196.

Klaveness, D. 1972. Coccolithus huxleyi (Lohmann) Kamptner. I. Morphological investigations on the vegetative cell and the process of coccolith formation. Protistologica 8:335-346.

Klaveness, D. 1976. Emiliania huxley: (Lohmann). Hay and Mohler. III. Mineral deposition and the origin of the matrix during coccolith formation. Protistologica 12:217-224.

Kellenberger, E., and R. S. Edgar. 1971. Structure and assembly of phage particles. Pages 271-295 in A. D. Hershey, ed. Cold Spring Harbor Laboratory, New York.

Kuratana, A. 1974. The isolation and preliminary characterization of the coccoliths of Hymenomonas carterae. Master's Thesis. Iowa State University. 69 pp.

Labavitch, J., L. Freeman, and P. Albersheim. 1976. Structure of plant cell walls. Purification and characterization of a β-1,4-galactanase which degrades a structural component of the primary cell walls of dicots. J. Biol. Chem. 251:5904-5910.

Lamport, D. T. A. 1970. Cell wall metabolism. Ann. Rev. Plant Physiol. 21:235-270.

Lamport, D. T. A. 1974. The role of hydroxyproline-rich proteins in the extracellular matrix of plants. Symp. Soc. Dev. Biol. 30: 113-130.

Lamport, D. T. A. 1977. Structure, biosynthesis and significance of cell wall glycoproteins. Recent Adv. Phytochem. 11:79-115.

Leadbeater, B. S. C. 1970. Preliminary observations on differences of scale morphology at various stages in the life cycle of Apistonema-Syracosphaera sensu von Stosch. Br. Phycol. J. 5:57-69.

Leadbeater, B. S. C. 1971. Observations on the life history of the haptophycean alga Pleurochrysis scherffelii with special reference to the microanatomy of the different types of motile cells. Ann. Bot. 35:429-439.

Lefort, F. 1971. Sur l'appartenance a une seule et même espece de deux Coccolithophoracees, Cricosphaera carterae et Ochrosphaera verrucosa. Comp. Rend., D, 272:2540-2543.

Levine, R. P., and W. T. Ebersold. 1960. The genetics and cytology of Chlamydomonas. Ann. Rev. Microbiol. 14:197-216.

Lowry, O. H., N. J. Rosebrough, A. L. Farr, and R. J. Randall. 1951. Protein measurement with the folin phenol reagent. J. Biol. Chem. 193:265-275.

Luft, J. H. 1964. Electron microscopy of cell extraneous coats as revealed by ruthenium red staining. J. Cell Biol. 23:54A.

Makino, S., J. A. Reynolds, and C. Tanford. 1973. The binding of deoxycholate and Triton X-100 to proteins. J. Biol. Chem. 248: 4926-4932.

Manton, I. 1966. Observations on scale production in Prymnesium parvum. J. Cell Sci. 1:375-380.

Manton, I. 1967a. Further observations on the fine structure of Chryschromulina chiton with special reference to the haptonema, "peculiar" Golgi structure and scale production. J. Cell Sci. 2:265-272.

Manton, I. 1967b. Further observations on scale formation in Chrysochromulina chiton. J. Cell Sci. 2:411-418.

Manton, I. 1968. Further observations on the microanatomy of the haptonema in Chrysochromulina chiton and Prymnesium parvum. Protoplasma 66:35-53.

Manton, I., and G. F. Leedale. 1969. Observations on the microanatomy of Coccolithus pelagicus and Cricosphaera carterae, with special reference to the origin and nature of coccoliths and scales. J. Mar. Biol. Assoc. U.K. 49:1-16.

Manton, I., and L. S. Peterfi. 1969. Observations on the fine structure of coccoliths, scales, and the protoplast of a freshwater coccolithophorid, Hymenomonas roseola Stein, with supplementary observations on the protoplast of Cricosphaera carterae. Roy. Soc. (London) Proc. B. 172:1-15.

Marchant, H. J. 1979. Microtubules, cell wall deposition and the determination of plant cell shape. Nature 278:167-168.

Marchant, H. J., and L. C. Fawke. 1977. Preparation, culture, and regeneration of protoplasts from filamentous green algae. Can. J. Bot. 55:3080-3086.

Marchant, H. J., and E. R. Hines. 1979. The role of microtubules and cell-wall deposition in elongation of regenerating protoplasts of Mangeotia. Planta 146:41-48.

Marchant, R. A., and A. W. Robards. 1968. Membrane systems associated with the plasmalemma of plant cells. Ann. Bot. 32:457-471.

Mathews, M. B., and L. Decker. 1971. Determination of molecular weight of acid mucopolysaccharides by gel electrophoresis. Biochim. Biophys. Acta 244:30-34.

McCandless, E. L., and S. J. Craigie. 1978. Sulfated polysaccharides in red and brown algae. Ann. Rev. Plant Physiol. 30:41-53.

McGuckin, W. F., and B. F. McKenzie. 1958. An improved periodic acid fuchsin sulfite staining method for evaluation of glycoproteins. Clin. Chem. 4:476-483.

Mesquita, J. F. 1974. Autoradiographic study of the function of the plasmalemmasomes in root tip cells. J. Submicr. Cytol. 6:391-397.

Meyer, Y., and W. Herth. 1978. Chemical inhibition of cell wall formation and cytokinesis, but not of nuclear division, in protoplasts of Nicotiana tabacum L. cultivated in vitro. Planta 142:253-262.

Miller, D. H. 1978. Cell wall chemistry and ultrastructure of Chlorococcum oleofaciens (Chlorophyceae). J. Phycol. 14(2):189-194.

Miller, D. H., D. T. A. Lamport, and M. Miller. 1972. Hydroxyproline heterooligosaccharides in Chlamydomonas. Science 176:918-920.

Miller, D. H., K. Mellman, D. T. A. Lamport, and M. Miller. 1974. The chemical composition of the cell wall of Chlamydomonas gymnogama and the concept of a plant cell wall protein. J. Cell Biol. 63:420-429.

Monro, J. A., D. Penny, and R. W. Bailey. 1976. The organization and growth of primary cell walls of lupin hypocotyl. Phytochemistry 15:1193-1198.

Muller, S. C., R. M. Brown, and T. K. Scott. 1976. Cellulose microfibrils: Nascent stages of synthesis in higher plant cell. Science 149:949-951.

Nagata, T., and I. Takebe. 1970. Cell wall regeneration and cell division of isolated tobacco mesophyll protoplasts. Planta 92: 301-308.

Outka, D. E., and D. C. Williams. 1971. Sequential coccolith morphogenesis in Hymenomonas carterae. J. Protozool. 18(2):285-297.

Paasche, E. 1963. The adaptation of the carbon-14 method for the measurement of coccolith production in Coccolithus huxleyi. Physiol. Plant. 16:186-200.

Paasche, E. 1964. A tracer study of inorganic carbon uptake during coccolith formation and photosynthesis in the coccolithophorid Coccolithus huxleyi. Physiol. Plant. Suppl. 111:1-82.

Paasche, E. 1965. The effect of 3-(P-chlorophenyl)-1,1-dimethylurea (CMV) on photosynthesis and light dependent coccolith formation in Coccolithus huxleyi. Physiol. Plant. 18:138.

Paasche, E. 1966a. Action spectrum of coccolith formation. Physiol. Plant. 19:770-779.

Paasche, E. 1966b. Adjustment to light and dark rates of coccolith formation. Physiol. Plant. 19:271-278.

Paasche, E. 1968. Biology and physiology of coccolithophorids. Ann. Rev. Microbiol. 22:71-86.

Paasche, E. 1969. Light dependent coccolith formation in the two forms of Coccolithus pelagicus. Arch. Mikrobiol. 67:199.

Paddock, T. B. B. 1968. A possible aid to survival of the marine coccolithophorid Cricosphaera and similar organisms. Br. Physiol. Bull. 3:519-523.

Palevitz, B. A., and P. K. Hepler. 1976. Cellulose microfibril orientation and cell shaping in developing guard cells of Allium. The role of microtubules and ion accumulation. Planta 132:71-93.

Parke, M., and I. Adams. 1960. The motile (Crystallolithus hyalinus Gaarder and Markali) and nonmotile phases in the life history of Coccolithus pelagicus (Wallich) Schiller. J. Mar. Biol. Assoc. U.K. 39:263-264.

Parker, B., and A. G. Diboll. 1966. Alcian stains for histochemical localization of acid and sulfated polysaccharides in algae. Phycologia 6:37.

Pearce, R. S., and E. C. Cocking. 1973. Behaviour in culture of isolated protoplasts from "Paul's Scarlet" rose suspension culture cells. Protoplasma 77:165-180.

Pearlmutter, N. L., and C. A. Lembi. 1976. The composition and structure of Pithophora cell walls. J. Phycol. (Suppl.) 12:24.

Pearlmutter, N. L., and C. A. Lembi. 1978. Localization of chitin in algal and fungal cell walls by light and electron microscopy. J. Histochem. and Cytochem. 26:782-791.

Peberdy, J. F. 1979. Protoplasts--Applications in microbial genetics. Pages 1-60 in J. F. Peberdy, ed. A handbook of experimental methods. Department of Botany, University of Nottingham, Nottingham, England.

Pickett-Heaps, J. D. 1966. Incorporation of radioactivity into wheat xylem walls. Planta 71:1-14.

Pickett-Heaps, J. D. 1967. The use of radioautography for investigating wall secretion in plant cells. Protoplasma 64:49-66.

Pickett-Heaps, J. D. 1968a. Xylem wall deposition; radioautographic investigations using lignin precursors. Protoplasma 65:181-205.

Pickett-Heaps, J. D. 1968b. Further ultrastructural observations on polysaccharide localization in plant cells. J. Cell Sci. 3:55-64.

Pienaar, R. N. 1969a. The fine structure of Cricosphaera carterae. I. External morphology. J. Cell Sci. 4:561-567.

Pienaar, R. N. 1969b. The fine structure of Hymenomonas (Cricosphaera) carterae. II. Observations on scale and coccolith production. J. Phycol. 5:321-331.

Pienaar, R. N. 1971. Coccolith production in Hymenomonas carterae. Protoplasma 73:217-224.

Pintner, I. J., and L. Provasoli. 1968. Heterotrophy in subdued light of three Chrysochromulina species. Bull. Misaki Mar. Biol. Inst., Kyoto Univ. 12:25-31.

Preston, R. D. 1974. The physical biology of plant cell walls. Chapman and Hall Ltd, London. 491 pp.

Rayns, D. G. 1962. Alternation of generations in a coccolithophorid, Cricosphaera carterae (Braarud and Fagerl.) Braarud. J. Mar. Biol. Assoc. U.K. 42:481-484.

Reimann, B. 1961. Zur Verwendbarkeit von Rutheniumrot als elektronenmikroskopische Kontratierungsmittel. Mikroskopie 16:224.

Reynolds, C. S. 1963. The use of lead citrate at high pH as an electron-opaque stain in electron microscopy. J. Cell Biol. 17:208-212.

Roberts, K. 1974. Crystalline glycoprotein cell walls of algae: Their structure, composition, and assembly. Phil. Trans. Roy. Soc. London, Series B, 268:129-146.

Roberts, K. 1979. Hydroxyprolline: Its asymmetric distribution in a cell wall glycoprotein. Planta 146:275-279.

Roberts, K., and G. J. Hills. 1976. The crystalline glycoprotein cell wall of the green alga Chlorogonium elongatum: A structural analysis. J. Cell Sci. 21:59-71.

Roberts, K., M. Gurney-Smith, and G. J. Hills. 1972. Structure, composition, and morphogenesis of the cell wall of Chlamydomonas reinhardi. I. Ultrastructure and preliminary chemical analysis. J. Ultrastruct. Res. 40:599-613.

Robinson, D. G., and H. Quader. 1978. Reestablishment of cell wall microfibrils orientation after removal of microtubule inhibitors in Oacystis solitaria. Cytobiologie 18:210.

Robinson, D. G., and P. M. Ray. 1973. Separation of the synthesis of cellulose and noncellulosic wall polysaccharides. Plant Physiol. 51:59.

Romanovicz, D. K., and R. M Brown, Jr. 1976. Biogenesis and structure of Golgi derived cellulosic scales in Pleurochrysis. II. Scale composition and supramolecular structure. Appl. Polym. Symp. 28: 587-610.

Safa, A. R. 1977. Physiological and microscopic studies of the life cycle of the unicellular marine algae, Hymenomonas carterae. Master's Thesis, Iowa State University, Ames, Iowa. 146 pp.

Satoh, S., K. Matruda, and K Tamari. 1976a. β-1,4-glucan occurring in homogenate of Phaseolus aureus seedlings. Possible nascent stage of cellulose biosynthesis in vivo. Plant Cell Physiol. 17:1243-1254.

Satoh, S., M. Takahara, and K. Matsuda. 1976b. Inhibition of the synthesis of microbial cellulose by coumarin. Plant Cell Physiol. 17:1077-1080.

Schlosser, U. G., H. Sachs, and D. G. Robinson. 1976. Isolation of protoplasts by means of a "species-specific" autolysin in Chlamydomonas. Protoplasma 88:51-64.

Smith, R. W., and H. Koffler. 1971. Bacterial flagella. Advan. Microbial Physiol. 6:219-339.

Spurr, A. R. 1969. A low viscosity epoxy resin embedding medium for electron microscopy. J. Ultrastruct. Res. 26:31-43.

Swift, E., and W. R. Taylor. 1966. The effect of pH on the division rate of the coccolithophorid Cricosphaera elongata. J. Phycol. 2:121-125.

Takebe, I. 1975. The use of protoplasts in plant virology. Ann. Rev. Phytopathol. 13:105-125.

Talmadge, K. W , K. Keegstra, W. D Bauer, and P. Albersheim. 1973. The structure of plant cell walls. I. The macromolecular components of the walls of suspension-cultured sycamore cells with a detailed analysis of the pectic polysaccharides. Plant Physiol. 51:158-173.

Turvey, J. R. 1978. Biochemistry of algal polysaccharides. Pages 151-177 in D. J. Manners, ed. Biochemistry of carbohydrates II. University Park Press, Baltimore.

Umetsu, N. S. Satoh, and K. Matsuda. 1976. Effects of 2,6-dichlorobenzonitrite on suspension-cultured soybean cells. Plant and Cell Physiol. 17:1071-1075.

Vannini, G. L., M. P. Fasulo, and A Bruni. 1977. First observations on the cytological changes induced in Euglena gracilis by coumarin treatment. Z. Pflanzen. Physiol. 84:183-187.

Vernon, L. P., and E. R. Shaw. 1969. Oxidation of 1,5-diphenylcarbozid as a measure of photosystem 2 activity in subchloroplast fragments. Biochem. Biophys. Res. Commun. 36:878.

Vina, B., and J. C. Roland. 1972. Différentiation des cytomembranes et renouvment du plasmalemme dans les phénomenes de sécrétions végetales. J. Microscopie 13:119-136.

von Stosch, H. A. 1955. Ein morphologischer Phasenwechsel bei einer Coccolithophoride. Naturwissenschaften 42:423.

von Stosch, H. A. 1967. Haptophyceae. Encycl. Plant Phys. 18: 646-656.

Waechter, C. J., and W. J. Lennarz. 1976. The role of polyprenol-linked sugars in blycoprotein synthesis. Ann. Rev. Biochem. 45:95-112.

Watabe, N. 1967. Crystallographic analysis of the coccolith of Coccolithus huxleyi. Calc. Tiss. Res. 1:114-121.

Weber, K., and M. Osborn. 1969. The reliability of molecular weight determinations by dodecyl sulfate-polyacrylamide gel electrophoresis. J. Biol. Chem. 244:4406-4412.

Weinstein, L., and P. Albersheim. 1979. Structure of plant cell walls. IX. Purification and partial characterization of a wall-degrading endo-arabanase and an arabinosidase from Bacillus subtilis. Plant Physiol. 63:425-432.

Weiss, R. E., and K. M. Wilbur. 1978. Effects of cytochalasin B on division and calcium carbonate extrusion in calcareous algae. Experimental Cell Res. 112:47-54.

Westbroek, P., E. W. deLong, W. Dam, and L. Bosch. 1973. Soluble intracrystalline polysaccharides from coccoliths of Coccolithus huxleyi (Lohmann) Kampther (1). Calc. Tiss. Res. 12:227-238.

Wilbur, K. M., and N. Watabe. 1963. Experimental studies on calcification in molluscs and the alga Coccolithus huxleyi. Ann. N. Y. Acad. Sci. 190:82-112.

Williams, D. C. 1972. Golgi associated calcification in the coccolithophorid phytoflagellate Hymenomonas carterae. Ph.D. Thesis. Iowa State University (Lib. Congr. Card No. Mic. 72-26,951), 159 pp. Univ. Microfilms, Ann Arbor, Michigan.

Williams, D. C. 1974. Studies on Protistan mineralization. I. Kinetics of coccolith secretion in Hymenomonas carterae. Calc. Tiss. Res. 16:227-237.

Willison, J. H. M., and R. M. Brown. 1977. An examination of the developing cotton fibre: Wall and plasmalemma. Protoplasma 92: 21-41.

Willison, J. H. M., and R. M. Brown. 1978. Cell wall structure and deposition in Glaucocystis. J. Cell Biol. 77:103-119.

Willison, J. H. M., and E. C. Cocking. 1975. Microfibril synthesis of the surfaces of isolated tobacco mesophyll protoplasts, a freeze-etch study. Protoplasma 84:147-159.

Willison, J. H. M , and B W. W Grout. 1978. Further observations on cell-wall formation around isolated protoplasts of tobacco and tomato. Planta 140:53-58.

Wuytack, R., and C. Gillet. 1978. The nature of the bonds holding the calcium ion in the cell wass of Nitella flexilis algae. Can. J. Bot. 12:1439-1443.

Yu, J., D. A. Fishman, and T. L. Steck. 1973. Selective solubilization of proteins and phospholipids from red blood cell membranes by nonionic detergents. J. Supramol. Struct. 1:233-248.

Zacharius, R. M., T. E. Zell, J. H. Morrison, and J. Woodlock. 1969. Glycoprotein staining following electrophoresis on acrylamide gels. J. Anal. Biochem. 30:148-152.

ACKNOWLEDGMENTS

I wish to express my sincere appreciation to my major professor, Dr. D. E. Outka, for his understanding, guidance, counsel, and patience during the completion of this dissertation. I would like to thank Drs. M. A. Rougvie and D. J. Nevins for their helpful discussions and for the use of their laboratory facilities and equipment. Also, I would like to thank Dr. H. T. Horner, Jr. for the use of his EM facilities and especially scanning electron microscope. In addition, I wish to thank my friend and colleague, Mr. Zieg, for his encouraging discussions during my stay in Ames.

I would particularly like to acknowledge my parents for their patience, encouragement, and moral support during my graduate work.

APPENDIX A

Culture Media and Antibiotic Mixture (PMW II)

Standard Growth Medium

Component	Amount
NaCl	20.0 g
KCl	0.6 g
$MgSO_4 \cdot 7H_2O$	2.465 g
$CaCl_2$	1.11 g
Na·glycerophosphate	0.315 g
$NaNO_3$	0.5 g
Tris (2-amino-2-(hydroxy-methyl)-1,3-propanedial)	1.0 g
Vitamin B_{12}	3×10^{-6} g
Thiamine HCl	1×10^{-4} g
Na·lactate	2.0 g
Na_2CO_3	1×10^{-4} g
Na_4·EDTA	0.1 g
Trace metals*	1.0 ml
Distilled H_2O	q.s. to 1000 ml

pH 7.7-7.9
autoclave at 15 lbs of pressure for 15 minutes

*Trace metals:

ERDT (Na_3 N-hydroxyethylethylene diamine Triacetate)	3.0 g
$FeSO_4 \cdot 7H_2O$	0.44 g
$MnCl_2$	0.1 g
$ZnCl_2$	0.05 g
$CaCl_2$	0.001 g
$CuCl_2$	0.002 g
Na_2MoO_4	0.05 g
H_3BO_3	0.2 g
Distilled H_2O	q.s. to 100 ml

Antibiotic Mixture PNPB

Component	Final concentration in growth medium
Penicillin G, Bufford Potassium (Lilly)	2000 units
NegGram (Winthrop Laboratories)	2 mg/ml
Polymyxin B sulfate (CALBIOCHEM)	100 units/ml
Bacitracin (CALBIOCHEM)	20 units/ml

APPENDIX B

Correction of Sedimentation Constant for Solvent Viscosity

Due to using SDS solutions as the solvent in some of the sedimentation experiments, correction of the observed values of the sedimentation coefficients is necessary. For this purpose, the knowledge of solution viscosity is essential. (The relative viscosity due to SDS as measured in 0.15 M NaCl solution was found from Table 10 of Kuratana (1974).)

Correction of the sedimentation coefficients to standard conditions was made using the following equation,

$$S_{20,w} = S_{obs}(\eta_{rel\cdot SDS})(\eta_{rel\cdot salt})\frac{(1-\bar{v}\rho_{20,w})}{(1-\bar{v}\rho T)},$$

in which $S_{20,w}$ is the standard sedimentation coefficient, $\bar{v}$ is the partial specific volume (about 0.64 cc/g), $\rho_{20,w}$ and ρT are the densities of water at 20 C and of the solven, respectively, $\eta_{rel\cdot SDS}$ is the relative viscosity of SDS as measured in 0.15 M NaCl, and $\eta_{rel\cdot salt}$ is the relative viscosity of 0.15 M NaCl to that of water at 20 C.